AD-A052 360 BOSTON UNIV MASS DEPT OF ASTRONOMY F/G 3/2
RADIO FLARE STUDIES AT 4 CM.(U)
JAN 78 M D PAPAGIANNIS, F L WEFER F19628-76-C-0027
UNCLASSIFIED SER-II-NO-66 AFGL-TR-78-0014 NL

1 OF 2
ADA
052360

AFGL-TR-78-0014

RADIO FLARE STUDIES AT 4 CM

Michael D. Papagiannis and Fred L. Wefer

Department of Astronomy
Boston University
725 Commonwealth Avenue
Boston, Massachusetts 02215

FINAL REPORT
July 1, 1975 - September 30, 1977

January 1978

Approved for public release; distribution unlimited

AIR FORCE GEOPHYSICS LABORATORY
AIR FORCE SYSTEMS COMMAND
UNITED STATES AIR FORCE
HANSCOM AFB, MASSACHUSETTS 01731

UNCLASSIFIED

SECURITY CLASSIFICATION OF THIS PAGE (When Data Entered)

AD51138

REPORT DOCUMENTATION PAGE

READ INSTRUCTIONS BEFORE COMPLETING FORM

1. REPORT NUMBER: AFGL-TR-78-0014	2. GOVT ACCESSION NO.
3. RECIPIENT'S CATALOG NUMBER	
4. TITLE (and Subtitle): RADIO FLARE STUDIES AT 4 CM.	5. TYPE OF REPORT & PERIOD COVERED: Final Scientific Rept. 1 Jul 75-30 Sep 77
6. PERFORMING ORG. REPORT NUMBER: A.C. B.U., SerII, No.66	
7. AUTHOR(s): Michael D. Papagiannis, Fred L. Wefer	8. CONTRACT OR GRANT NUMBER(s): F19628-76-C-0027
9. PERFORMING ORGANIZATION NAME AND ADDRESS: Department of Astronomy, Boston University, 725 Commonwealth Ave., Boston, MA 02215	10. PROGRAM ELEMENT, PROJECT, TASK AREA & WORK UNIT NUMBERS: 62101F; 03; 46430302
11. CONTROLLING OFFICE NAME AND ADDRESS: Air Force Geophysics Laboratory, Hanscom AFB, Massachusetts 01731, Contract Monitor: Donald Guidice/PHP	12. REPORT DATE: Jan 78; NUMBER OF PAGES: 106 (108 P.)
14. MONITORING AGENCY NAME & ADDRESS (if different from Controlling Office): SER-II-NO-66	15. SECURITY CLASS. (of this report): Unclassified
	15a. DECLASSIFICATION/DOWNGRADING SCHEDULE

16. DISTRIBUTION STATEMENT (of this Report)

Approved for public release; distribution unlimited

17. DISTRIBUTION STATEMENT (of the abstract entered in Block 20, if different from Report)

18. SUPPLEMENTARY NOTES

19. KEY WORDS (Continue on reverse side if necessary and identify by block number)

Solar Radio Maps
Solar Brightness Temperature
Circular Radio Polarization
Solar Active Regions
Solar Flare Events
Forecasting Flare Activity

20. ABSTRACT (Continue on reverse side if necessary and identify by block number)

This report describes the efforts made under the present contract to observe and analyze the morphology of solar active regions and flare events. The overall four-year effort (1973-1977) was undertaken in the hope of developing a forecasting scheme which would allow the prediction of major flare events based on the behavior of the brightness temperature $T_a = \frac{1}{2}(T_r + T_\ell)$ and the circular polarization $P = (T_r - T_\ell)/(T_r + T_\ell)$ in the hours, or possibly

DD FORM 1 JAN 73 1473 EDITION OF 1 NOV 65 IS OBSOLETE

UNCLASSIFIED

SECURITY CLASSIFICATION OF THIS PAGE (When Data Entered)

406 311 JOB

the days, prior to the erruption of such a flare.

During the years 1973-1977, we conducted 63 days of observations with the 120 ft. Haystack antenna at a 4 cm wavelength, logging a total of more than 330 hours of solar observations. Primarily because this was a period of solar minimum, the number of cases observed, and especially those pertaining to major flare events, was relatively small. This fact, compounded by the observed diversity in the behavior of active regions before and during flare events, made it impossible to extract from the data any dependable forecasting scheme. It was concluded, therefore, that this goal can be achieved only with a long term project using a dedicated facility which over the period of a solar cycle could obtain a large enough number of events to make any statistical interpretation of the results meaningful. Though the main goal of the project was not realized, our efforts allowed us to gain a better perspective of the magnitude of the task and an understanding of the ways through which the forecasting effort should be approached. Our work produced also several other results, in which we were more successful. These included theoretical work on radio emission from active regions, detailed analysis of a specific active region, observation and theoretical analysis of a large solar filament, and studies of coronal holes.

TABLE OF CONTENTS

LIST OF TABLES

LIST OF FIGURES

Chapter I

INTRODUCTION

1.1 The Scope of the Project

The purpose of this research contract was to study the morphology and characteristics of solar radio emission in the centimeter range, and in particular near 4 cm, prior and during flare events. In order to obtain radio data on flare activity, it is necessary to spend long periods of time observing solar active regions where the flares occur. During the years 1973, 1974, and 1975 we logged more than 330 hours of observations and many more hours plotting and analyzing the data obtained.

The study of solar flares is based not only on pure scientific interest, but also on practical considerations. Solar flares produce significant changes in the terrestrial environment ranging from variations in the ozone layer to disruptions of telecommunications, and from geomagnetic disturbances to hazardous conditions for astronauts in space. To understand the conditions which generate major solar flares and to gain some insight in the forecasting of solar activity, it is important to study the active regions where the flares occur and to try to build a library of active region behavior prior to a flare event.

These studies were carried out using the NEROC 120 ft. Haystack antenna in Westford, Massachusetts, which is one of the major national facilities for radio astronomical research. The

unique features of the Haystack antenna include the following: At wavelengths close to 4 cm it can record both left and right circularly polarized emission. It has a time resolution better than one second. It has excellent pointing accuracy (a few arc sec). It can perform automatically many intricate scanning procedures. The greatest disadvantage of the Haystack antenna is the fact that at 4 cm it has a beam width of about 4 arc min. This is too broad for studies of the detailed structure of active regions, but is sufficient for studying the overall behavior of active regions prior and during flare events, which was actually the main objective of our research.

The duration of this contract effort covered the period from 1 July 1975 through 30 September 1977.

1.2. Observations and Data

The dates and times of observations during the year 1975 are listed in Table I. In addition we have listed in Table I the observing dates and times during the years 1973 and 1974. These observations were conducted under the previous Research Contract (F 19628-73-C-0058) but the analysis of the data obtained was continued under the present contract and some of the results are included in this Final Report.

TABLE I

1973		1974		1975	
Date	Times (UT)	Date	Times (UT)	Date	Times (UT)
13 MAR	1900-2250	5 JUN	1940-2210	23 JUN	1610-1910
14 MAR	1940-2200	6 JUN	1710-2100	24 JUN	1320-1900
19 MAR	1940-2150	7 JUN	1700-2100	25 JUN	1320-1850
25 MAY	1430-2050	8 JUN	1650-2110	04 AUG	1410-1950
28 JUN	1550-2110	9 JUN	1300-1910	05 AUG	1430-2000
29 JUN	1210-1700	12 JUL	1440-1950	06 AUG	1410-1950
30 JUN	1150-2040	13 JUL	1310-1910	07 AUG	1420-2000
1 JUL	1050-1700	14 JUL	1320-2040	08 AUG	1640-2000
4 JUL	1250-1830	15 JUL	1410-2020	09 AUG	1350-2050
5 JUL	1200-1650	17 JUL	1400-2020	10 AUG	1340-2030
7 JUL	1230-1820	18 JUL	1330-1950	21 AUG	1320-2010
8 JUL	1200-1840	20 JUL	1320-1900	23 AUG	1310-1940
11 JUL	1410-1900	21 JUL	1320-1910	31 AUG	1400-1800
12 JUL	1310-1720	18 SEP	1350-1910	01 SEP	1220-1930
14 JUL	1100-1800	19 SEP	1250-1900	08 NOV	1240-2050
15 JUL	1200-1800	20 SEP	1310-1850	09 NOV	1240-2030
17 JUL	1530-1910	21 SEP	1310-2040	10 NOV	1230-2000
18 JUL	1520-2000	22 SEP	1300-1840		
21 JUL	1240-1810	23 SEP	1320-1850		
22 JUL	1250-1800	24 SEP	1320-1900		
26 JUL	1530-1850	25 SEP	1320-1850		
		26 SEP	1310-1850		
		27 SEP	1310-1910		
		28 SEP	1310-1930		
		29 SEP	1320-1900		
Total	92.5 HRS	Total	137.8 HRS	Total	101.8 HRS
				TOTAL	332.1 HRS

1.3 The Haystack-Westford Interferometer

During the summer of 1976 a combined proposal was submitted to the Haystack Observatory by Boston University, Tufts University, and AFGL, to reactivate the Haystack-Westford interferometer for solar work. At a wavelength of 3.75 cm, this interferometer can achieve an angular resolution of 5-10 arc sec, which is comparable to the angular resolution of the NRAO interferometer. It is capable also of achieving time resolution better than 1 sec, which is superior to the 30 sec capability of NRAO and the 8 sec of OVRO.

It was proposed to carry out the project in three Phases. In Phase 1 we were to use the Westford dish as a single antenna. Two days were allocated to us in the fall of 1976 and during those two days we became familiar with the somewhat antiquated but still operable driving mechanisms of the Westford antenna. The test showed that the tracking ability of the Westford antenna was more than adequate for our purposes. In Phase 2 we were to use the Haystack and the Westford antennas together in an interferometer mode. This test was carried out on January 19, 1977, and though in principle was successful, it showed that the high time resolution of the system could not be realized for relatively weak events due to the narrow bandwidth of the system. Phase 3 was to follow the previous two, assuming that the results of 1 and 2 had been encouraging, and was supposed to include one to two weeks of actual solar interferometric observations. The results of Phase 2, however, indicated that at the present state of the system and the prevailing low level of solar activity the experi-

ment did not hold any great expectations of success. It has been postponed, therefore, until a time closer to solar maximum with the hope that, in the meantime, funds will become available to increase the bandwidth of the system.

1.4 Personnel

The people involved in the two years of this project were:

a. Professor Michael D. Papagiannis, the Chairman of the Astronomy Department of Boston University who is also th Principal Investigator of this Research Contract. Professor Papagiannis receives only summer compensation from this contract but spends also a substantial amount of his time during the academic year conducting or supervising research work under this contract.

b. Dr. Fred Wefer, a Post-Doctoral Research Associate of the Department of Astronomy of Boston University. Dr. Wefer is paid full time by this contract and devotes all his time on this project. He joined our group on 1 September 1976, and his presense has given great impetus to our research efforts.

c. Mr. Morgan Besson, a graduate student of the Astronomy Department. He worked for one year, September 1975 to August 1976, on this project and was quite helpful with some of the 1975 observations as well as with subsequent data analysis.

d. Mr. Robert Rose, also a graduate student of the Astronomy Department. He worked during the summer of 1976 and was primarily involved in data analysis.

1.5 Publications

During the period covered by this contract the following papers, reports, and abstracts in meetings were published:

a. Study of a Filament with a Circularly Polarized Beam at 3.8 cm. R.M. Straka, M.D. Papagiannis, and J.A. Kogut. Solar Physics, 45, 131, 1975.

b. A Simple Derivation of Microwave Solar Brightness Temperatures and Polarizations from Thermal Regions. M.D. Papagiannis, and J.A. Kogut. Solar Physics, 48, 49, 1976.

c. Polarization Studies at 3.8 cm of McMath Region 12417 of 1973. M.D. Papagiannis, and R.M. Straka. AFGL-TR-77-0115, May 1977.

d. Analysis of Solar Active Region 158/73. M.D. Papagiannis, R.M. Straka, and J.A. Kogut. 147th Meeting of AAS, Chicago, Illinois. December, 1975. Bull. AAS, 7, 523, 1975.

e. Solar Radio Maps at Five Wavelengths in the Presence of a Large Coronal Hole. F.L. Wefer, M.D. Papagiannis, R.M. Straka and M.P. Bleiweiss. Topical Conference on Solar and Interplanetary Physics, Tuscon, Arizona, January 1977.

1.6 Scientific Content of the Report

The following three Chapters of this Final Report summarize the work carried out under this Research Contract. This includes also the analysis of data obtained during the previous research contract, which are now presented in a uniform manner together with the data of the present contract. Chapters II, III, and IV contain the following material:

a. Chapter II begins with a description of the techniques used to obtain and plot solar maps and includes a total of 40 solar maps (10 for 1973, 19 for 1974, and 11 for 1975). For each case there are two maps. One for the total brightness temperature $T_a = \frac{1}{2}(T_r + T_\ell)$ scaled to a base of 100 for a quiet region on the solar disk, and the other giving the polarization in the form of right circular minus left circular $(T_r - T_\ell)$.

b. Chapter III begins with an introduction, followed by a comprehensive listing of all the active regions monitored during our 332 hours of observations. It includes also plots of 22 selected flare events as a function of time. These plots are of significant interest not only because they show the time development of a flare event, both in terms of brightness temperature and polarization, but also because they indicate the conditions which prevailed in an active region during the hours before the erruption of a flare.

c. Chapter IV presents the conclusions drawn from the observations and the subsequent analysis of the data. It includes also some suggestions for the future based on the information obtained from the work of this Research Contract.

Chapter II

FULL DISK SOLAR RADIO MAPS

2.1 Introduction

The first contour maps of circularly polarized radio emission from the Sun were made by Edelson,et al. (1971). These observations were made at wavelengths of 9 and 3.5 mm with an antenna having half power beam widths of 3.5 and 1.2 arc min, respectively Kundu and McCullough (1972) have also made maps of solar polarization at 9.5 mm with an antenna having a half power beam width of 1.6 arc min. Maps of solar polarization at 3.8 cm made with the 120 ft. Haystack antenna were first published by Richards and Straka (1971). The equipment and observational techniques have been presented by Richards (1972).

2.2 Observational Techniques

During 1973, 1974, and 1975 we performed more than 330 hours of solar polarization observations with the NEROC Haystack radio telescope at a wavelength of 3.8 cm. The antenna used for the observations was a 36.6 m (120 ft.) diameter circular paraboloid on a computer controlled altitude-azimuth mount. At 3.8 cm (7.875 GHz) the half power beam width is 4.4 arc min. The receiver system employed was the one used for planetary radar experiments at Haystack. The antenna temperatures of left and right circular polarization (T_ℓ and T_r) at 7.875 GHz are measured in a rapidly switching sequence, using a waveguide

hybrid to synthesize the polarizations from the two orthogoral linear feeds of the antenna. The bandwidth of the receiver system was 6.67 MHz.

A reference temperature or the quiet sun was established by pointing the antenna close to the north or the south pole of the sun, depending on which hemisphere was quieter. The declination offset of this calibration region from the center of the sun was ±0°.238 which placed the center of the antenna beam less than half a beam width inside the northern or southern limb of the sun. During the 1974 and 1975 observing sessions, this declination offset was changed to ±0°.202 which placed the entire beam clearly inside the solar disk and the center of the beam better than half a beam width from the limb of the sun.

A temperature value of 100 was taken to represent the difference between the solar emission from the quiet region near the polar limb mentioned above, and the emission from the background sky at an offset from the sun's center of 5° azimuth/cos (elevation), which corresponds to a distance of about 20 solar radii from the center of the solar disk. The antenna temperature of an active region is by definition equal to one half the sum of the antenna temperatures of the left and right circular polarized components.

$$T_a = \frac{1}{2}(T_r + T_\ell) \qquad (1)$$

Typical T_r and T_ℓ values observed in active regions were 150-300, i.e., 1.5 to 3 times the value of the quiet sun. On a few occasions, however, we observed temperatures in excess of 500, i.e., more than 5 times the temperature of the quiet sun. These values, of course, include a dilution effect produced by the antenna beam which in general is considerably larger than the hot active region.

The uncertainty ΔT in the antenna temperature T_a is given by the expression

$$\Delta T = \frac{T_a + T_s}{\sqrt{\tau \Delta \nu}} \qquad (2)$$

where T_s is the system temperature, $\Delta\nu$ the bandwidth, and τ the time constant of the observations. For our observations we had

$$\begin{aligned} T_a &\sim 18{,}000 \text{ K} \\ T_s &\sim 2{,}000 \text{ K} \\ \Delta\nu &\sim 6.7 \times 10^6 \text{ Hz} \\ \tau &\sim \frac{0.3}{2} \text{ sec} \end{aligned} \qquad (3)$$

In the value of τ, 0.3 seconds is the time constant of the receiver which is divided by 2 because of the switching between the two polarizations. Introducing the values of (3) into Eq. (2) we obtain

$$\Delta T \simeq \frac{T_a}{1000} \simeq 20^{\circ}K \qquad (4)$$

The antenna voltage measured at Haystack is digitized into steps of 1 milliVolt. The calibration voltage V_c, which was used for the reference temperature of the quiet region near the pole of the sun, was usually set equal to 0.15 Volts, so as to allow a large linear scale (up to 10 Volts) for major flare events. This meant that the temperature resolution was 1/150 of the quiet region temperature (150 × 1mV=0.15V) i.e.,

$$\Delta T = \frac{T_a}{150} = 120^{\circ}K \qquad (5)$$

From the above it follows that ΔT from (5) is much larger than the theoretical limit from (4), but it was dictated by the need to have available a large voltage range in order to be able to follow sudden large increases in the antenna voltage during major flare events. Under quiet conditions, however, this is a disadvantage because it quantizes the reference scale of 100 for the quiet regions in steps of approximately six times the theoretical limit. It is advisable, therefore, when detailed maps of quiet solar regions are made, to increase V_c to a level of about 1 Volt.

Each day's observations began with the making of a map of the sun in order to determine the locations of the active regions to be observed. Some of these maps covered only the declination range in which the active regions were known to reside.

On most occasions, however, the map covered the entire sun. It is these full disk solar maps with which we will deal in this Chapter.

The data for a map were collected by directing the telescope to perform a boustrophedonic raster with lines perpendicular to celestial north-south. The 20 lines of a map were spaced 2.2 arc min apart in declination, each line spanning 1°.1 in right ascension. The sampling rate was 0.6 s, with each scan line taking 72 s. Hence, the spacing in right ascension between sampling points was 0.55 arc min. The completion of the data acquisition for a map required 24 min.

2.3 Data Reduction

The first step in the data reduction process was the determination of the interval in Right Ascension which would result in a square grid of 20 rows and 39 columns. Antenna temperatures were determined at these points along the scan line by 4 point Lagrangian interpolation using the two nearest points on each side of the desired position. The result is a grid of points with a 2.2 arc min spacing N-S and 1.1 arc min spacing E-W, i.e., a square 41.8 arc min on each side.

In normalizing the 3.8 cm-λ maps we have adopted a technique similar to that used by Kundu and McCullough (1972). We have assumed that the sum of the grid of antenna temperatures is proportional to the 8.8 GHz solar flux density as given in Solar-Geophysical Data, while the sum of the polarizations is zero.

Mathematically, the normalization may be written:

$$T_\ell(i,j) = p\, T'_\ell(i,j)$$
$$T_r(i,j) = q\, T'_r(i,j) \qquad (6)$$

We assume:

$$\sum_{i=1}^{39} \sum_{j=1}^{20} [T_r(i,j) + T_\ell(i,j)] = K\, S(8.8\ \text{GHz}) \qquad (7)$$

and

$$\sum_{i=1}^{39} \sum_{j=1}^{20} [T_r(i,j) - T_\ell(i,j)] = 0 \qquad (8)$$

where: $T'_\ell(i,j)$ = antenna temperature (left circular polarization) at grid point (i,j),

$T_\ell(i,j)$ = normalized antenna temperature (left circular polarization) at grid point (i,j),

$T'_r(i,j)$ and $T_r(i,j)$ have the same meanings for right circular polarization,

$S(8.8\ \text{GHz})$ = 8.8 GHz solar flux density,

p and q are normalization factors and K is a proportionality constant.

Solving for p and q gives:

$$p = \frac{K\ \ S(8.8\ \text{GHz})}{2\ \Sigma\Sigma\ \ T_\ell(i,j)}\ , \quad q = \frac{K\ \ S(8.8\ \text{GHz})}{2\ \Sigma\Sigma\ \ T_r(i,j)} \qquad (9)$$

The proportionality constant K was chosen so as to make the normalized antenna temperature of the central disk quiet area approximately 100. In practice the two normalization factors are nearly equal, indicating that the original radiometer calibrations were of adequate accuracy. Two types of 3.8 cm radioheliograms are presented in this report: $T_a = 0.5\ (T_r+T_\ell)$ and $P = (T_r-T_\ell)$. All of these maps are plotted from the normalized data.

2.4 Contour Maps

The computer program used to contour the map grids was adapted from the program used at the La Posta Astrogeophysical Observatory. In traversing the map grid at a particular contour level, "high ground" is kept always on the right. Ambiguities, such as those that occur at saddle points, are resolved by the program always attempting first to make a right turn. Linear interpolation is used in determining where along a row or column the contour level crosses. These points are connected sequentially by straight line segments. In order to make the direction of decreasing temperature readily apparent, short tic marks are placed on the low side of the contour level at the mid-point of each line segment.

The interval between contours is <u>not constant</u> on these maps. Rather, it is varied using larger intervals where the temperature gradient is high. The smallest contour intervals appear where the surface is most flat. Contour labels are in units of percent of the central disk quiet area temperature.

Because not all of the contours are labelled, we state here the levels at which contours are drawn. On the temperature maps, the contoured levels are: 50, 60, 70, 80, 90, 95, 98, 100, 102, 105, 110, 120, 130, 140, 150, 170, 190, 210, 230, ... On the polarization maps, the contoured levels are 0, ±5, ±10, ±15, ±20, ±30, ±40, ...

At the bottom of each plot are listed the universal time at the start of data acquisition, the date, and the radio wavelength of the observation. The area covered by the data is enclosed in a box. The scale of each plot is shown at the lower left-hand corner of this box by the 1.0 arc min square and three additional tics at 1.0 arc min intervals along both the horizontal and vertical directions. A circle, corresponding to the photospheric disk on the date of the map, is also plotted and the location of the rotation axis is shown. Table II lists the dates and starting times for the 40 full disk radio maps obtained during the 1973, 1974, and 1975 observing programs. Because the weather during the observations affects the quality of the maps, we have included a brief description of it in this table.

TABLE II

Dates and times of 3.8 cm wavelength full disk antenna temperature and polarization radioheliograms.

Date	Starting Time (UT)	Weather Comments
13 March 1973	20:25	Clear
25 May 1973	14:27	Cloudy
25 May 1973	20:26	Cloudy
28 June 1973	16:04	Cirrus
29 June 1973	13:17	Rain
30 June 1973	11:52	Rain
01 July 1973	11:03	Cloudy
14 July 1973	13:37	Ptly Cldy
14 July 1973	17:33	Ptly Cldy
21 July 1973	17:21	Rain
12 July 1974	14:57	Clear
13 July 1974	13:37	Ptly Cldy
14 July 1974	13:39	Clear
15 July 1974	14:22	Cirrus
17 July 1974	14:03	Clear
18 July 1974	13:54	Cloudy
20 July 1974	13:32	Ptly Cldy
21 July 1974	13:44	Ptly Cldy
18 Sept. 1974	14:01	Clear
19 Sept. 1974	13:02	Cloudy
20 Sept. 1974	13:15	Cloudy
21 Sept. 1974	13:23	Rain

TABLE II (continued)

Date	Starting Time (UT)	Weather Conditions
22 Sept. 1974	13:13	Clear
23 Sept. 1974	13:28	Clear
24 Sept. 1974	13:26	Clear
25 Sept. 1974	13:22	Ptly Cldy
26 Sept. 1974	13:24	Cloudy
28 Sept. 1974	13:14	Fog, Cldy
29 Sept. 1974	13:27	Fog, Cldy
24 June 1975	13:43	Clear
24 June 1975	18:07	Clear
25 June 1975	13:28	Clear
21 August 1975	12:29	Clear
23 August 1975	13:10	Clear
23 August 1975	19:21	Clear
31 August 1975	14:14	?
01 Sept. 1975	12:52	Clear
08 Nov. 1975	13:18	Rain
09 Nov. 1975	13:08	Clear
10 Nov. 1975	13:12	Fog, Cldy

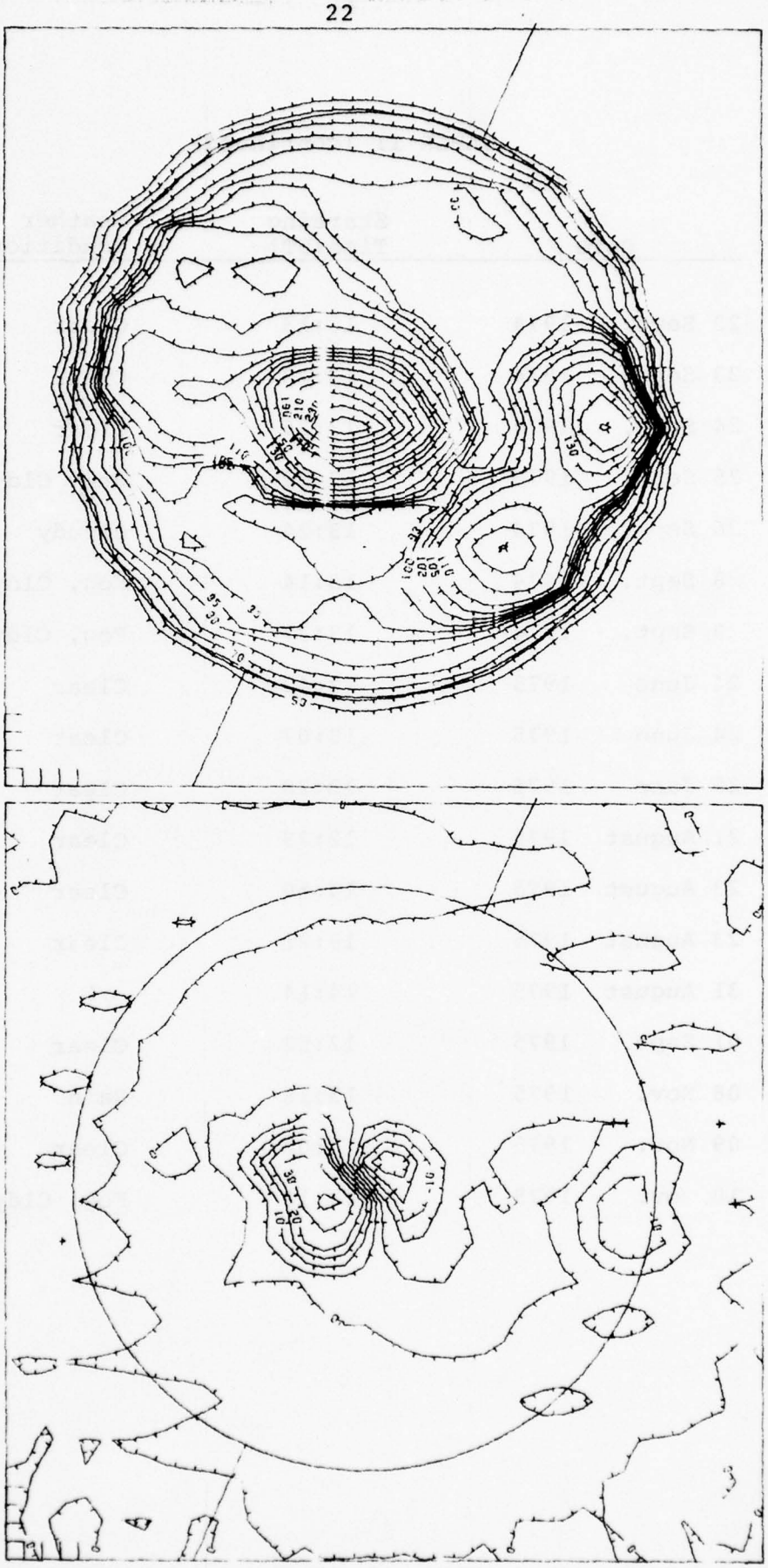

FIGURE 2.1

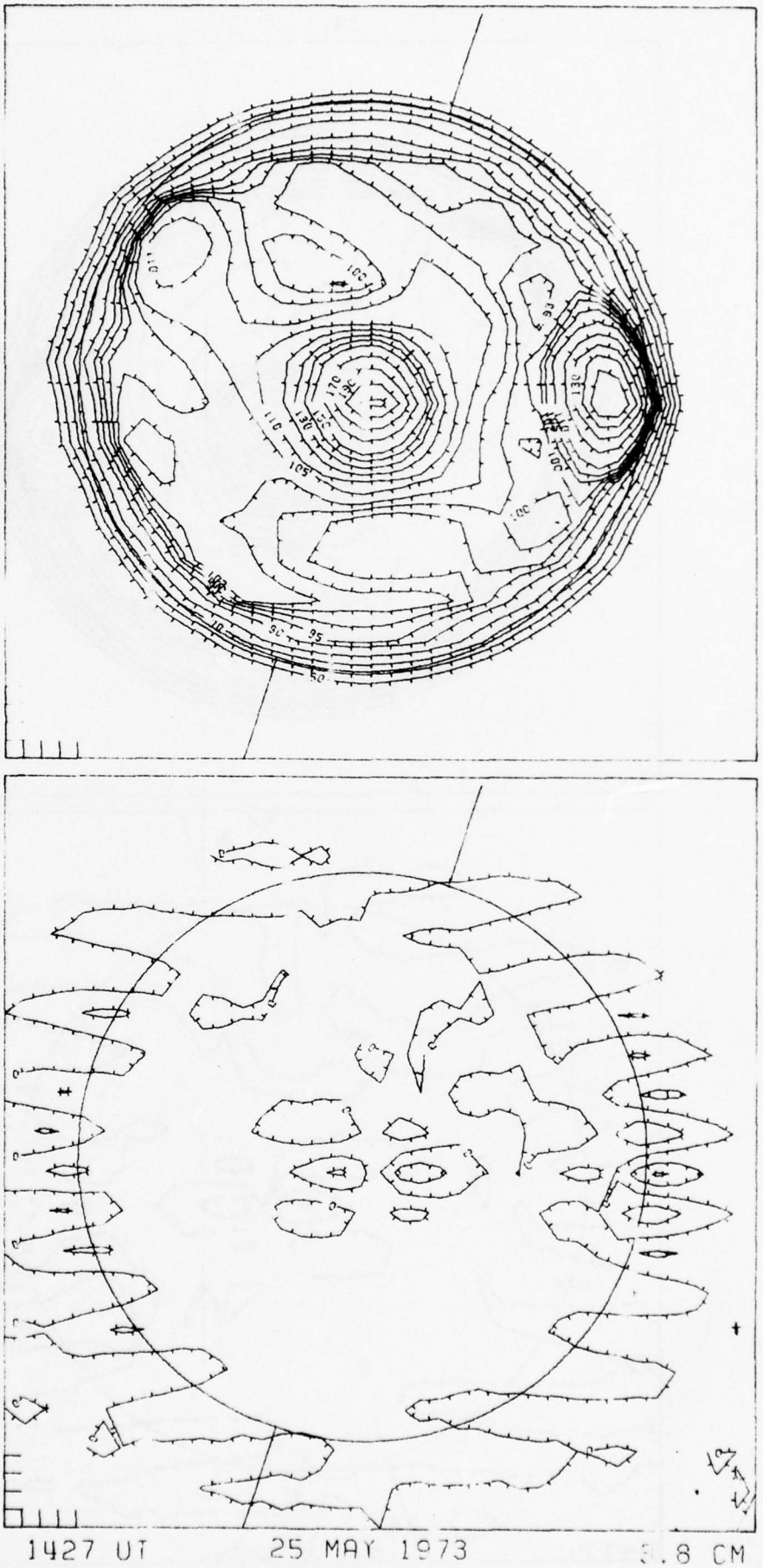

FIGURE 2.2

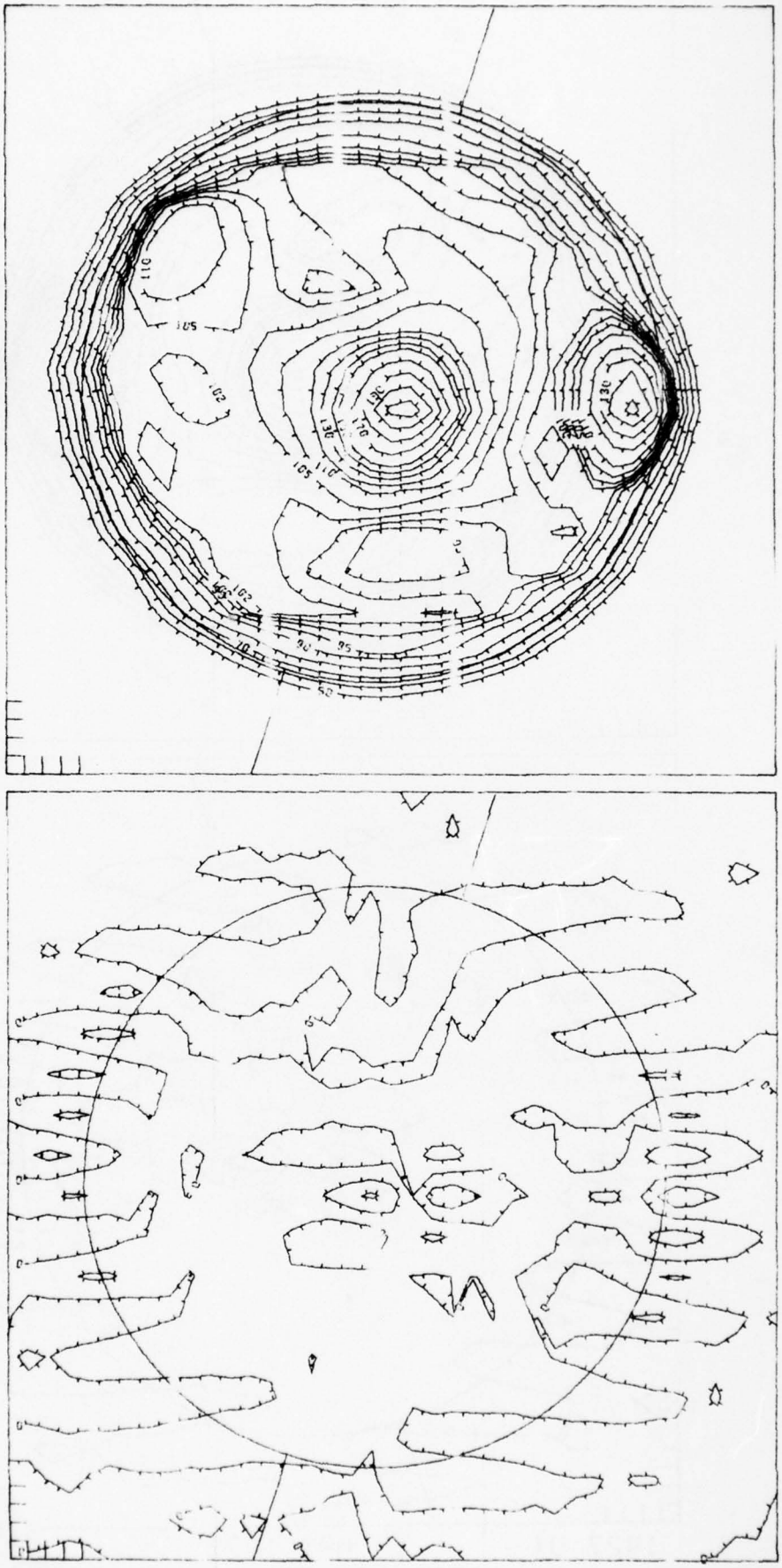

FIGURE 2.3

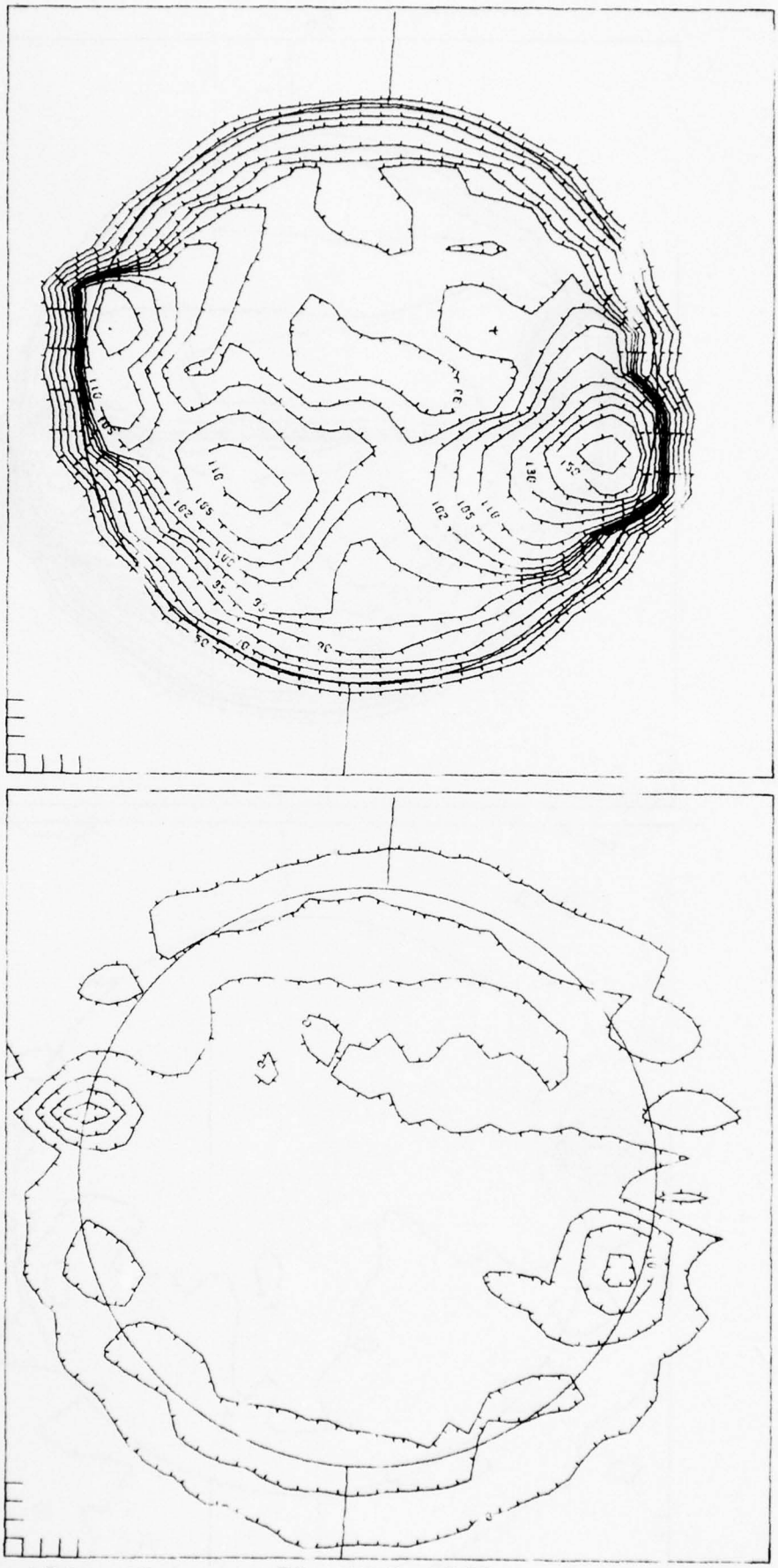

FIGURE 2.4

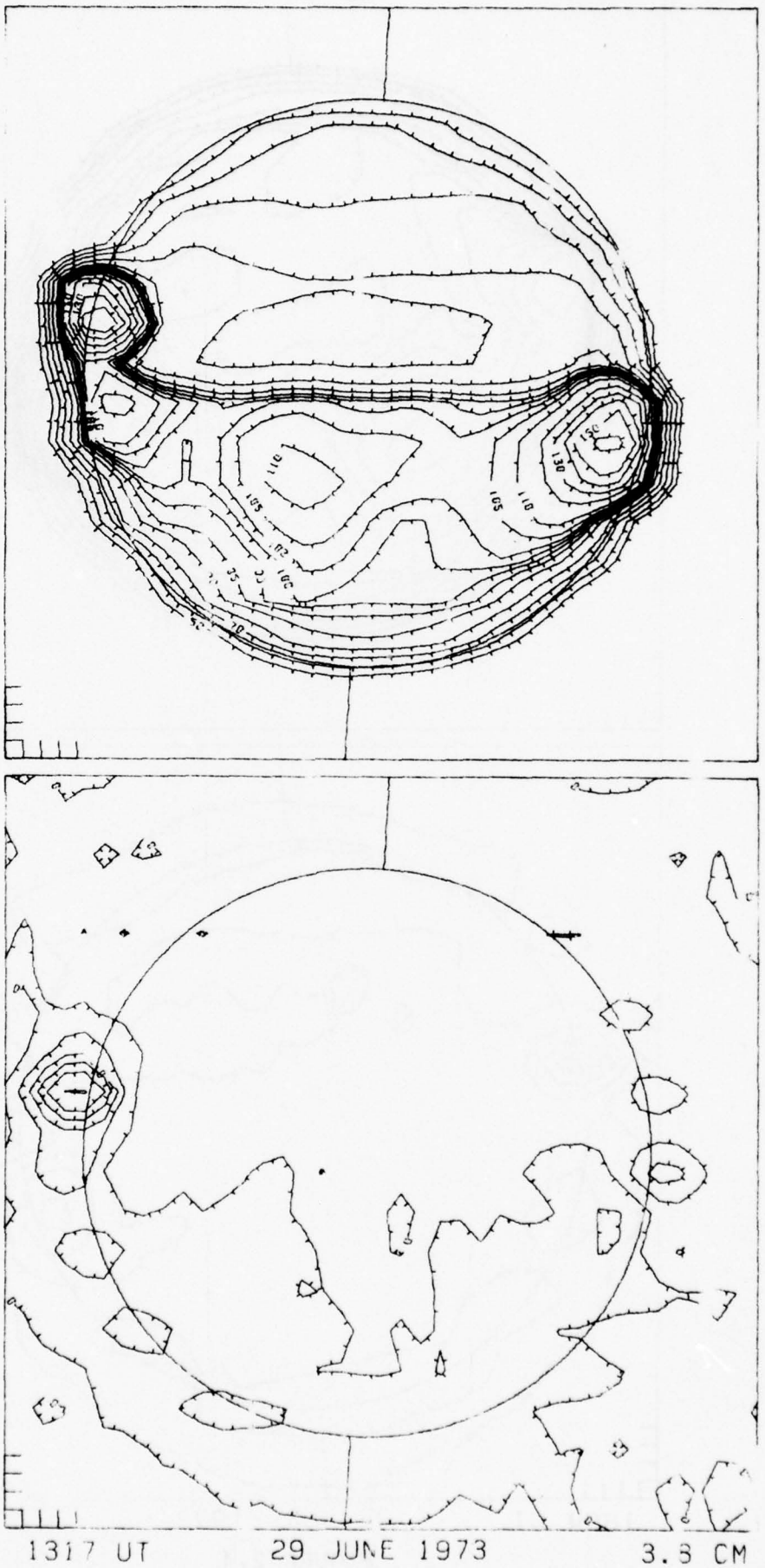

FIGURE 2.5

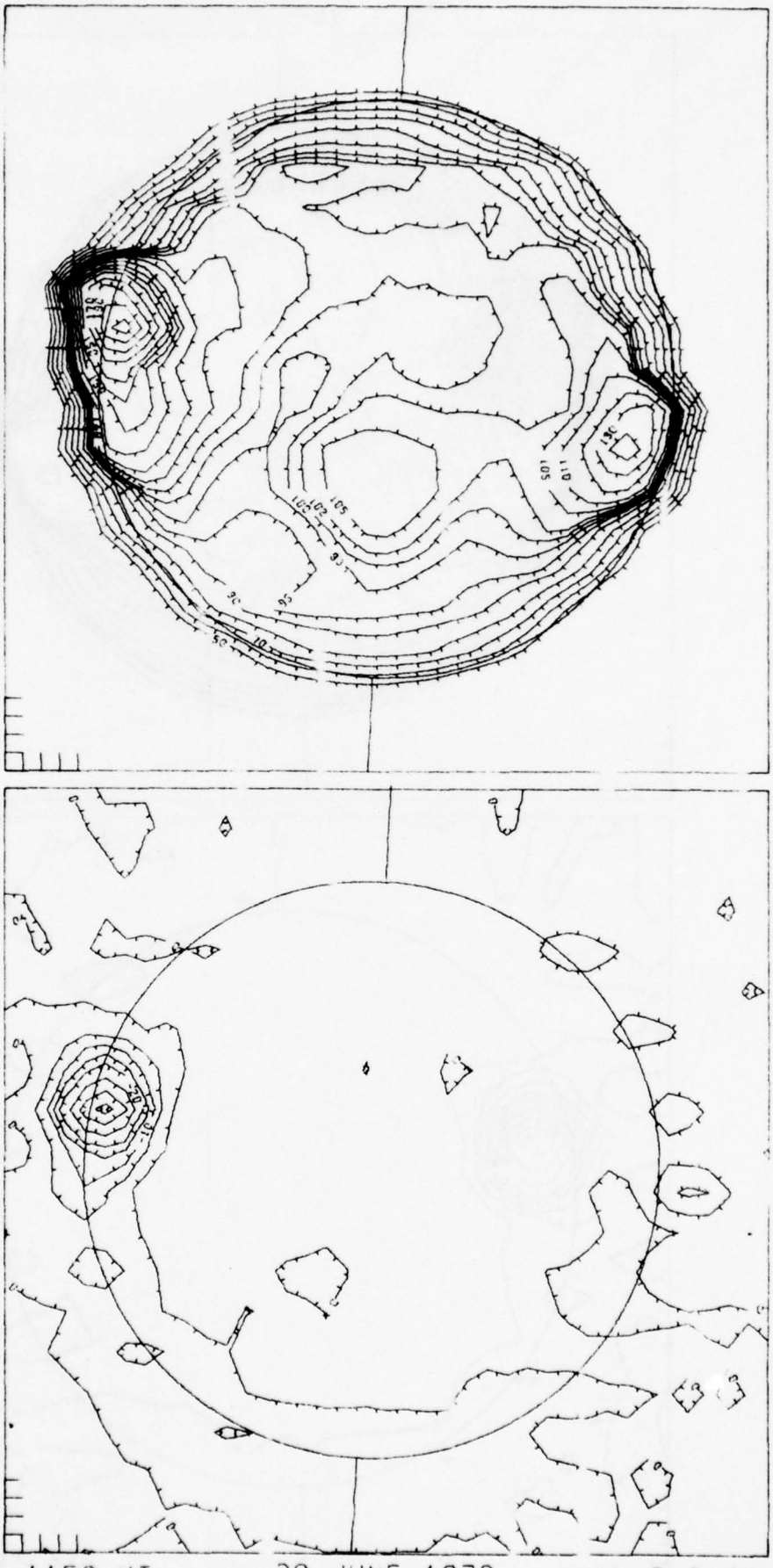

FIGURE 2.6

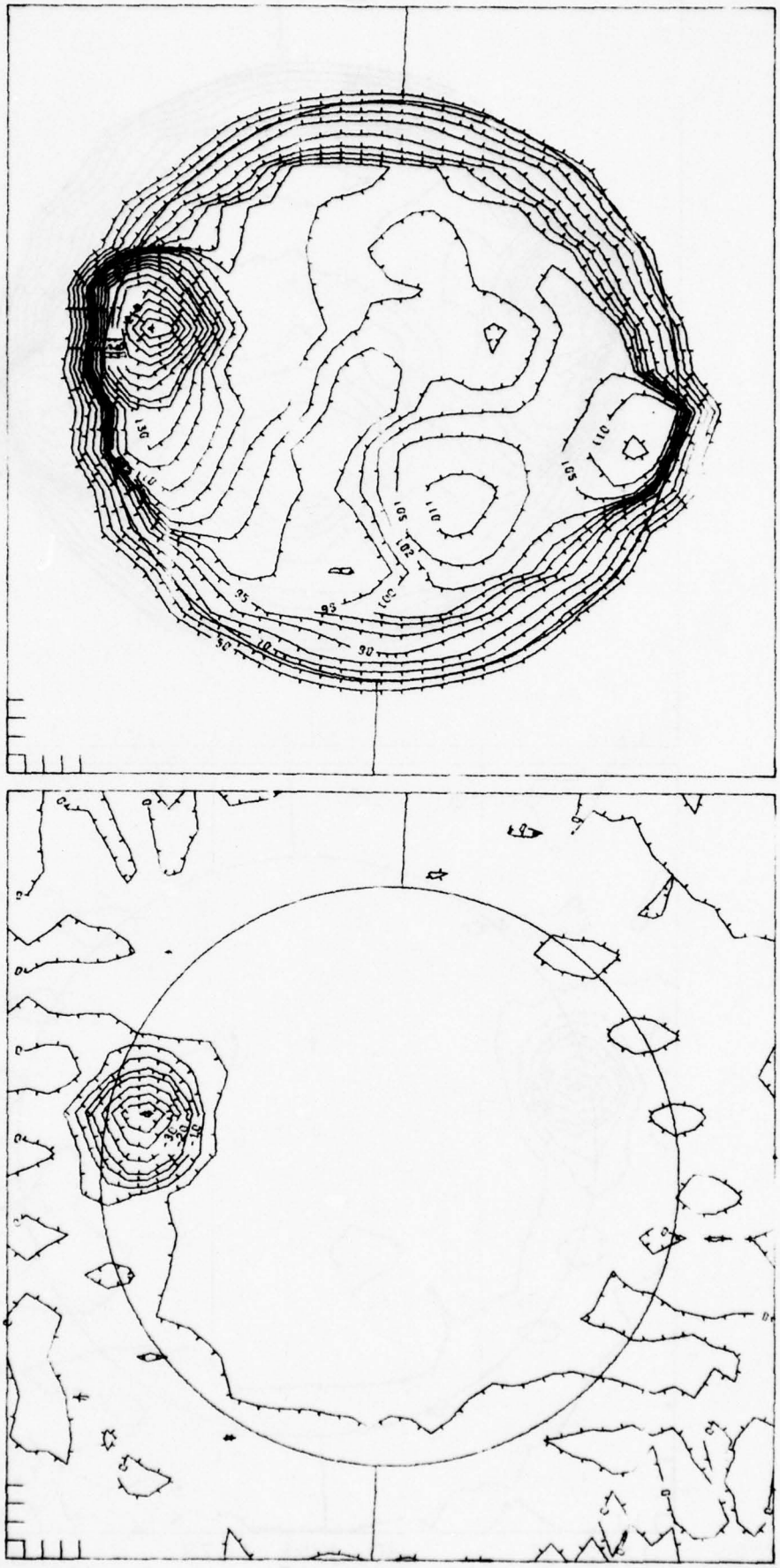

FIGURE 2.7

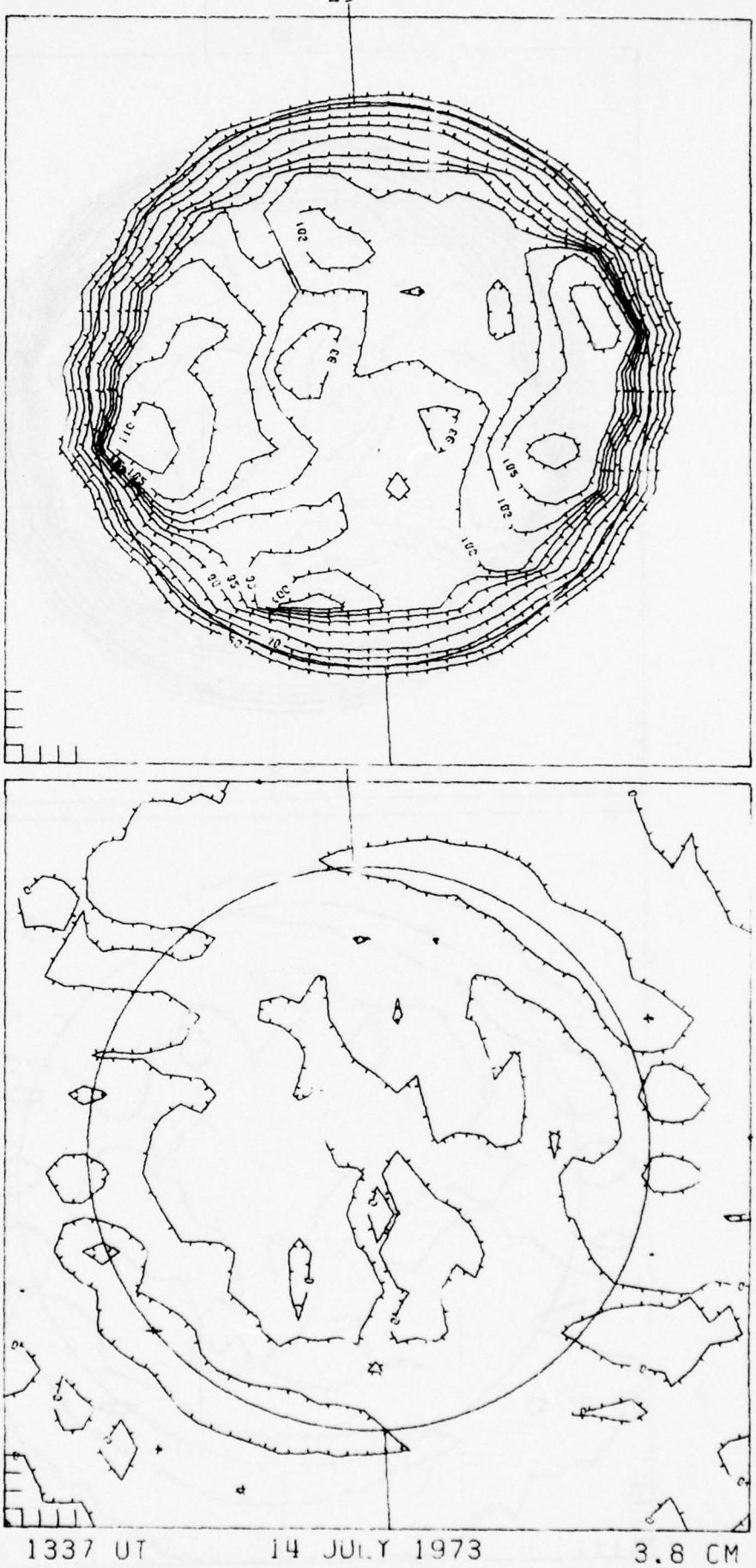

FIGURE 2.8

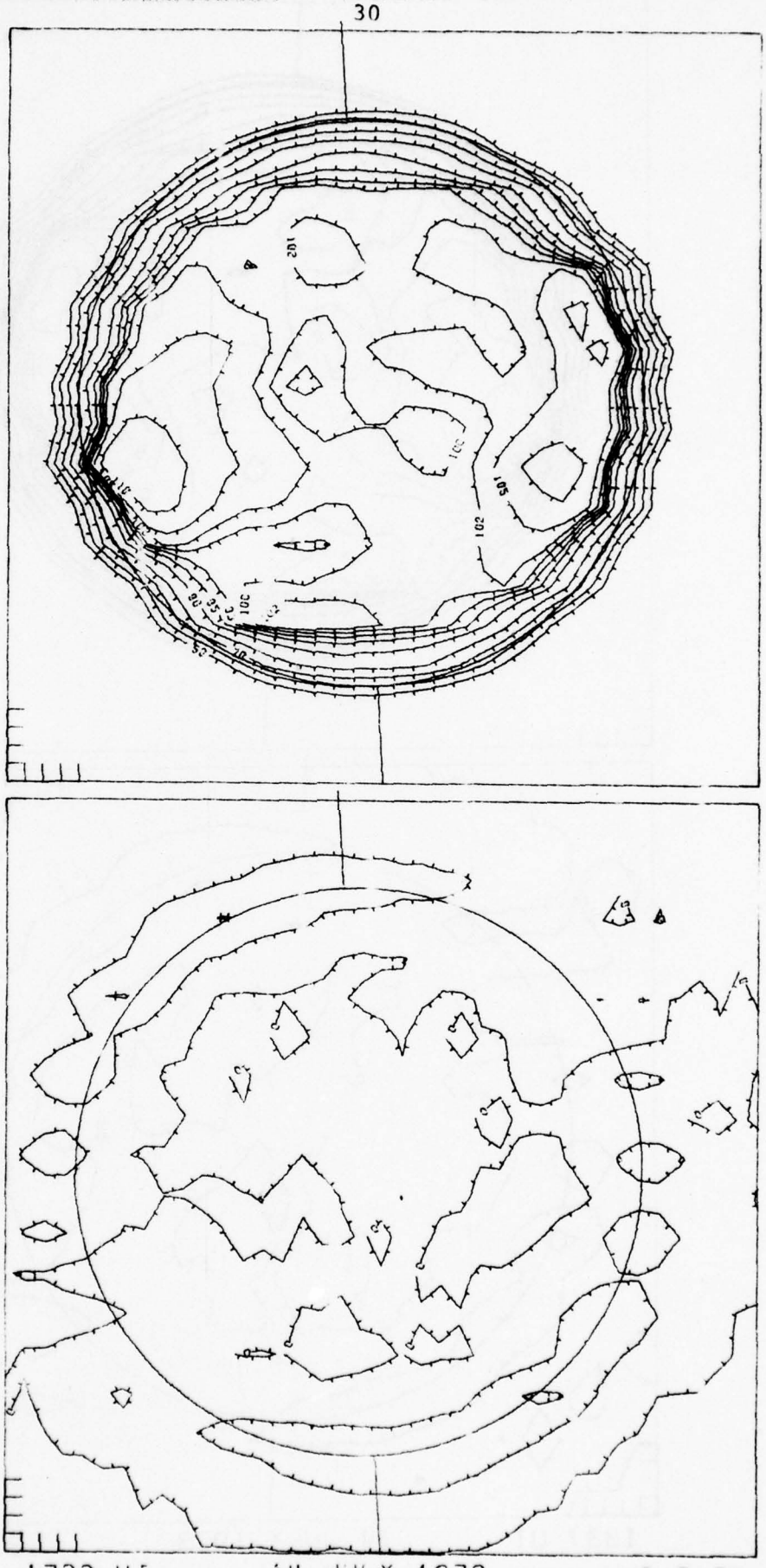

FIGURE 2.9

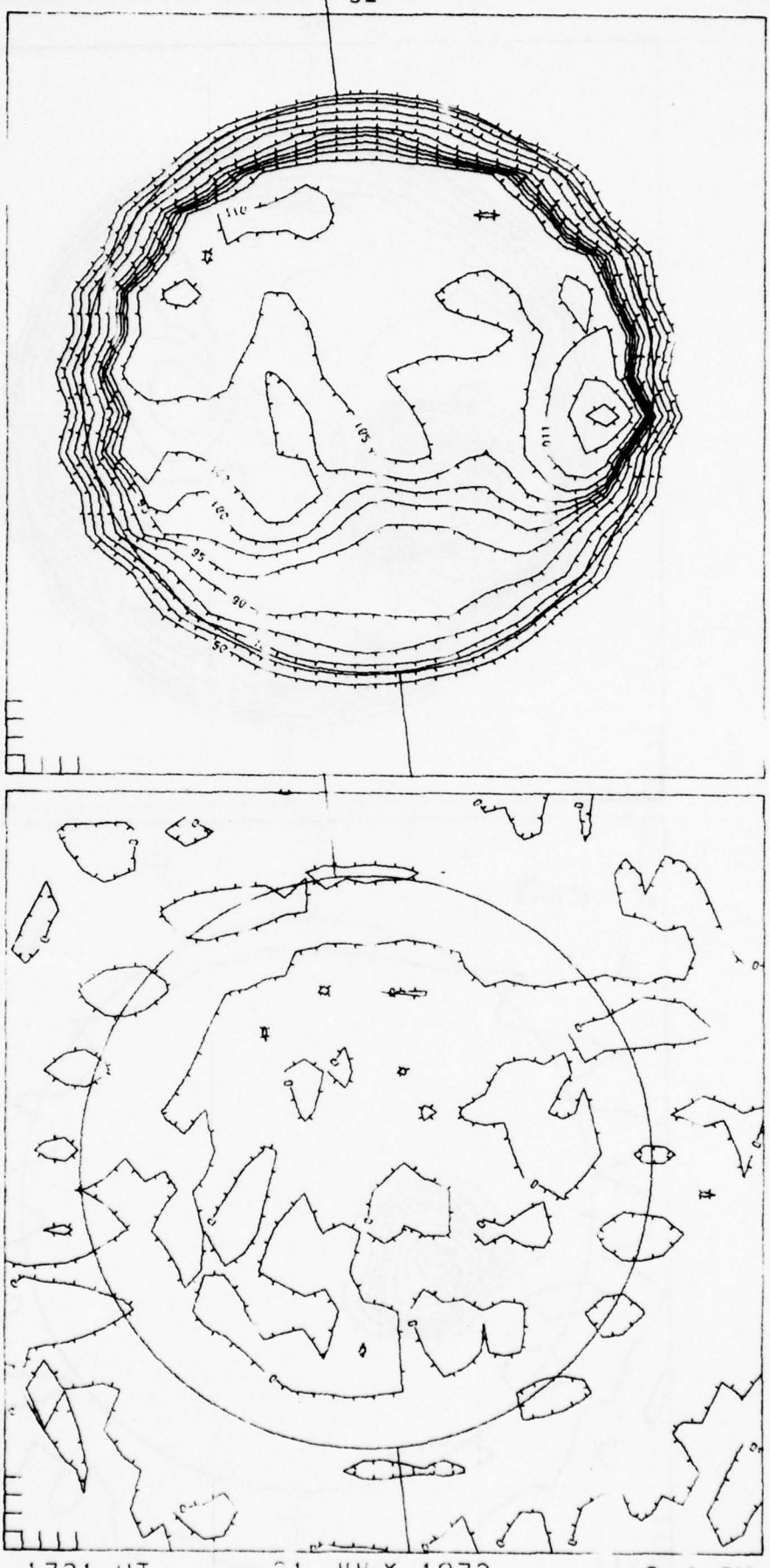

FIGURE 2.10

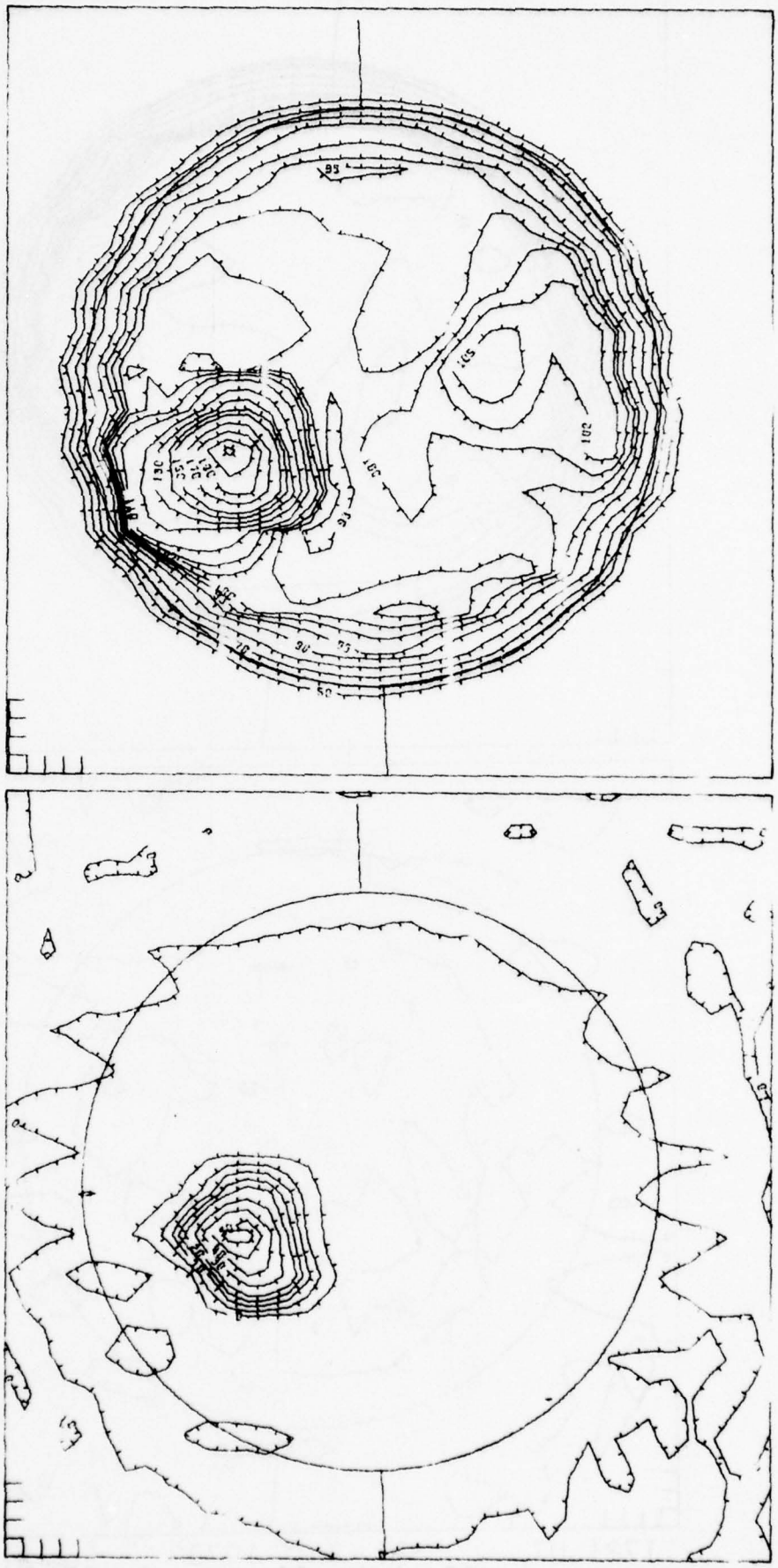

FIGURE 2.11

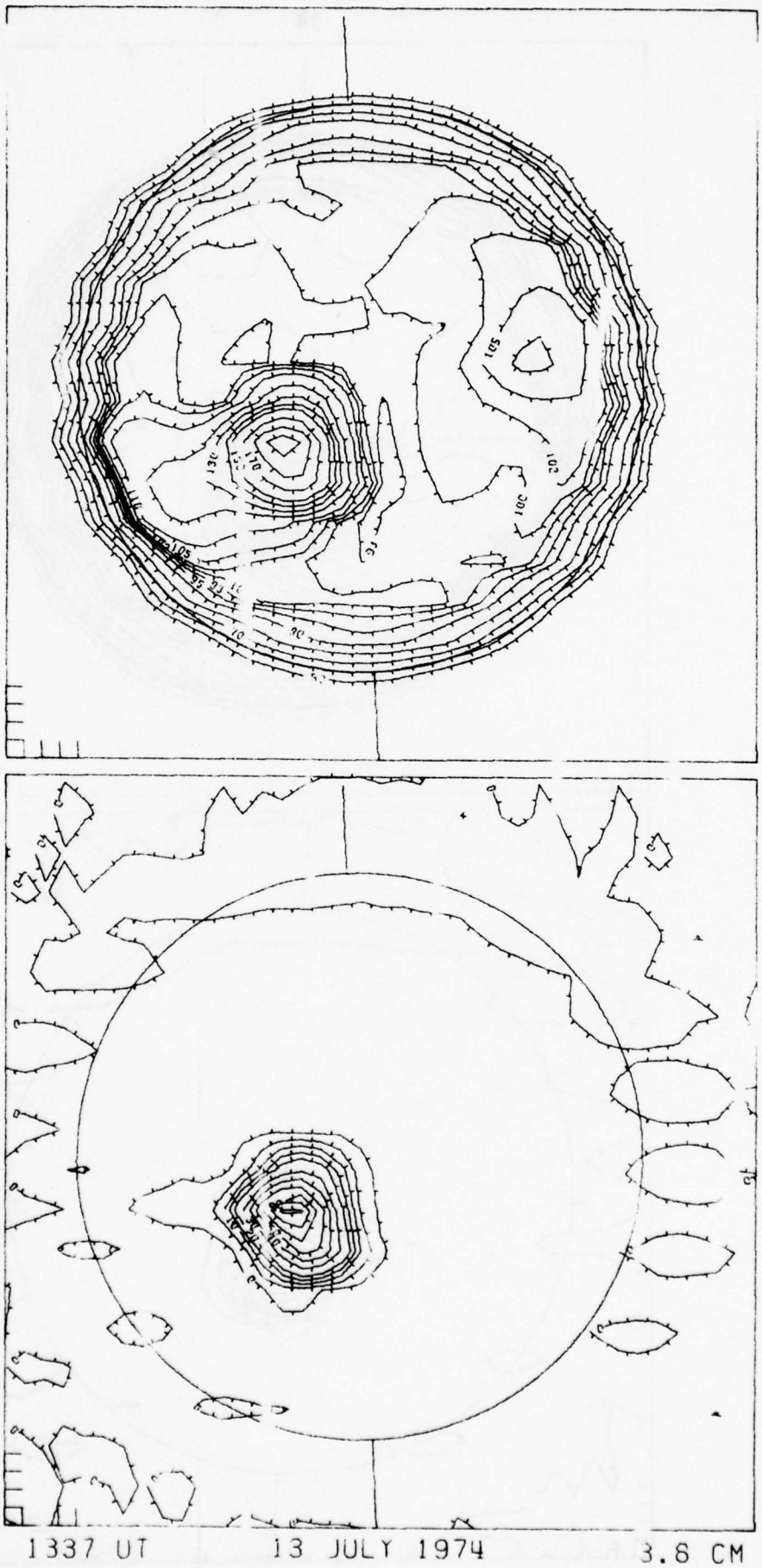

FIGURE 2.12

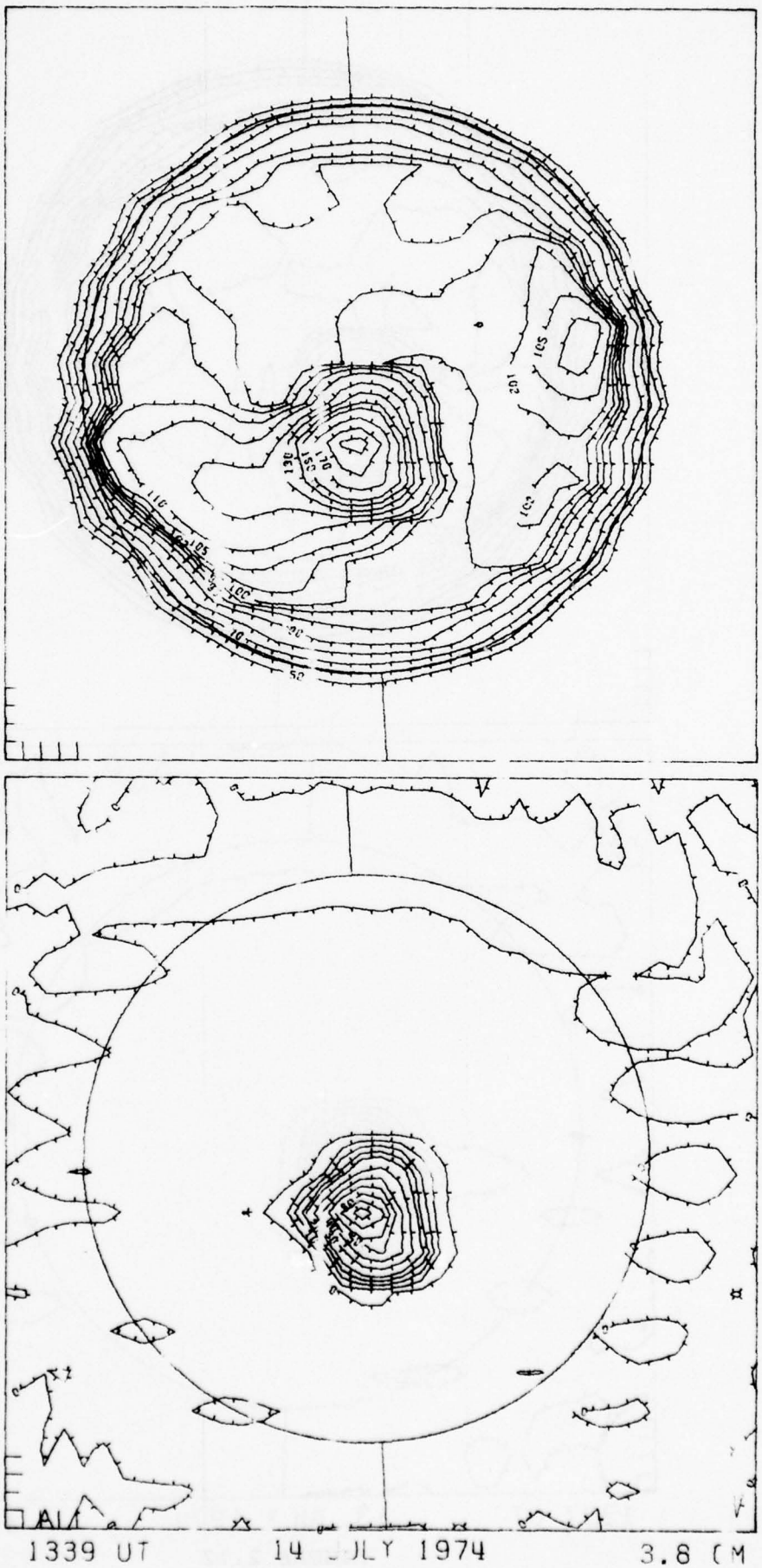

FIGURE 2.13

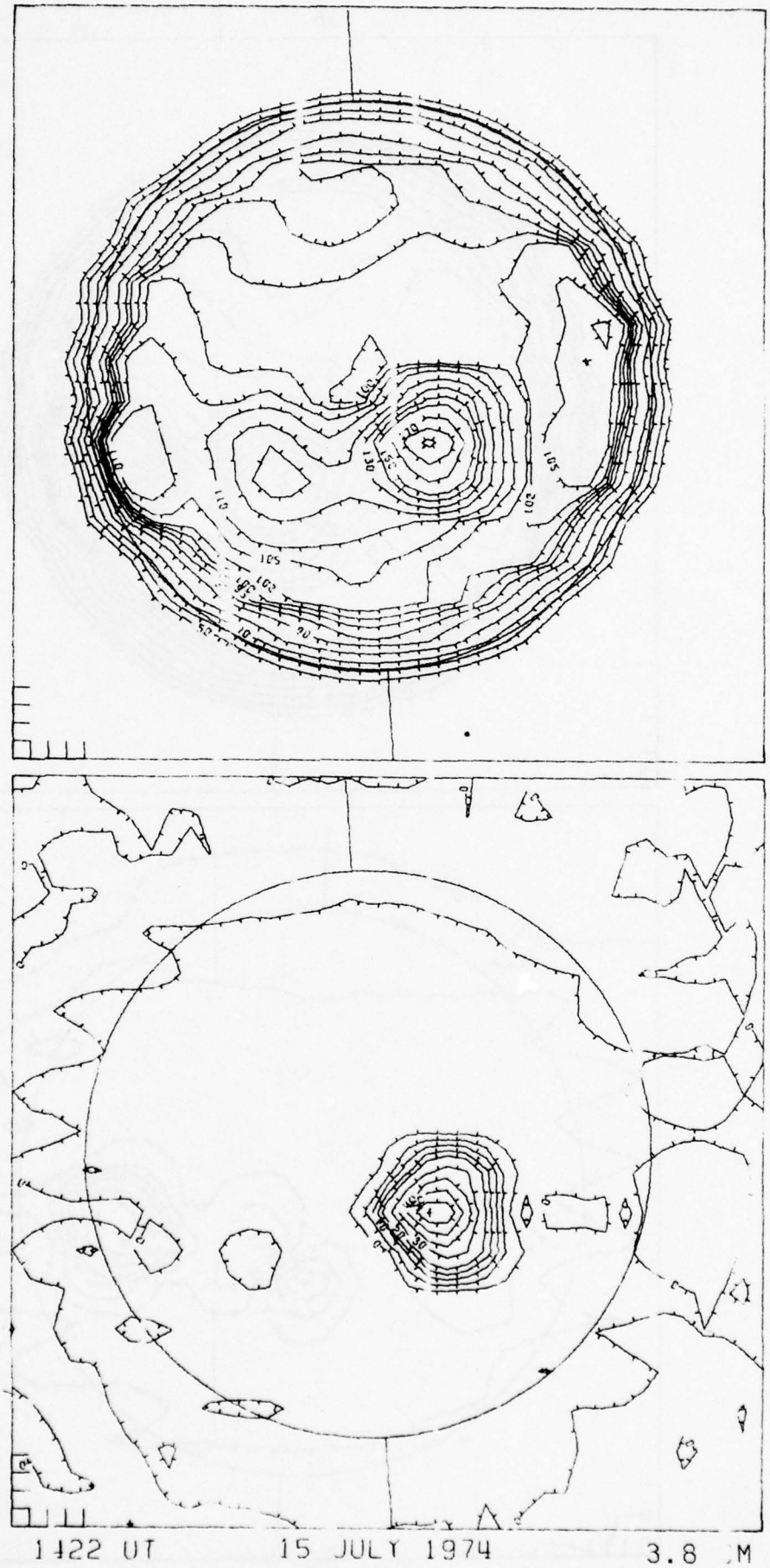

1422 UT 15 JULY 1974 3.8 M

FIGURE 2.14

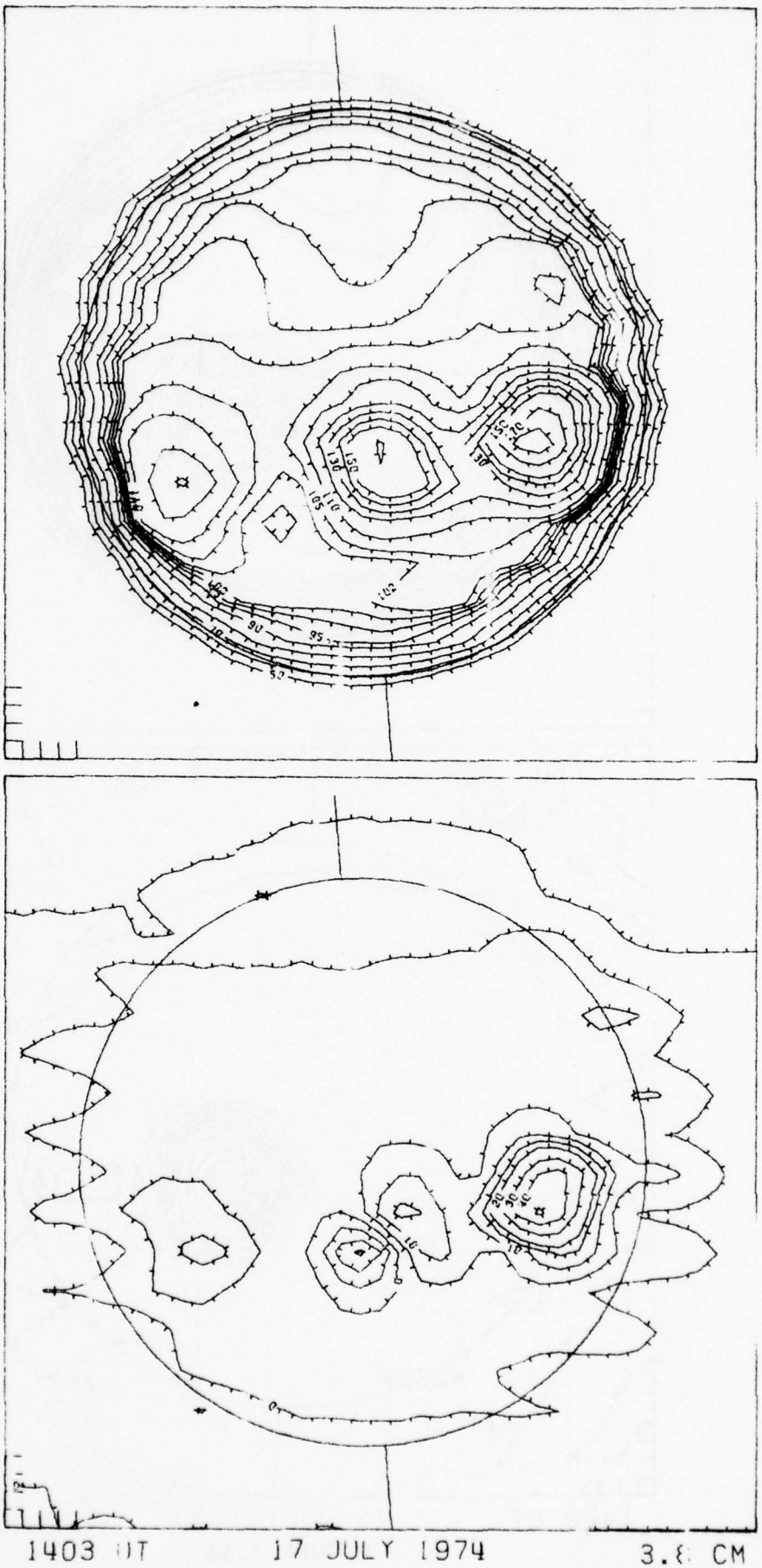

FIGURE 2.15

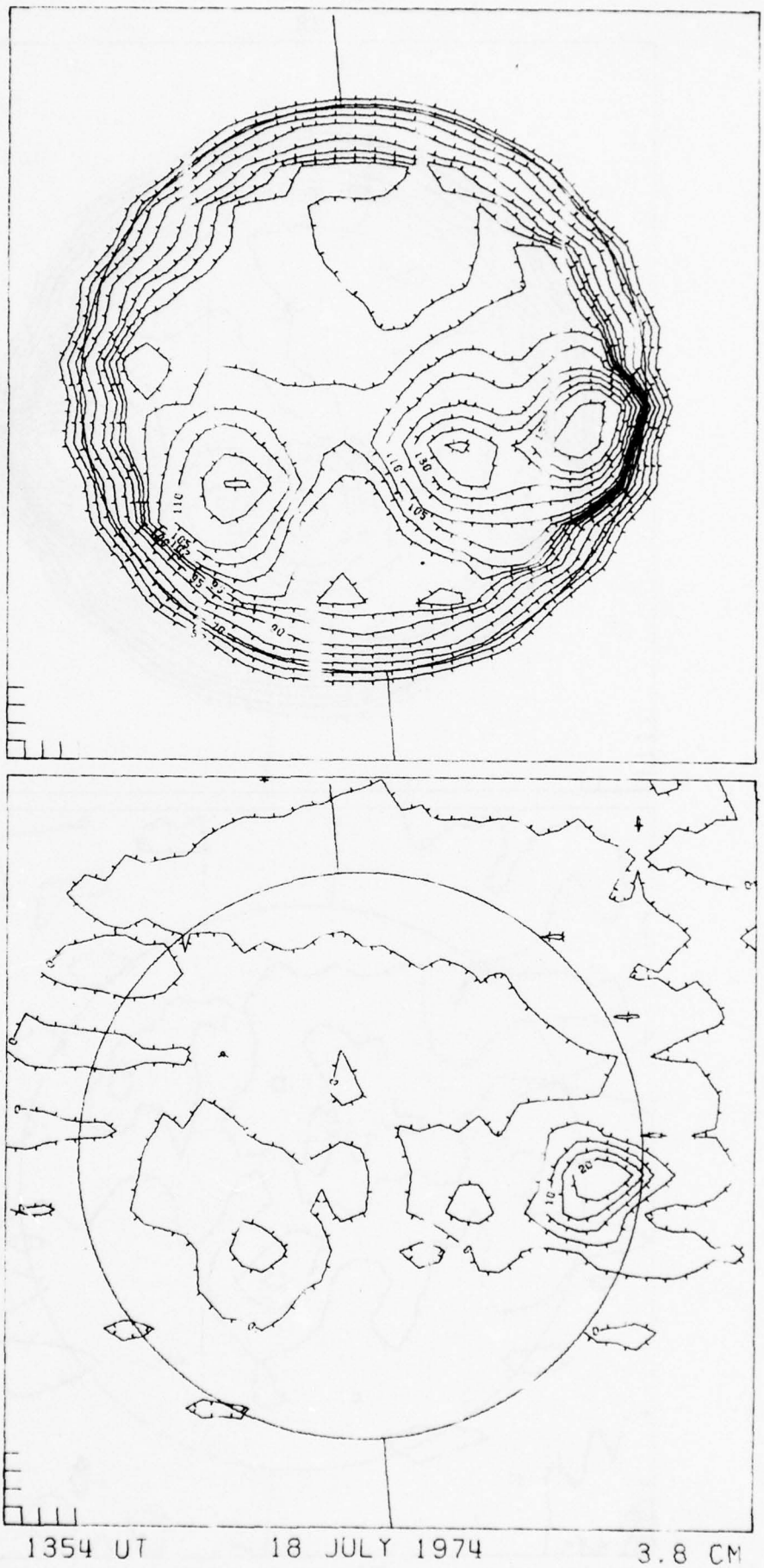

FIGURE 2.16

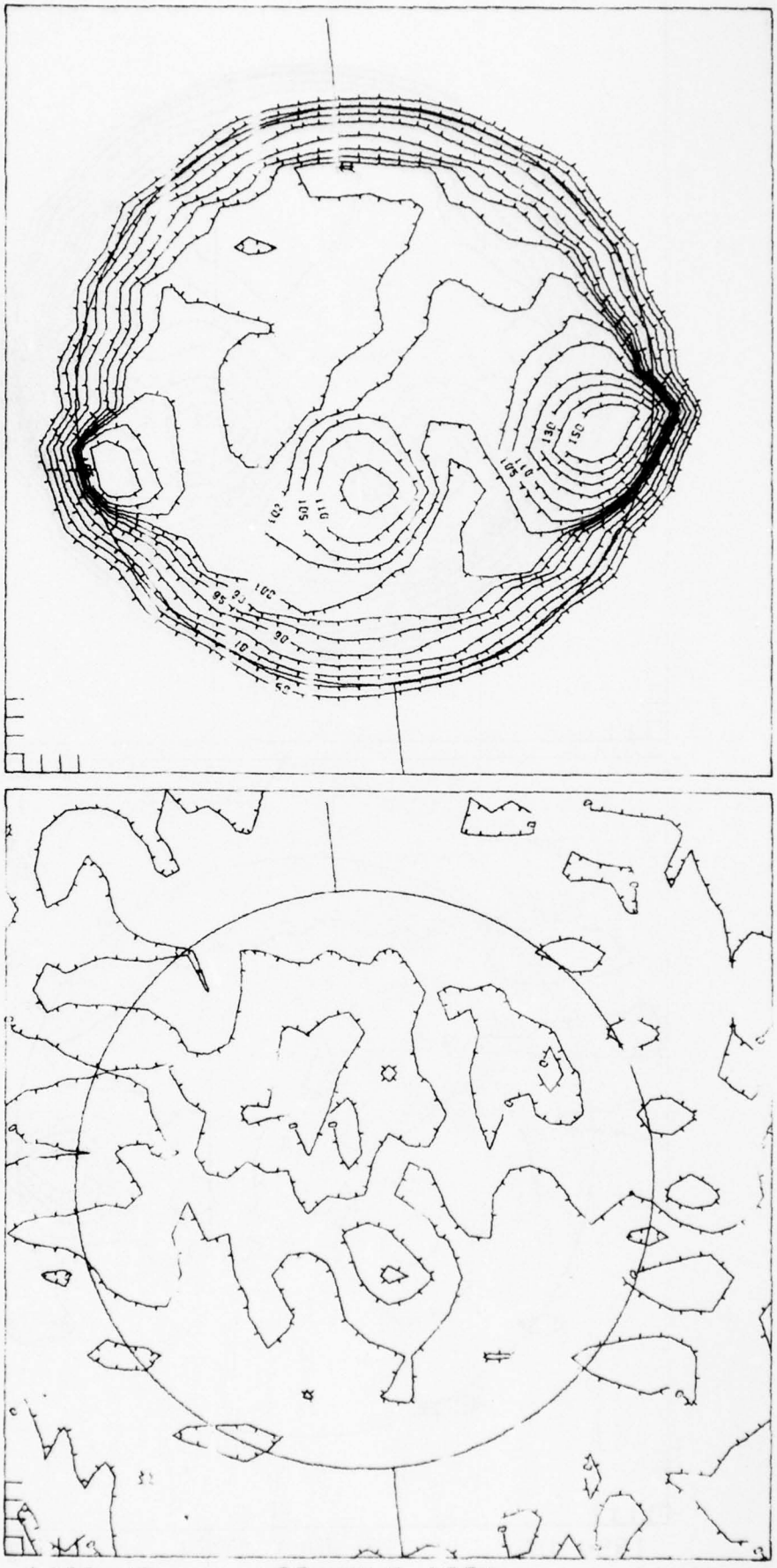

FIGURE 2.17

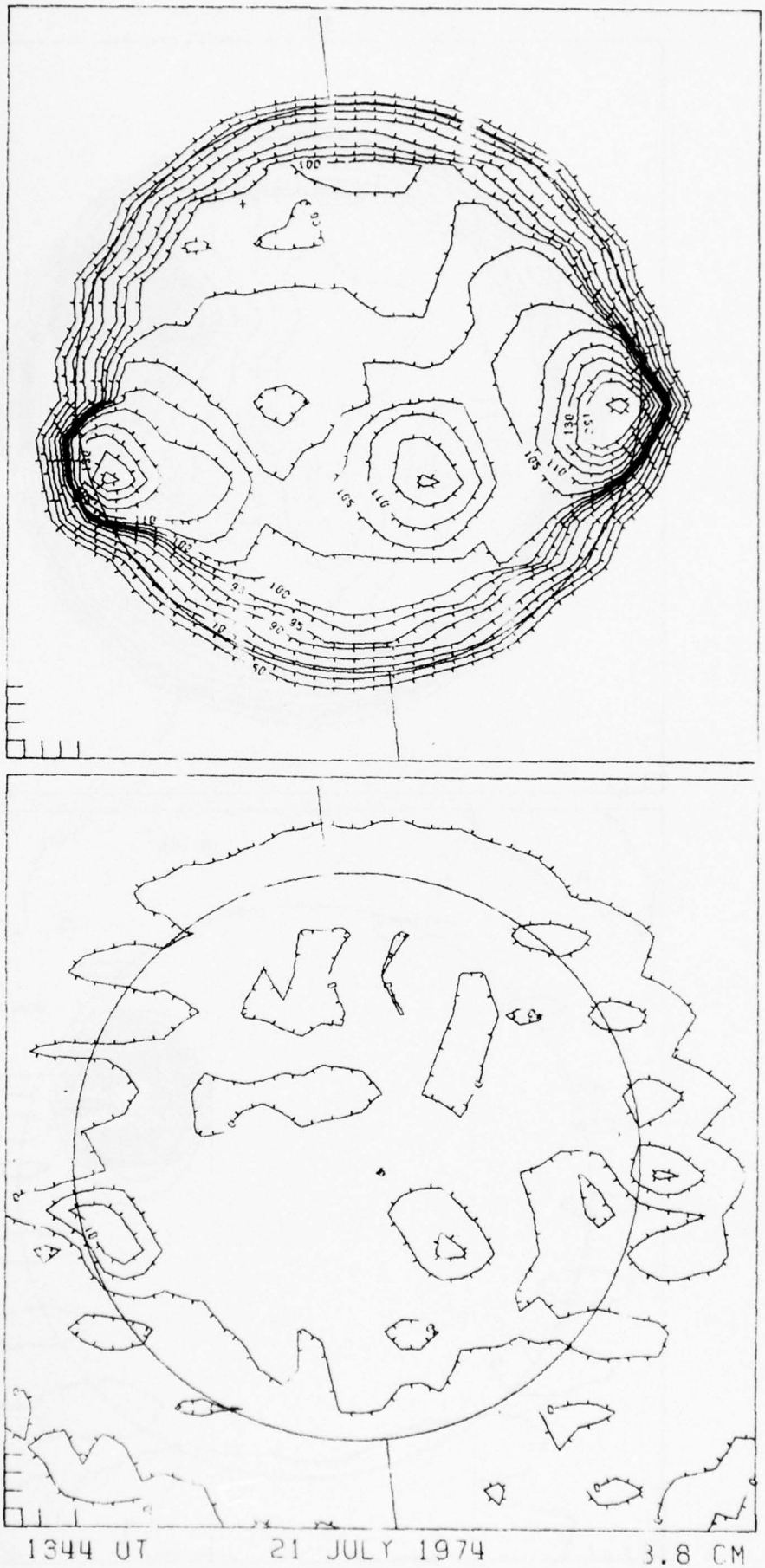

FIGURI 2.18

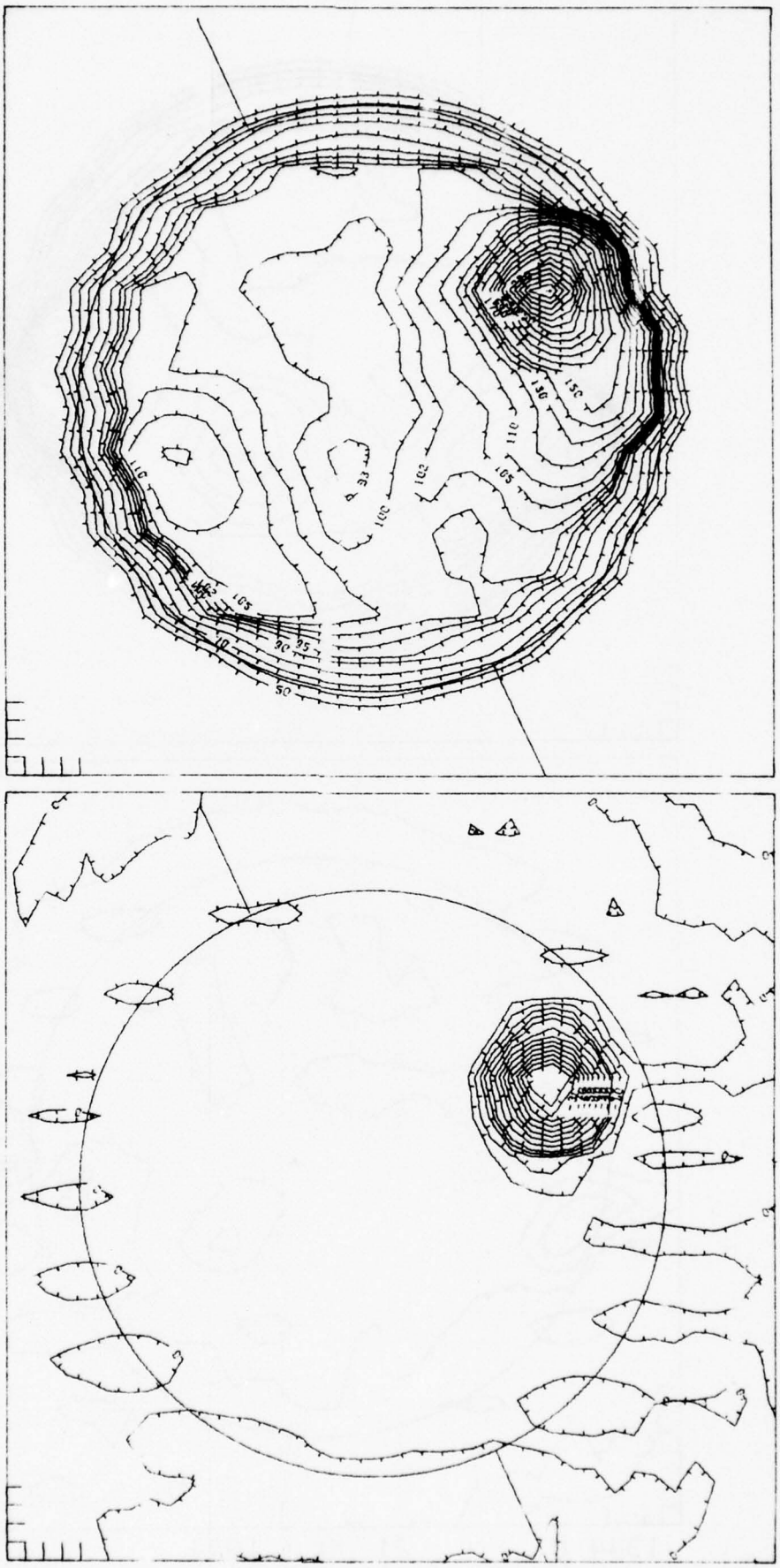

FIGURE 2.19

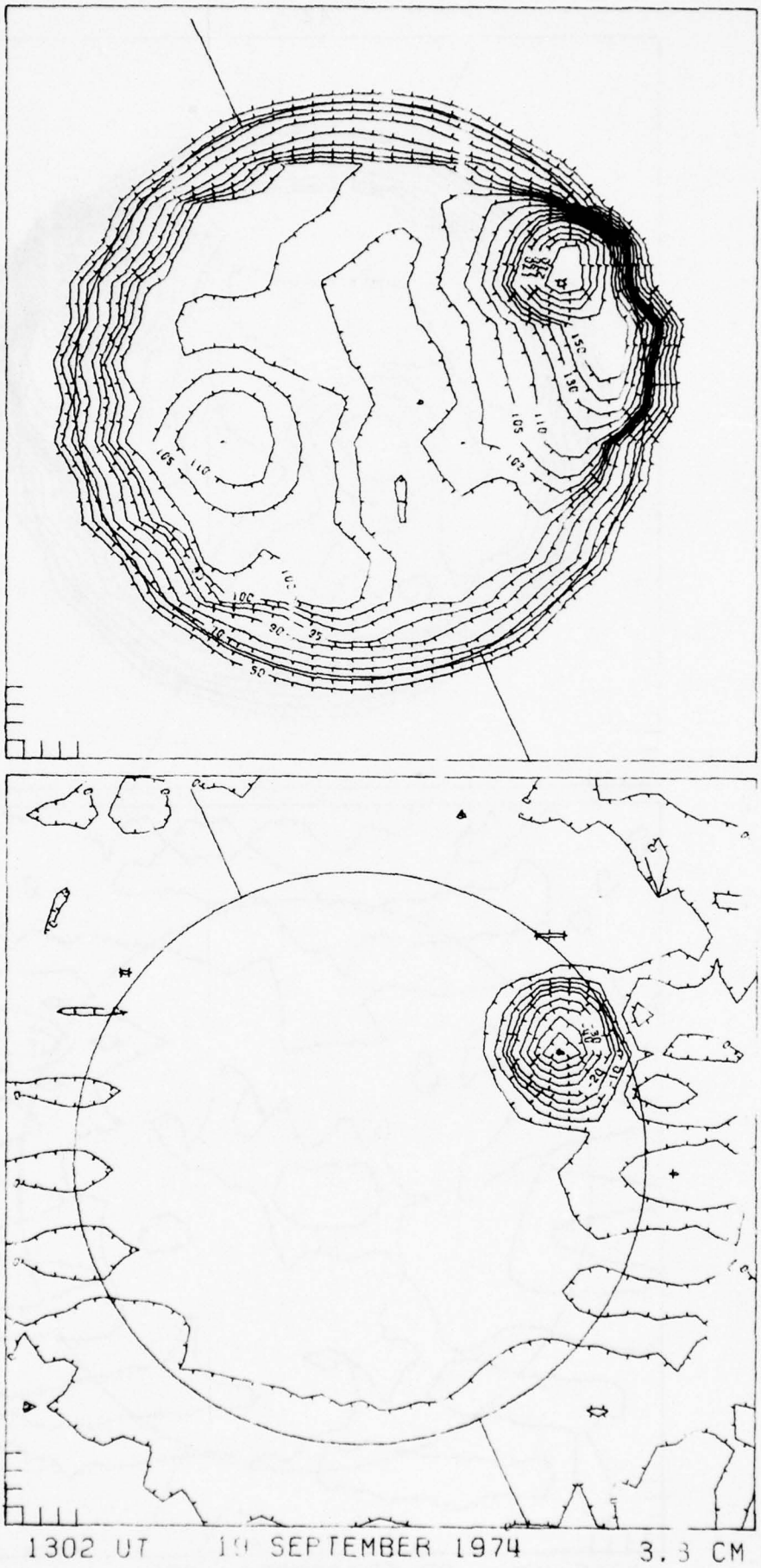

FIGURE 2.2)

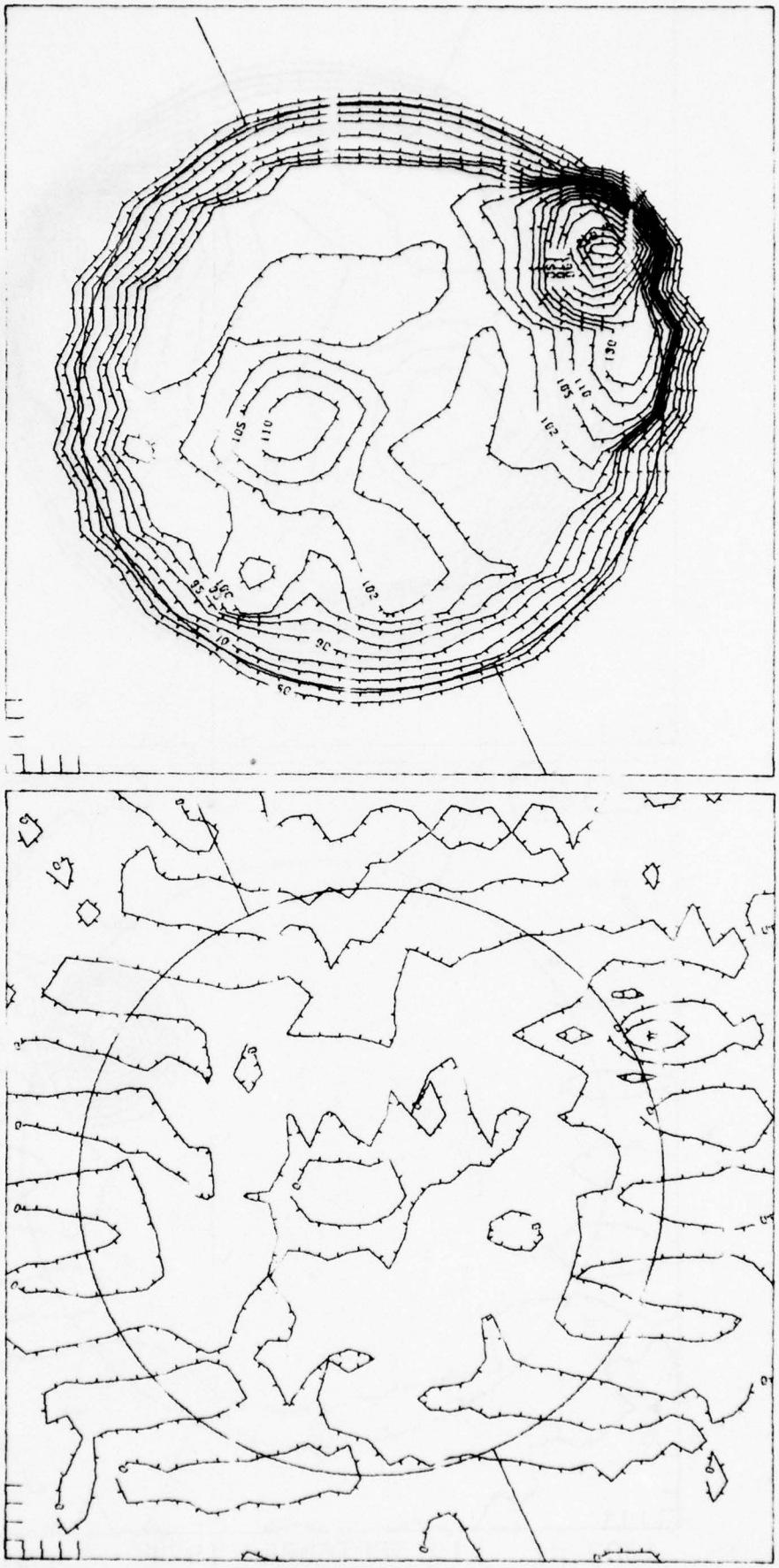

FIGURE 2.21

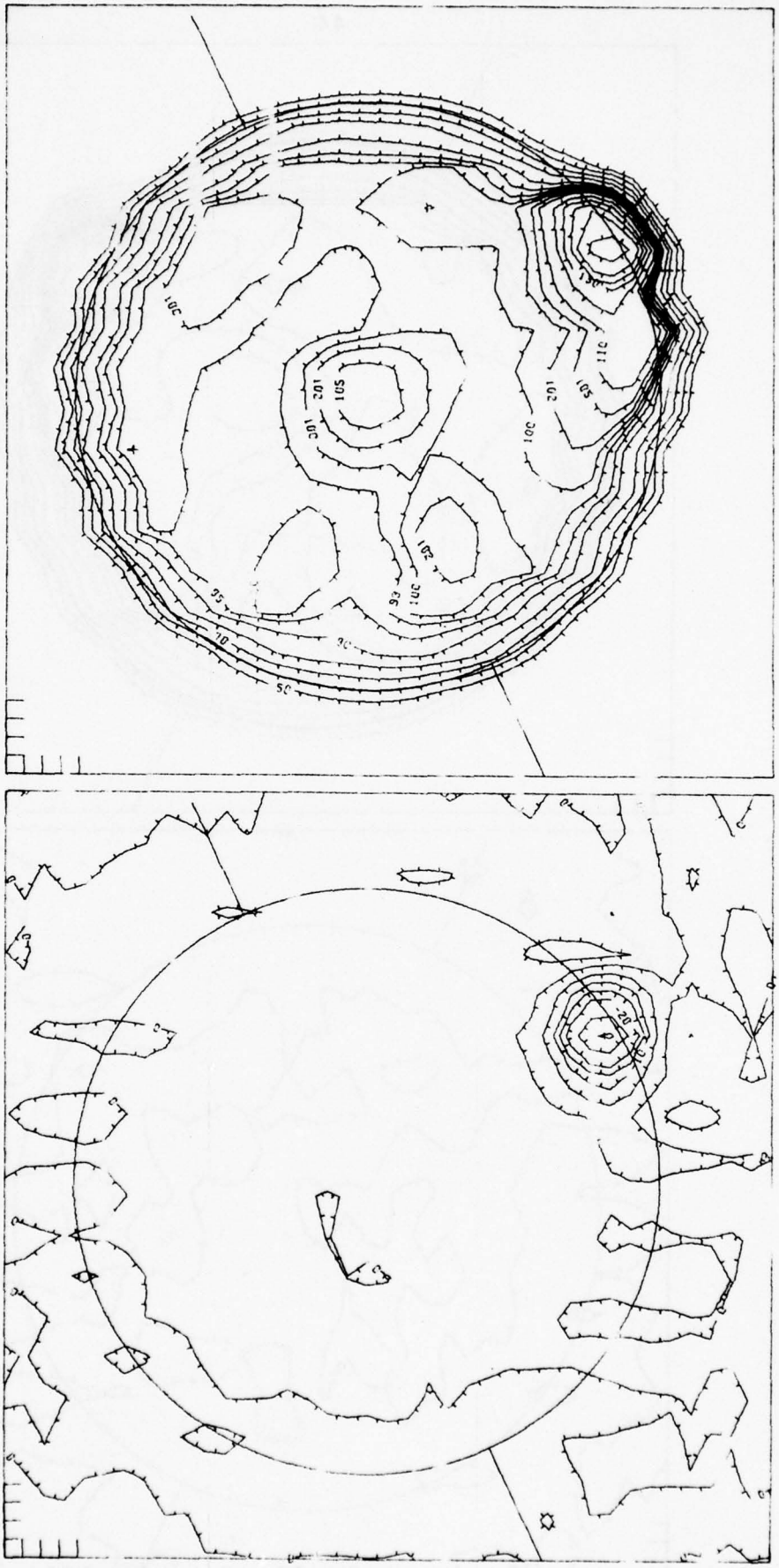

FIGURE 2.2

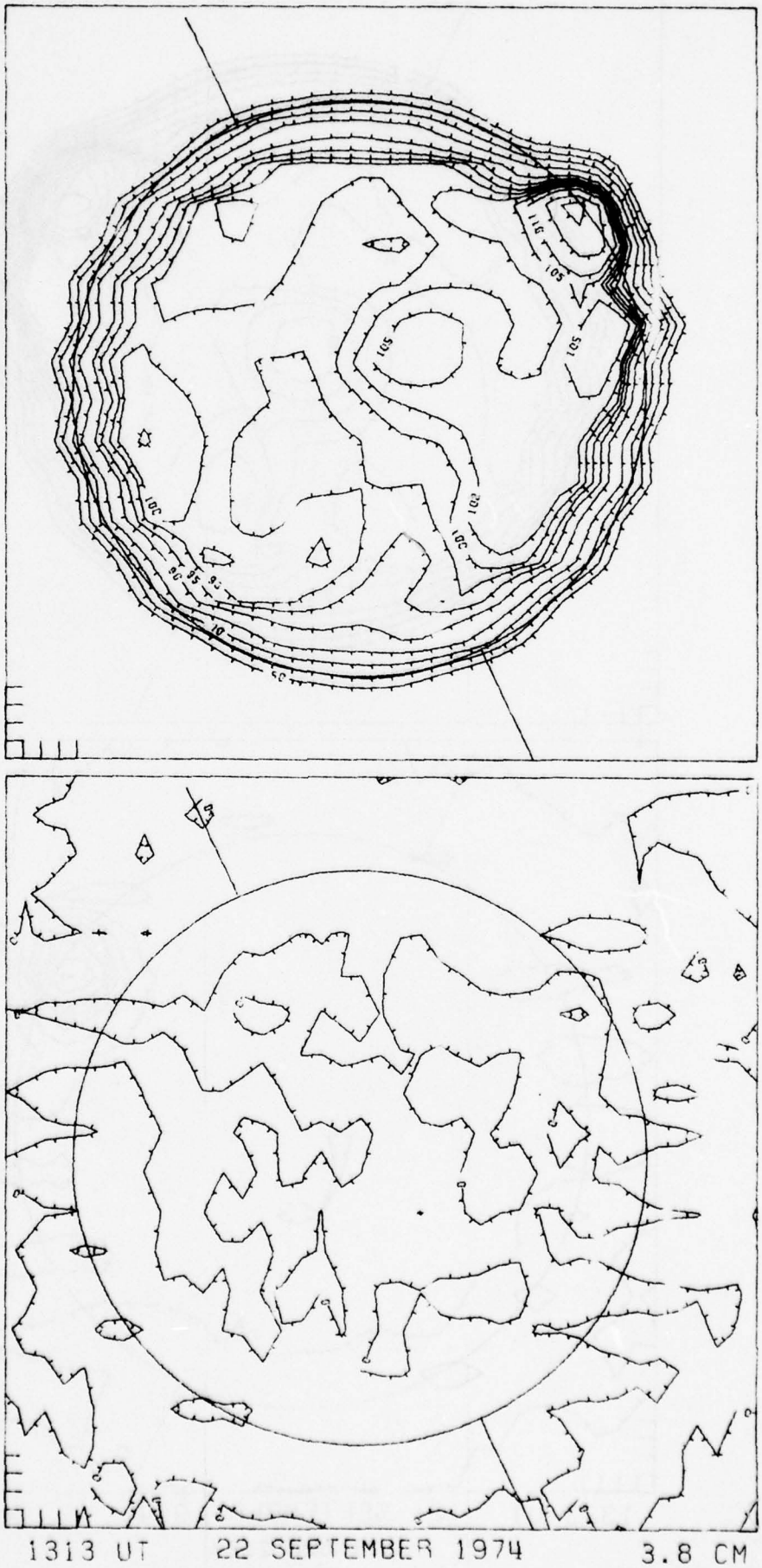

FIGURE 2.13

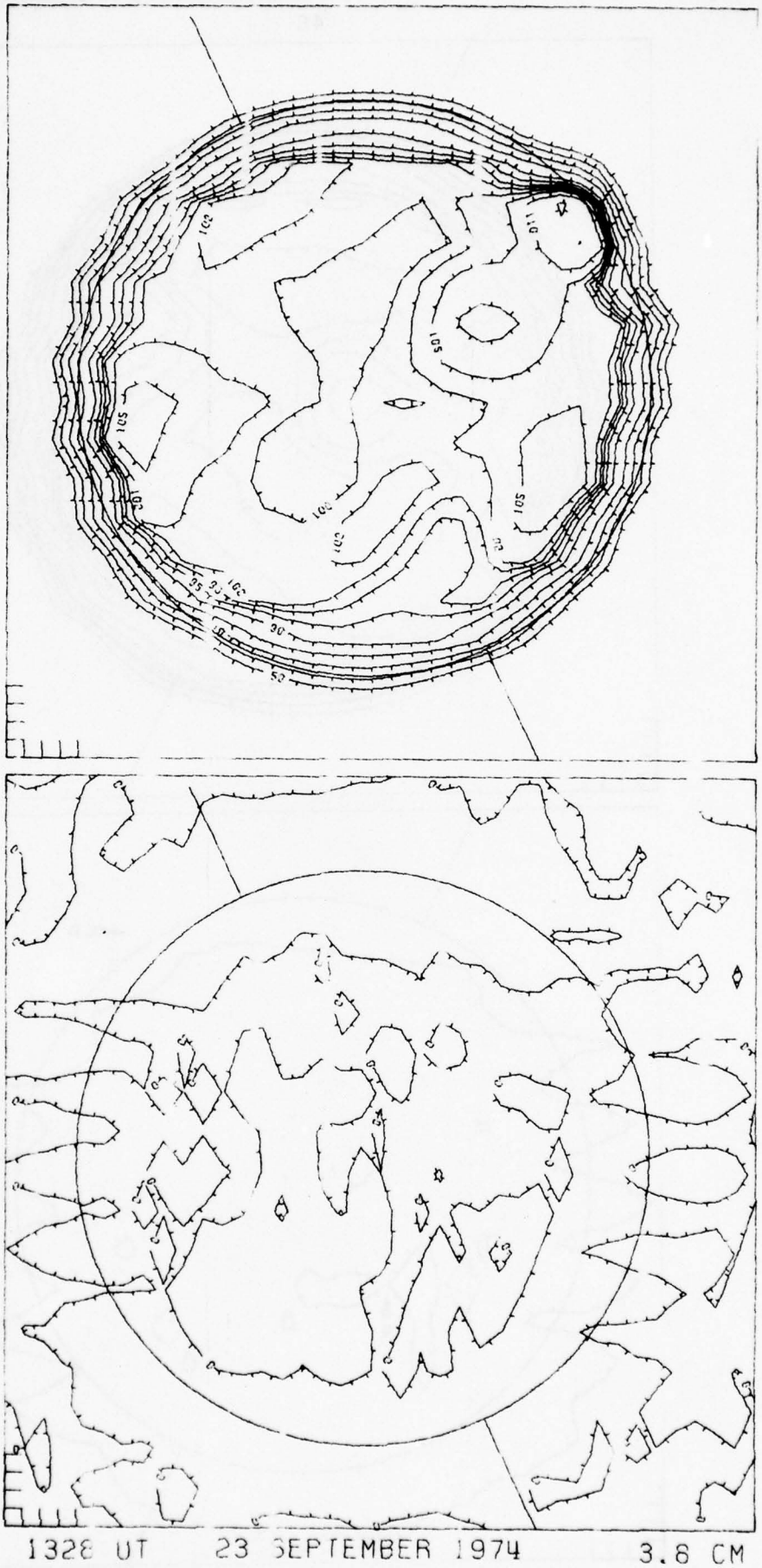

FIGURE 2.24

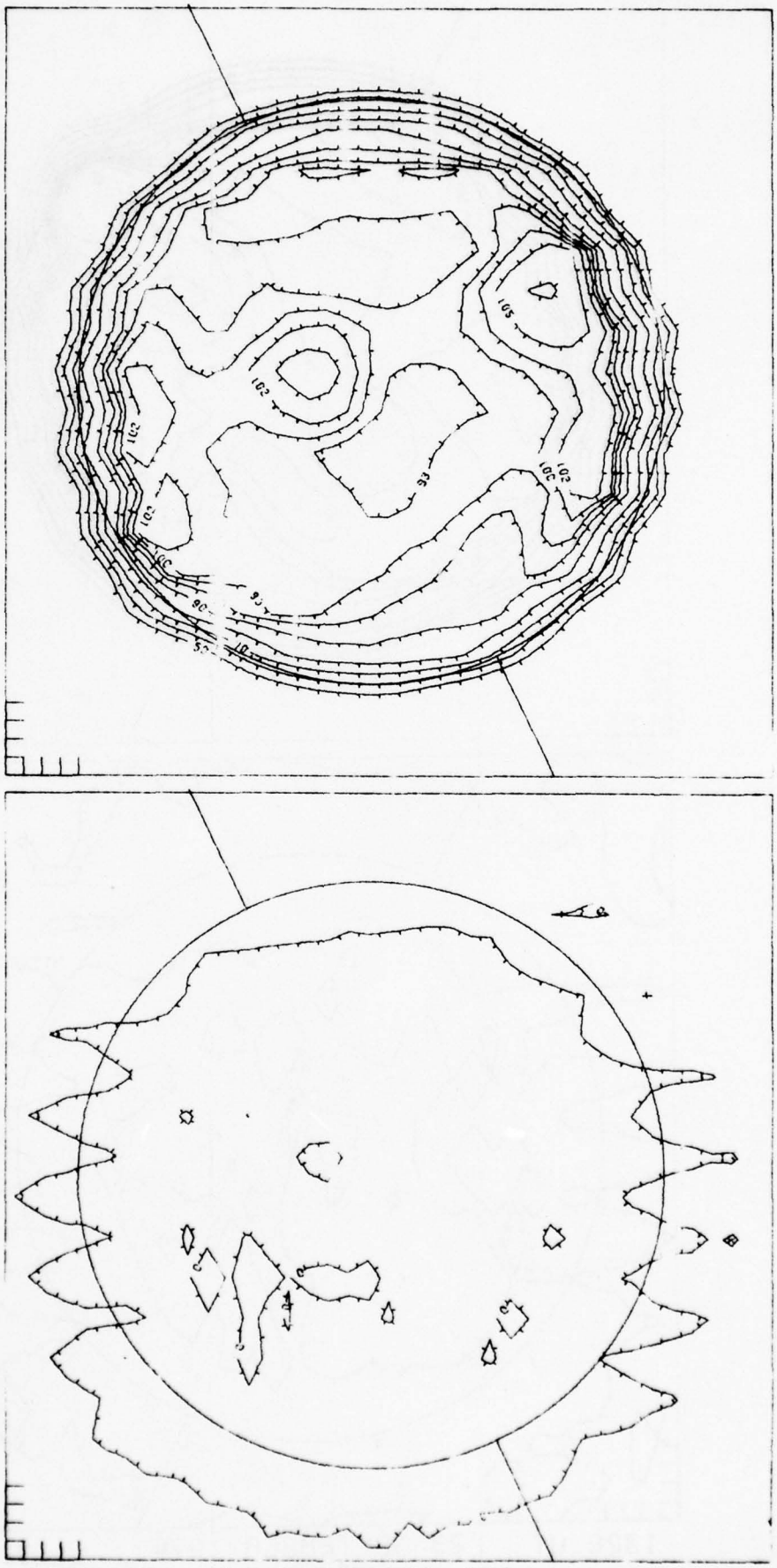

FIGURE 2.25

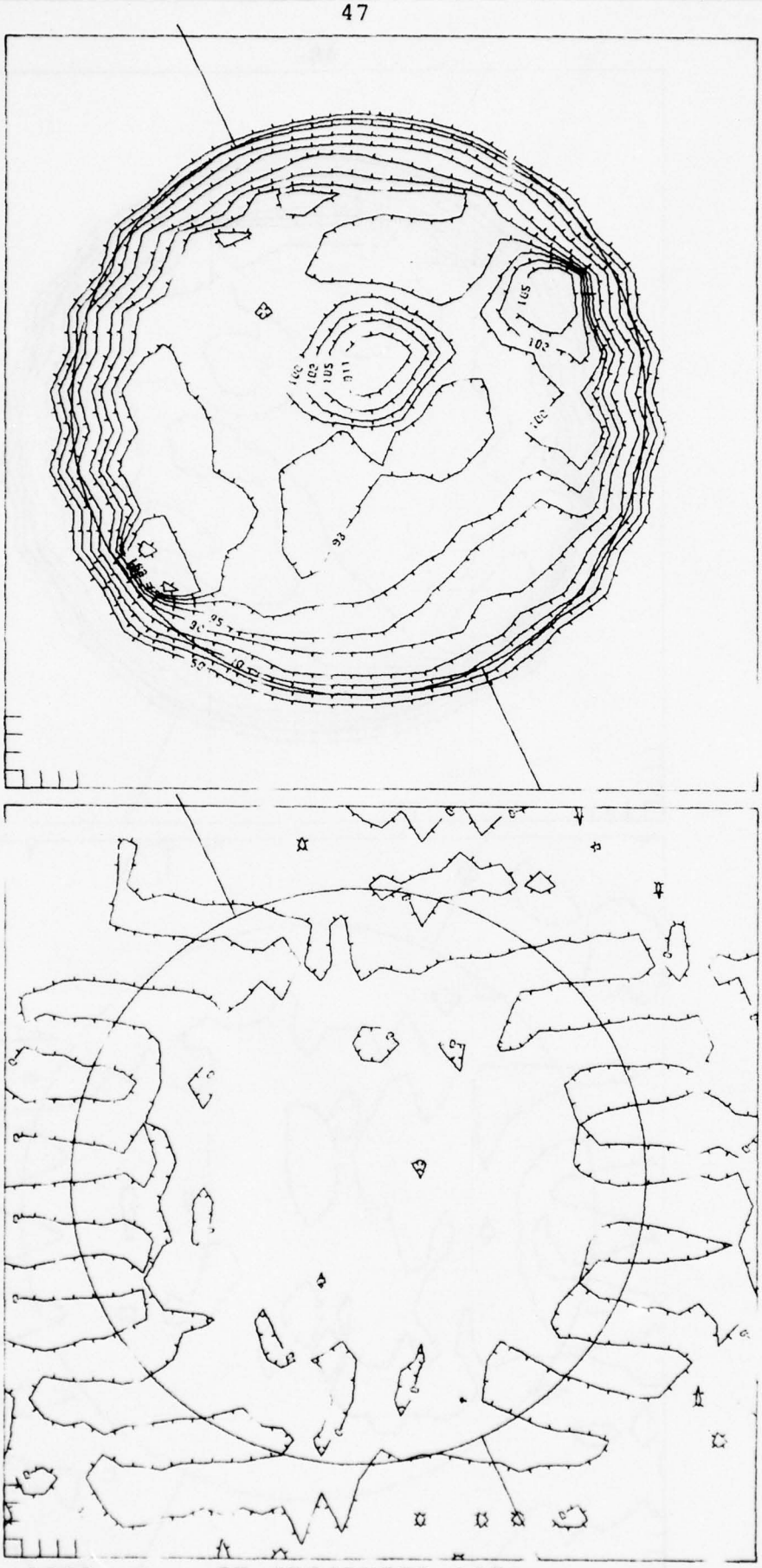

FIGURE 2.26

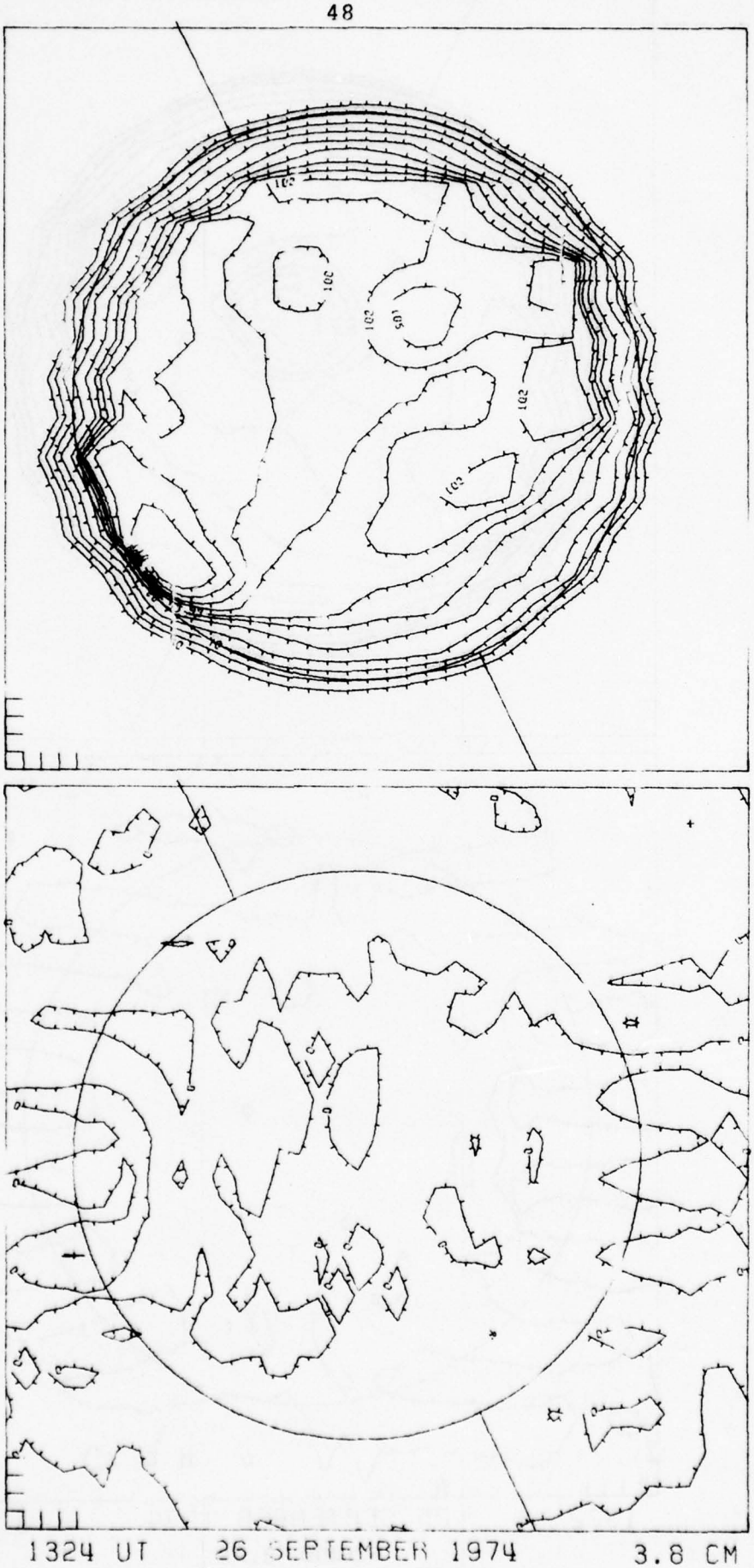

FIGURE 2.27

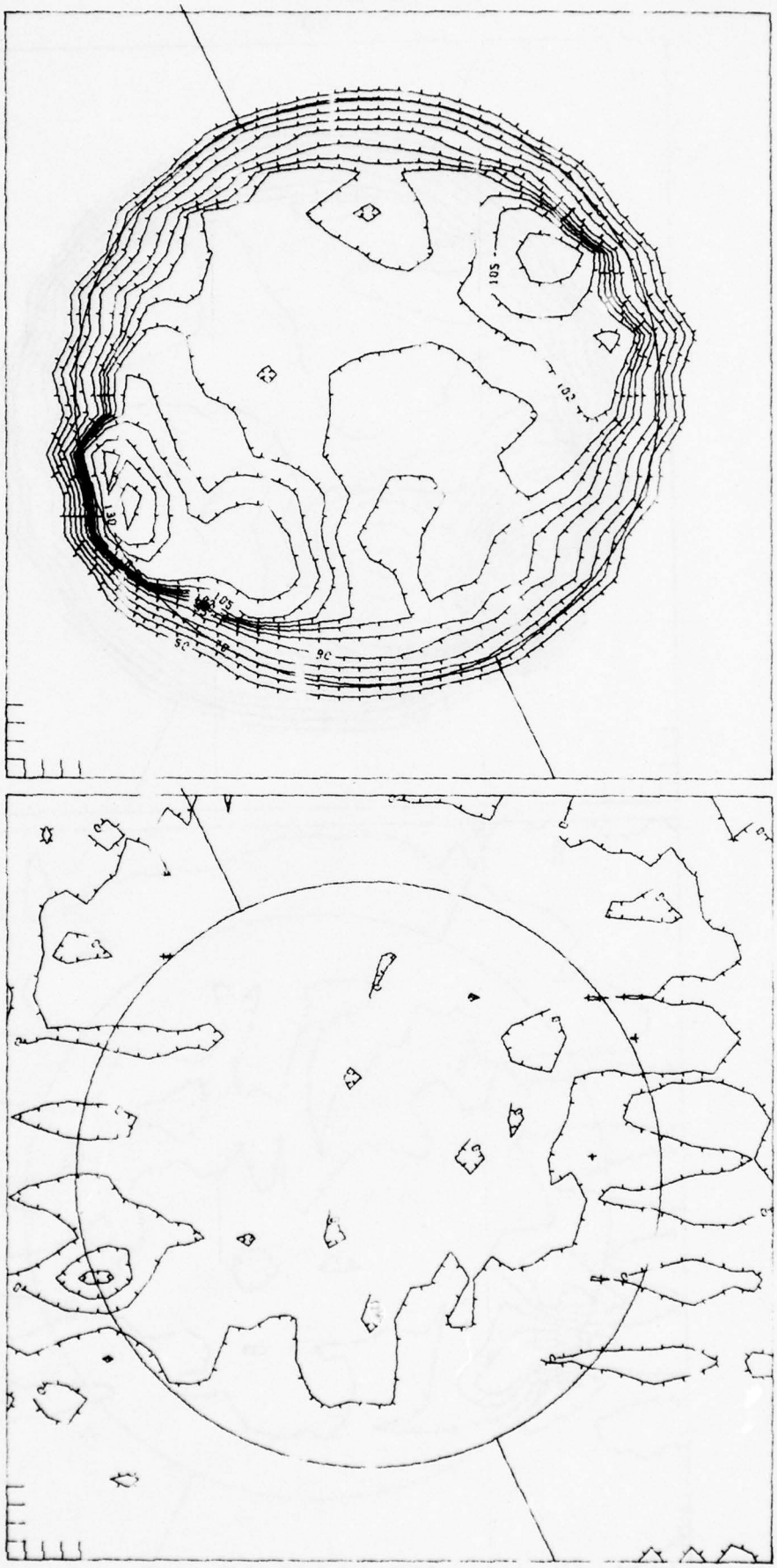

FIGURE 2.28

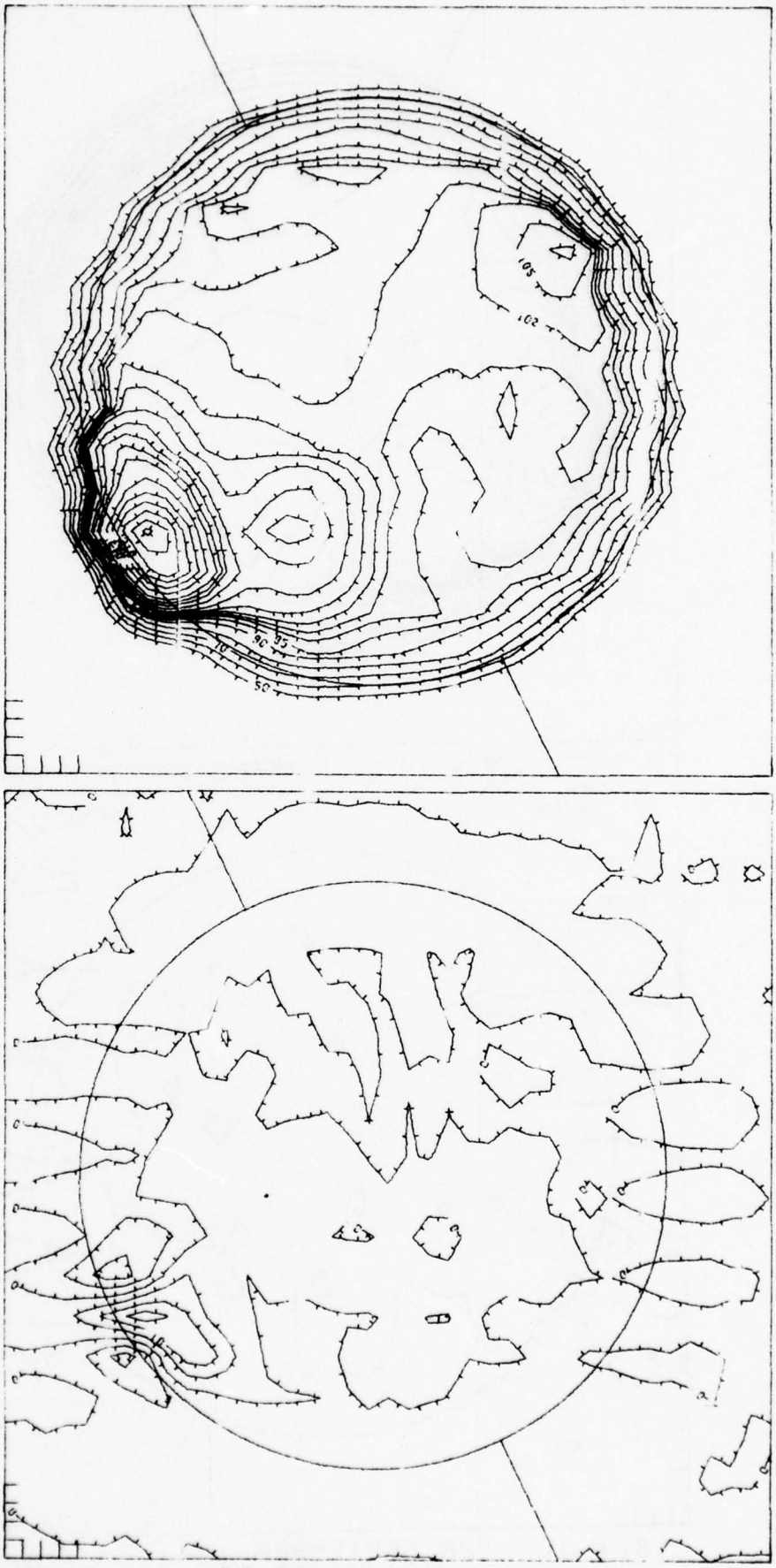

FIGURE 2.29

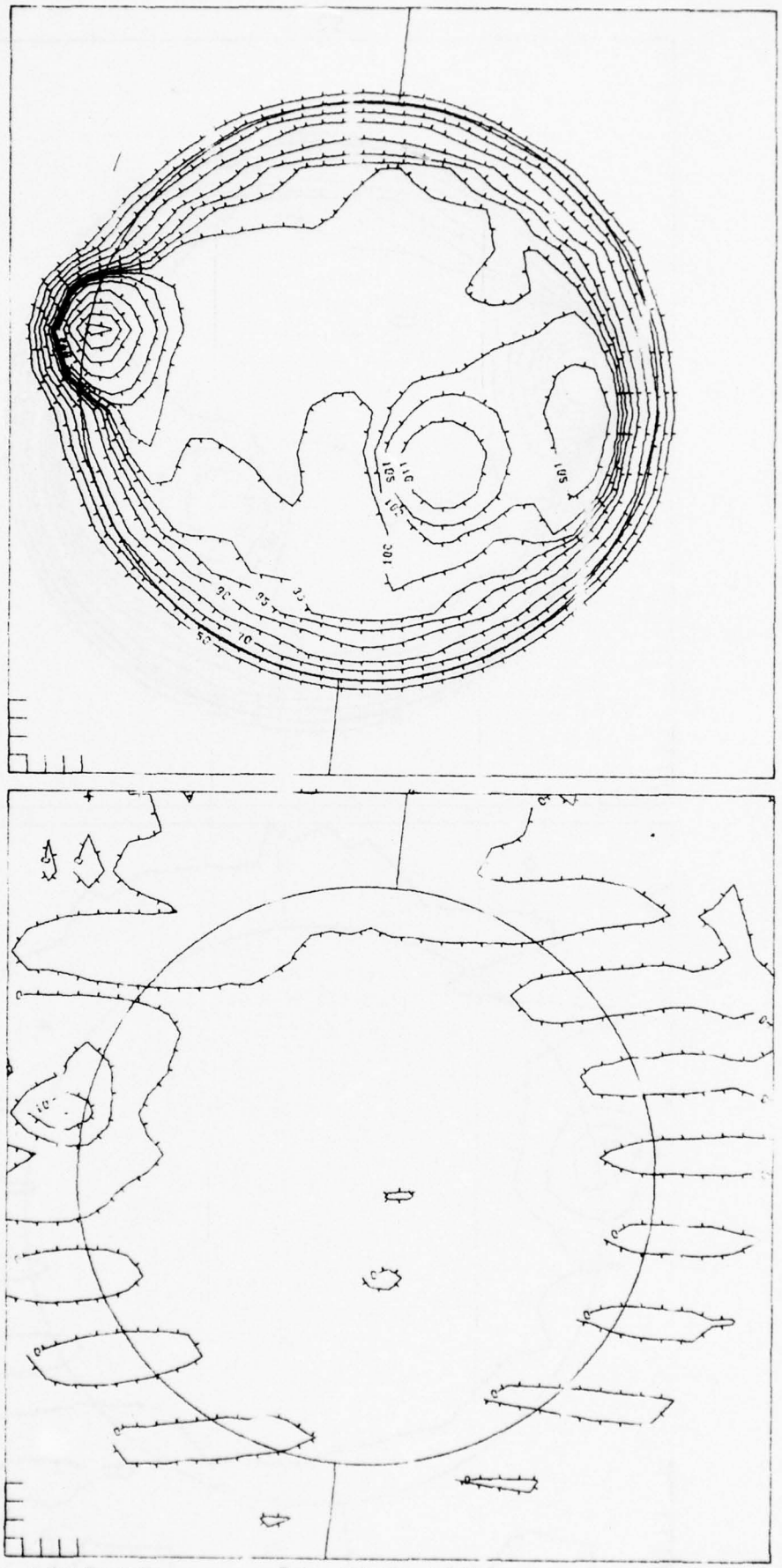

FIGURE 2.30

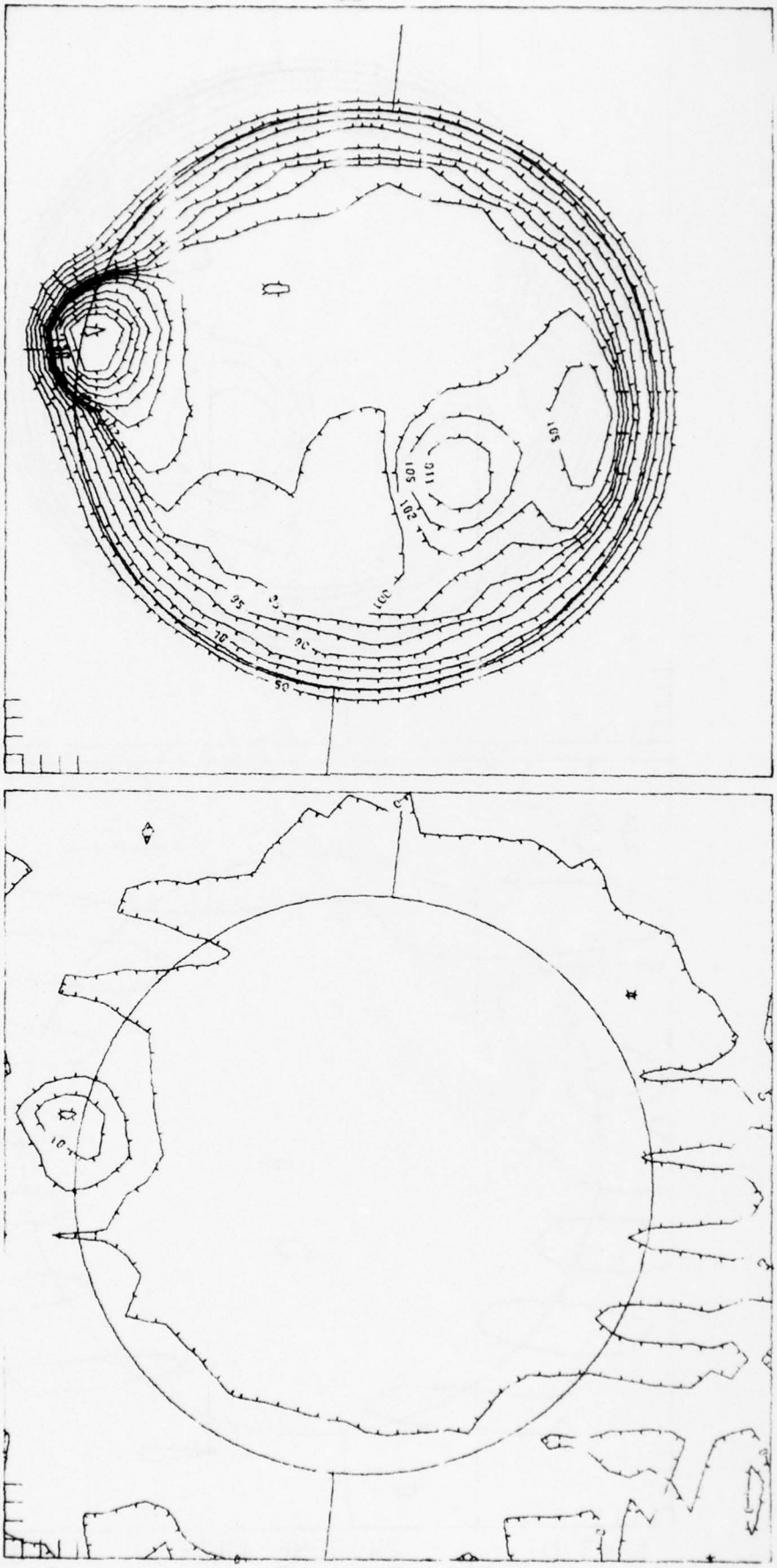

FIGURE 2.31

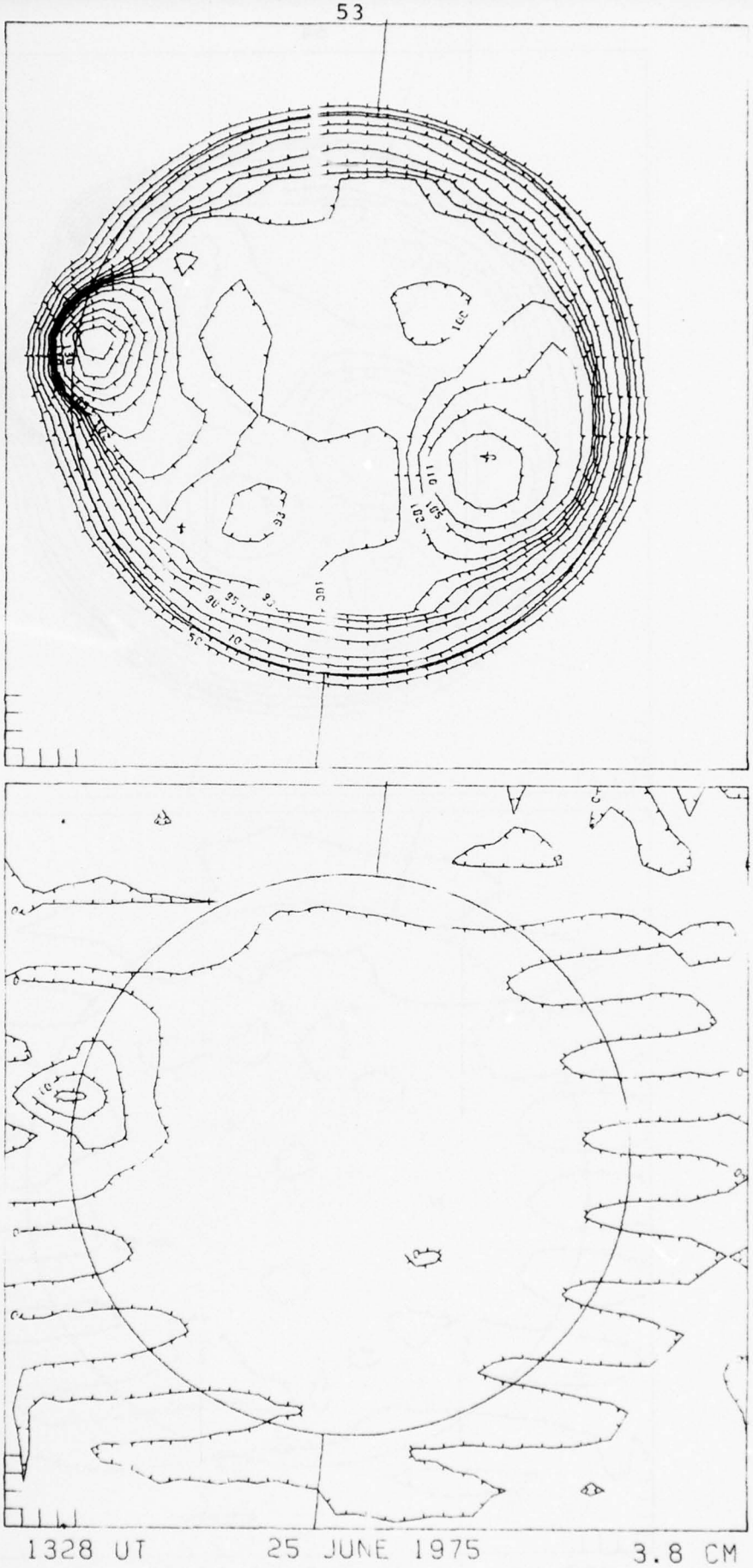

FIGURE 2.32

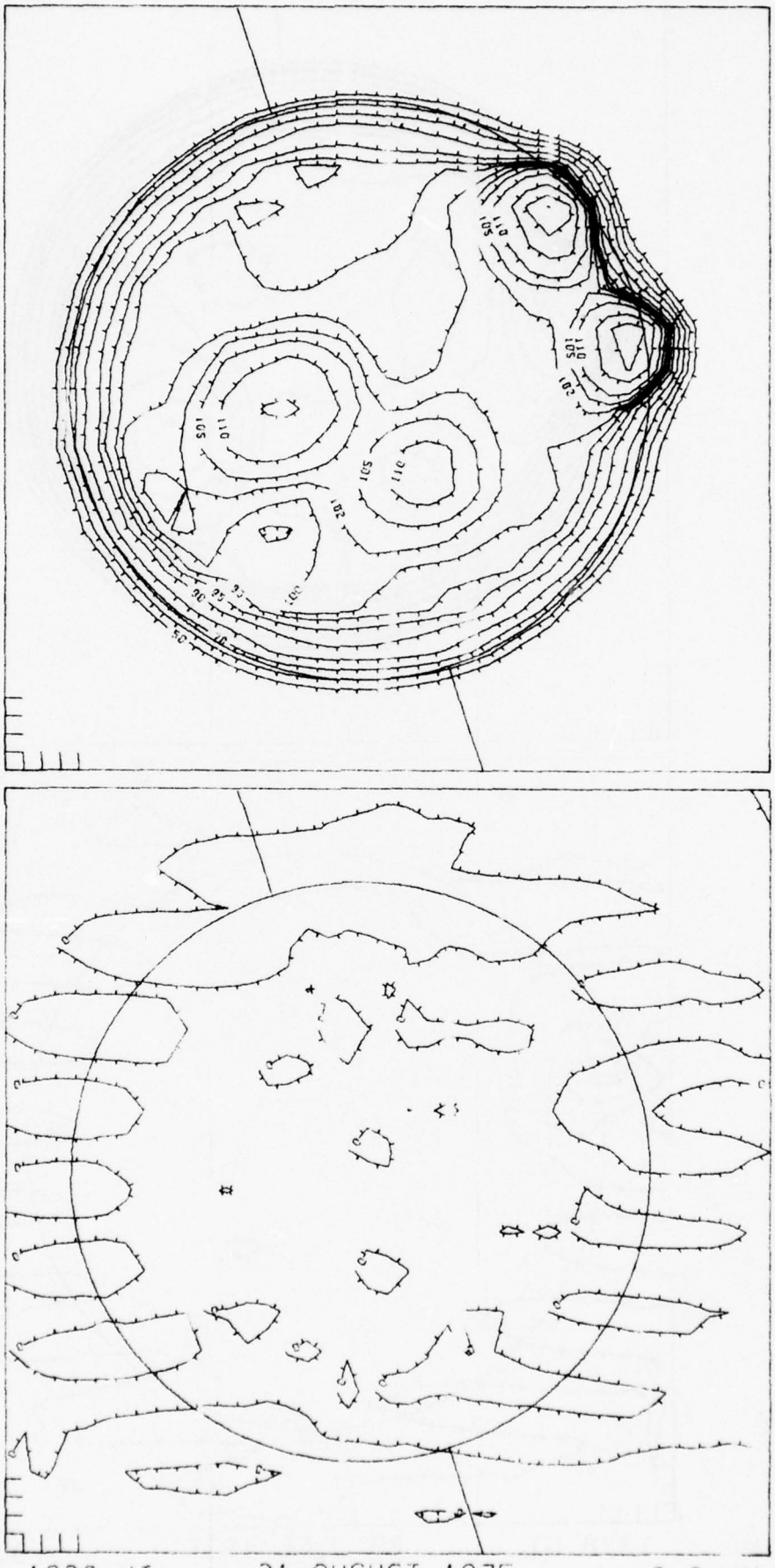

FIGURE 2.33

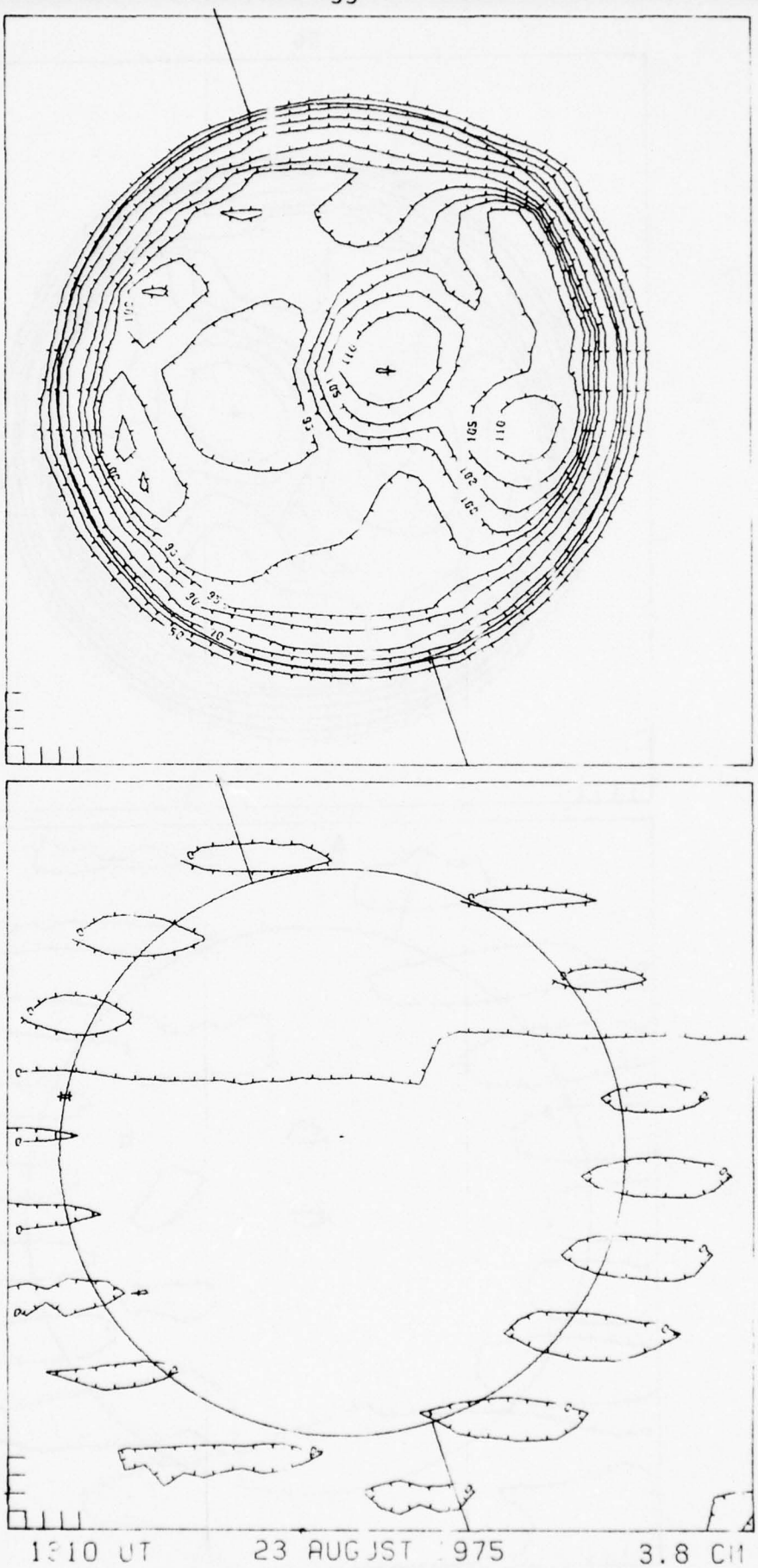

FIGURE 2.34

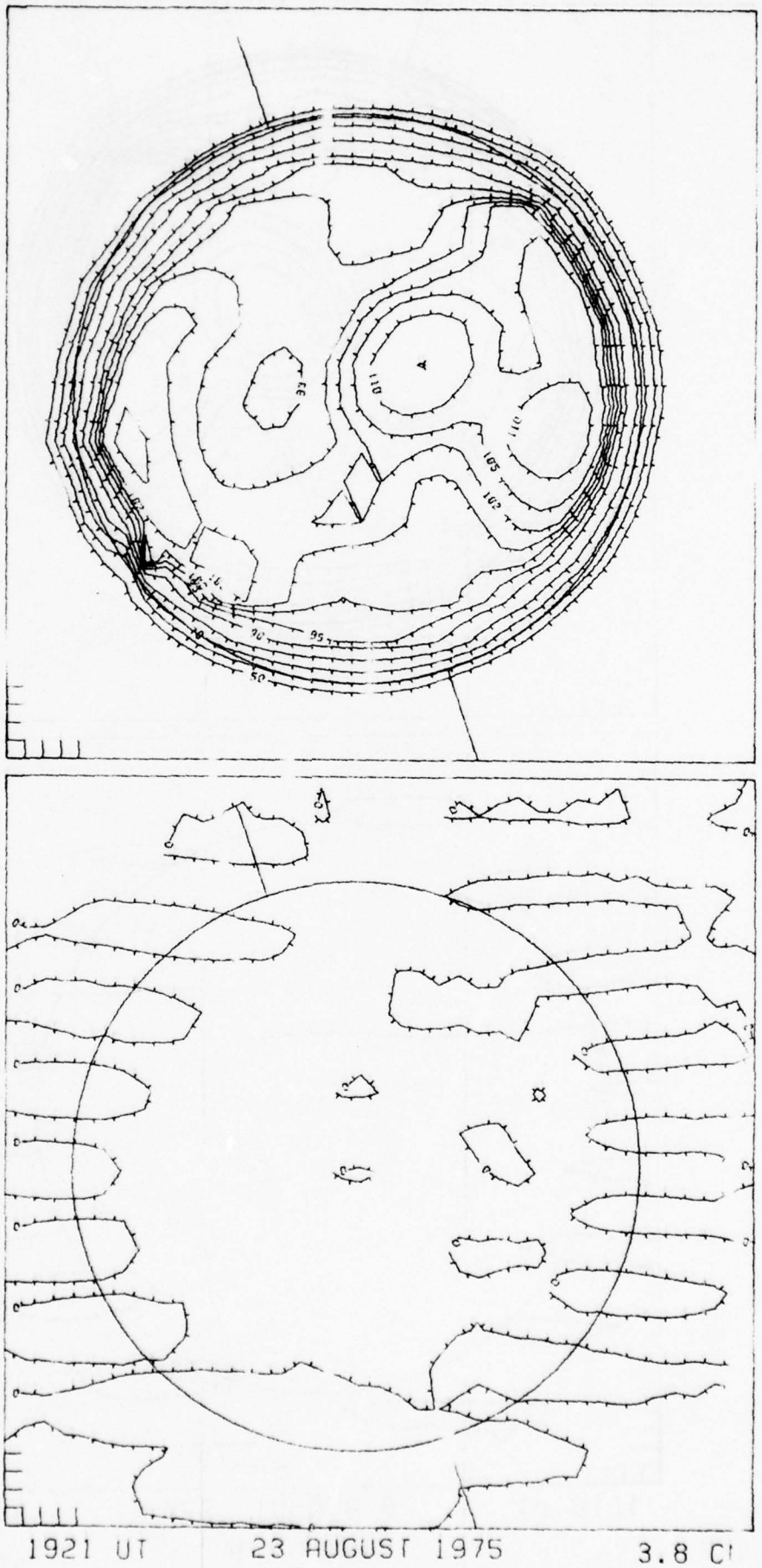

FIGURE 2.35

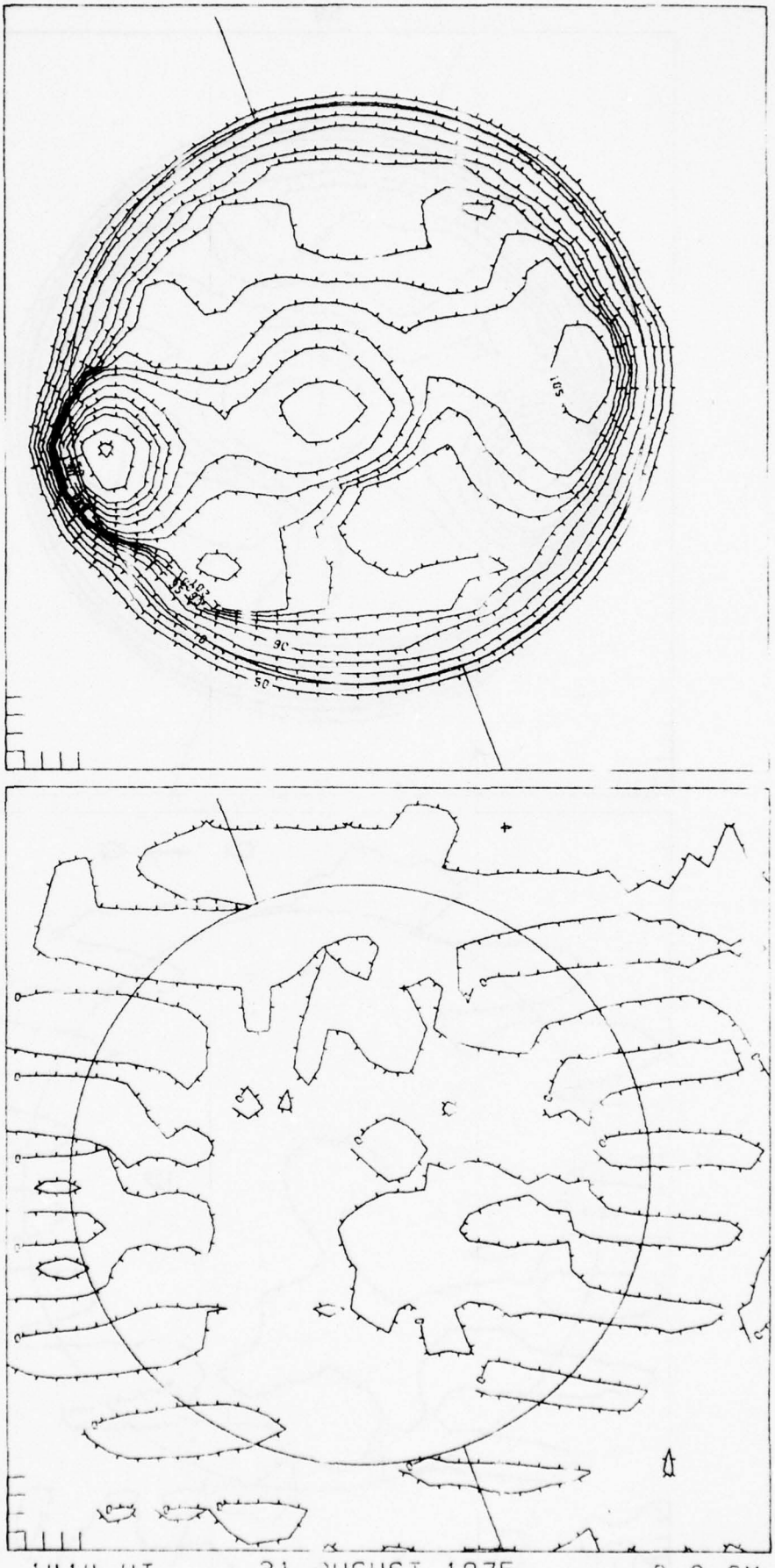

FIGURE 2.36

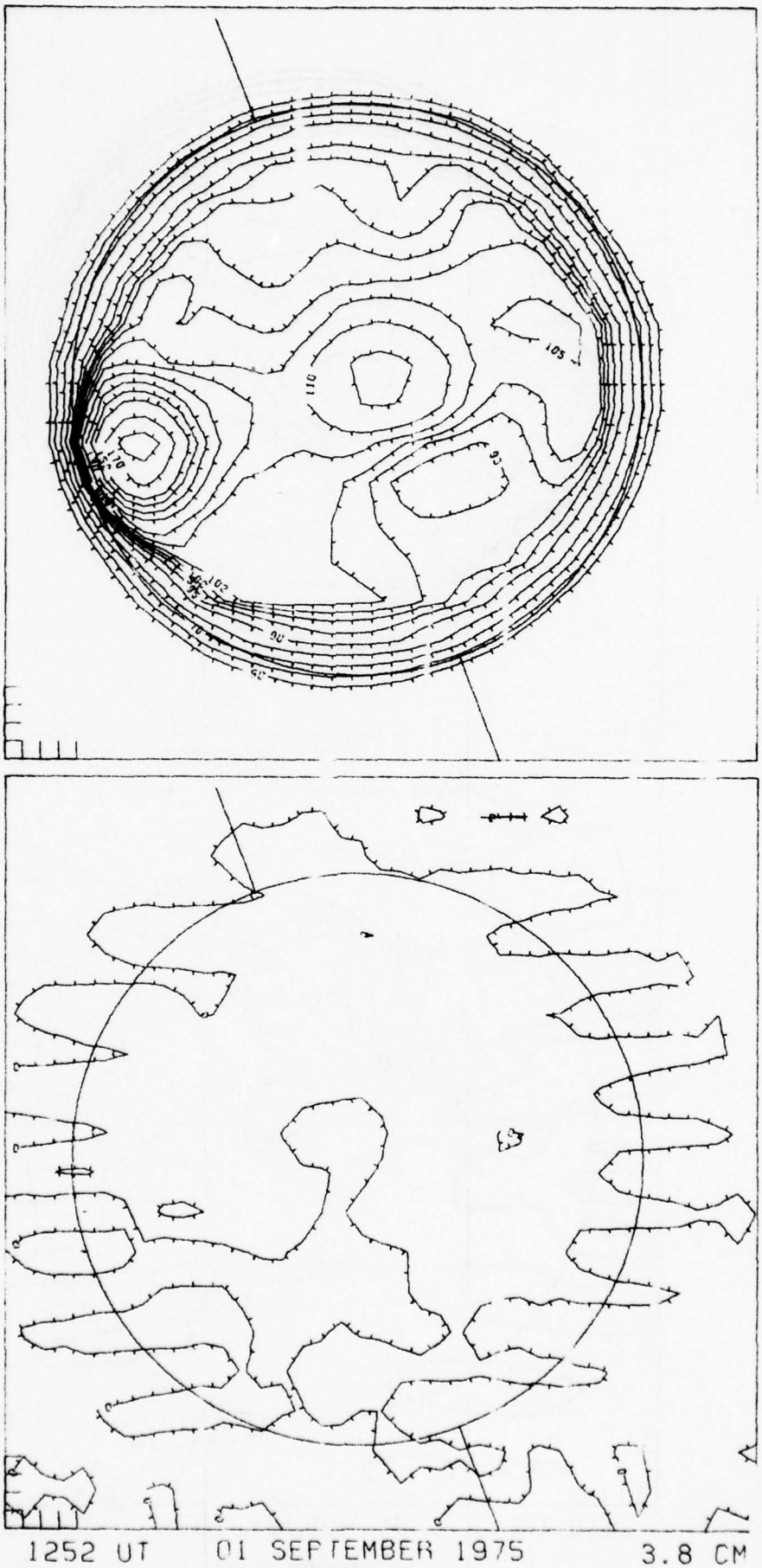

FIGURE 2.37

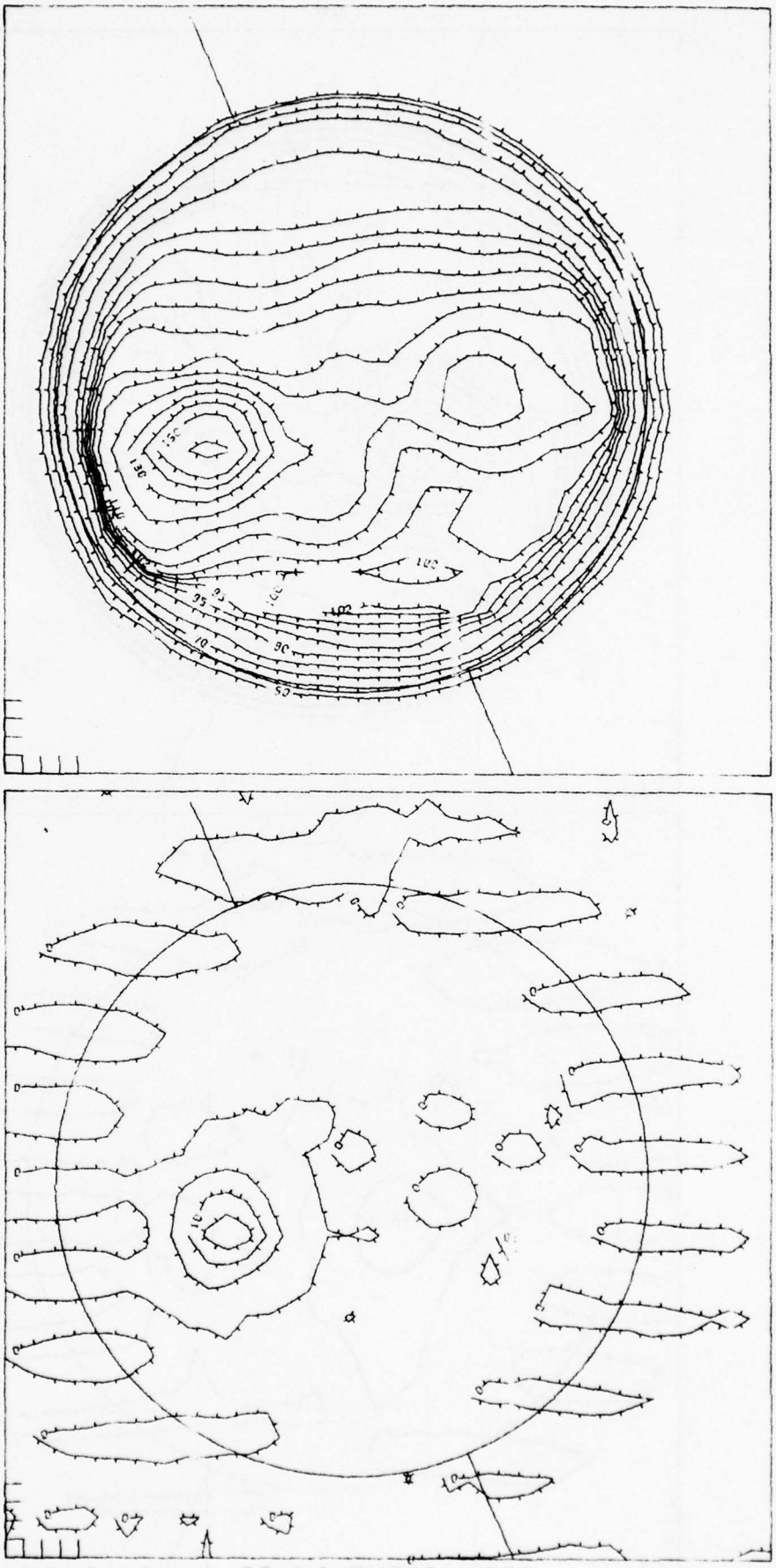

FIGURE 2.38

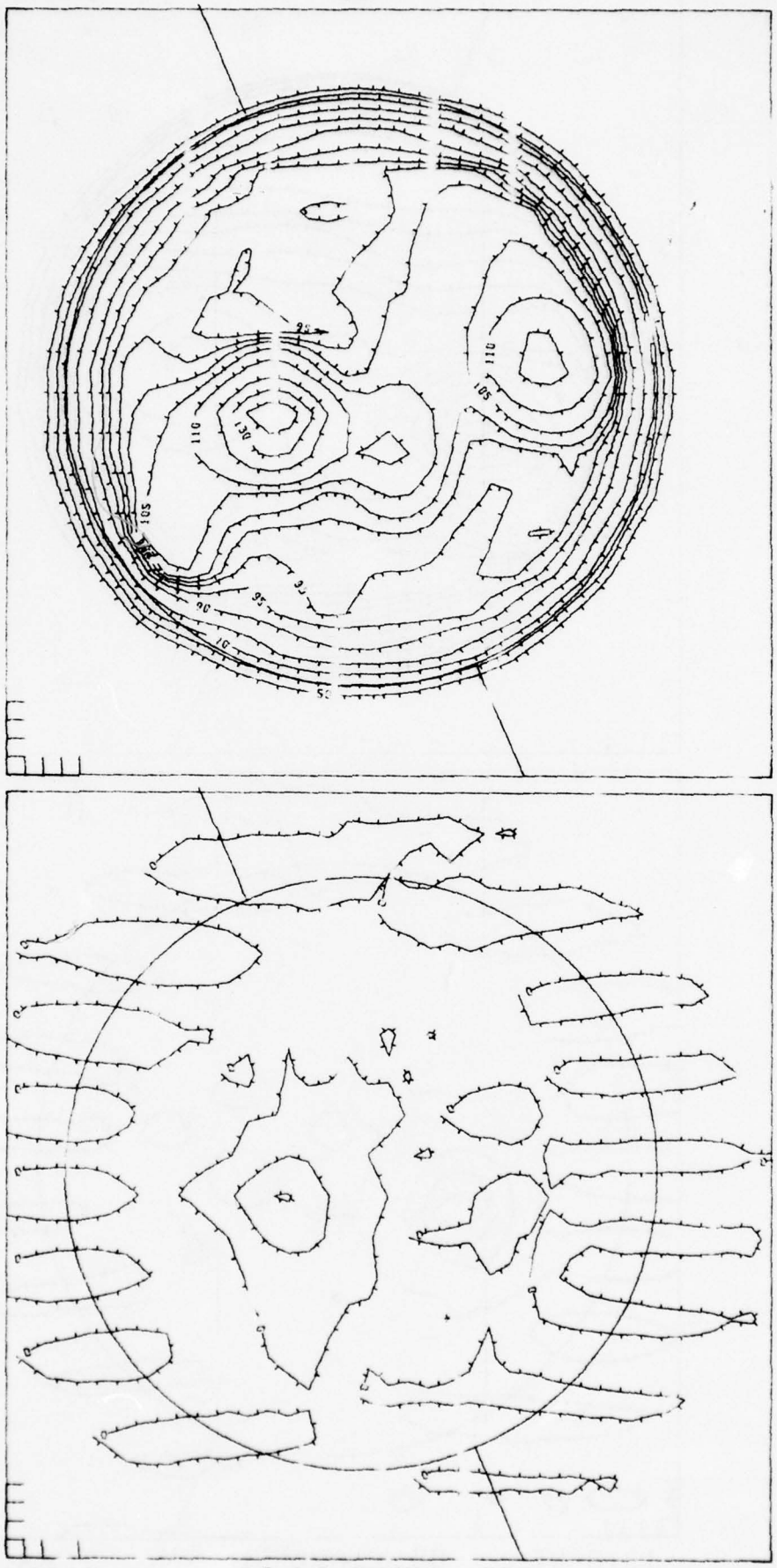

FIGURE 2.39

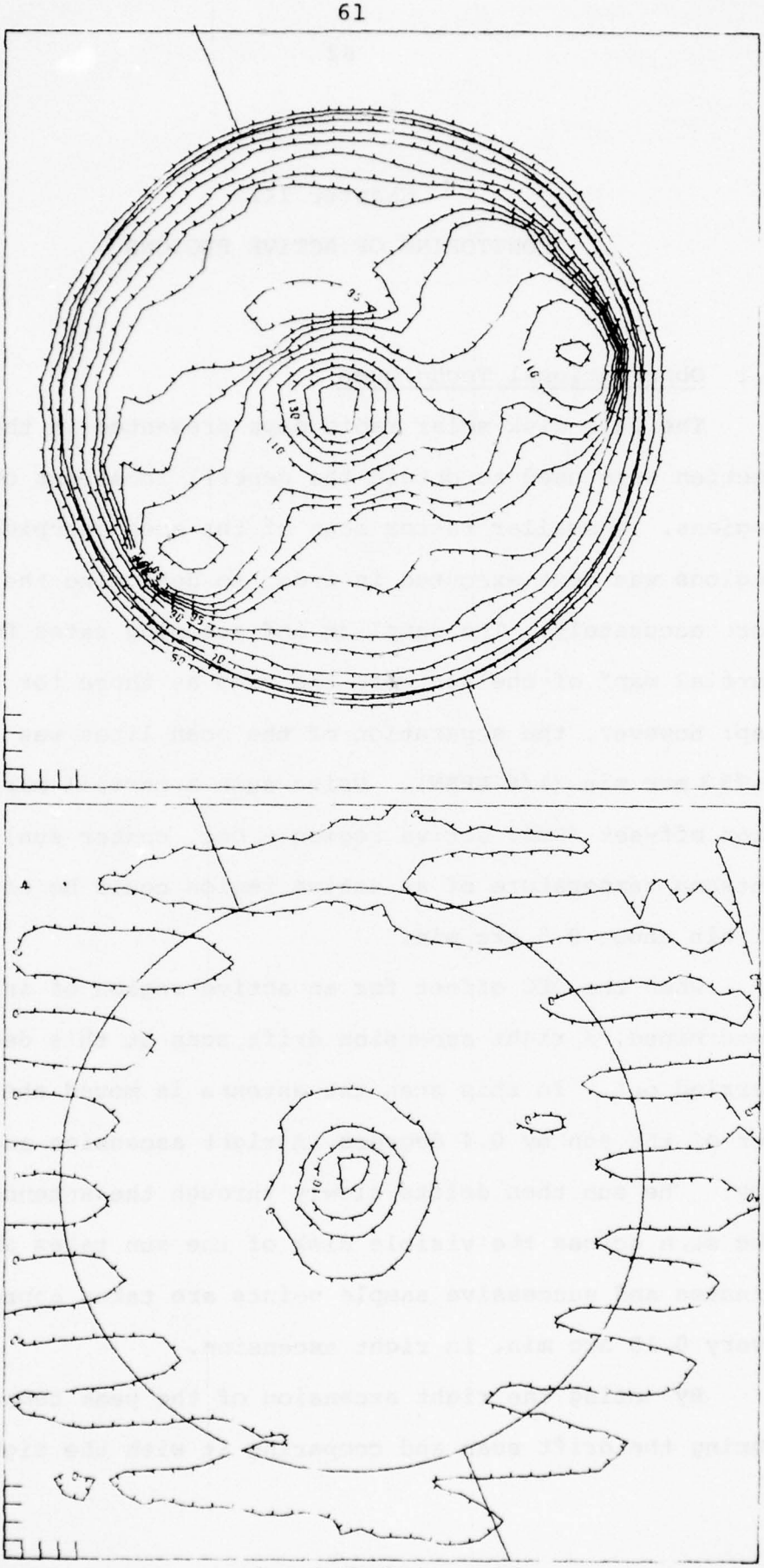

FIGURE 2.40

Chapter III

MONITORING OF ACTIVE REGIONS

3.1 Observational Techniques

The full disk solar radio maps presented in the preceeding section were used to obtain the general locations of the active regions. A smaller raster scan of the area occupied by the active regions was next executed in order to determine the location more accurately. The sampling and scanning rates for this "partial map" of the sun were the same as those for the full disk map; however, the separation of the scan lines was reduced to 0.733 arc min (1/6 HPBW). Using such a partial map, the Declination off-set (Dec. active region - Dec. center sun) of the peak antenna temperature of an active region could be estimated to within about 0.5 arc min.

When the DEC offset for an active region of interest was determined, a right ascension drift scan at this declination was carried out. In this scan the antenna is moved ahead of the center of the sun by 0.4 degrees in right ascension and held stationary. The sun then drifts slowly through the antenna beam. The scan across the visible disk of the sun takes about two minutes and successive sample points are taken approximately every 0.15 arc min. in right ascension.

By noting the right ascension of the peak temperature during the drift scan and comparing it with the right ascension

of the center of the sun for the same instant of time, we were able to determine the RA offset of the peak of the active region. The antenna was then set to execute a declination scan at the RA offset of the peak of the active region. This allowed us to determine more accurately the declination of the peak of the active region and hence its DEC offset from the center of the sun.

The RA and DEC offsets of the peak of the active region were then entered into the computer, and the antenna would lock onto this region and track it as the sun moved across the sky. The integration time for each sample point during these long monitoring periods, which often lasted several hours, was increased to three seconds to conserve computer tape and printout paper.

While making observations at Haystack, we were in continuous contact with the Sagamore Hill Observatory of AFGL which in turn received continuously updated information from the USAF Astrogeophysical Teletype Network (ATN), on the size, structure, and location of solar active regions. If we were informed at the beginning of our observations that a particular active region was likely to produce a flare, we would skip the full disk solar map and go directly to the partial map using the previous day's positions to set up the smaller scan.

3.2 Data Reduction

The first step in the data reduction process was to prepare a list of all the active regions which had been monitored for flare activity during the three observing seasons. The complete list is shown in Table III which gives the date of record, the starting time in UT, the SFC number for the active region, the McMath plage region number, the time interval between data points (SSP) which is usually 3 sec., the duration of the monitoring in minutes, the weather conditions, the Right Ascension and Declination offsets of the active region from the center of the solar disk (degrees), and finally whether any flare activity occurred during the monitoring period.

Computer line printer plots were made for each monitoring period. These preliminary plots showed the variation with time of T_r, T_ℓ, T_a, and %P, where

$$T_a = \frac{T_r + T_\ell}{2} \quad , \qquad \%P = 100 \times \frac{T_r - T_\ell}{T_r + T_\ell} \tag{10}$$

and were used to find the monitoring periods that showed any signs of solar activity. They were used to establish the maximum and minimum values of T_a and %P during the flare episodes. Plots were made then of the monitoring intervals which showed flare activity. In these final figures, for purposes of clarity, we plotted only the T_a and %P values. The %P scale, at the right side of the figures, was kept the same in all plots varying only the maximum and minimum values so as to accomodate the particular event. The T_a scale, on the other hand, was changed from plot to plot to accommodate the substantial variations in flare activity that were observed.

TABLE III

DATE	UT START	SFC	MPR	SSP	DUR	WEATHER	RA-OFF	DEC-OFF	ACT
14 MAR 73	20:06:24.6	054	263-4	0.3	2.03	CIRRUS	0.000	-0.043	NO
14 MAR 73	20:08:28.8	054	263-4	1.2	11.92	CIRRUS	0.000	-0.043	NO
14 MAR 73	20:20:35.7	054	263-4	3.0	42.25	CIRRUS	0.000	-0.043	NO
19 MAR 73	21:38:11.9	?	263-4	0.3	7.89	PTLY CLDY	-0.232	-0.165	NO
19 MAR 73	21:46:17.0	?	263-4	3.0	5.60	PTLY CLDY	-0.232	-0.165	NO
25 MAY 73	15:56:24.6	?	357	3.0	27.60	CLOUDY	-0.020	-0.018	YES
25 MAY 73	16:27:33.3	?	357	3.0	33.00	CLOUDY	-0.020	-0.018	NO
25 MAY 73	17:08:43.5	?	357	3.0	31.90	CLOUDY	-0.022	-0.018	NO
25 MAY 73	18:11:55.8	?	357	3.0	30.40	CLOUDY	-0.019	-0.018	NO
25 MAY 73	18:56:19.8	?	357	3.0	25.20	CLOUDY	-0.019	-0.018	YES
25 MAY 73	19:56:00.0	?	?	3.0	26.35	CLOUDY	0.022	-0.030	NO
28 JUN 73	17:07:29.8	147	397	3.0	42.55	CIRRUS	-0.233	-0.055	YES
28 JUN 73	17:50:04.6	147	397	0.6	22.59	CIRRUS	-0.233	-0.055	YES
28 JUN 73	18:44:45.1	147	397	3.0	39.80	CIRRUS	-0.240	-0.050	YES
28 JUN 73	20:56:50.5	158	417	0.6	3.28	CIRRUS	0.272	0.061	NO
28 JUN 73	21:00:09.7	158	417	3.0	17.85	CIRRUS	0.272	0.061	NO
29 JUN 73	14:27:00.4	158	417	3.0	40.65	RAIN	0.270	0.061	NO
29 JUN 73	15:11:28.6	158	417	3.0	57.95	RAIN	0.270	0.061	YES
29 JUN 73	16:31:58.6	158	417	3.0	28.75	RAIN	0.267	0.067	YES
30 JUN 73	13:33:57.3	158	417	3.0	95.05	RAIN	0.252	0.061	NO
30 JUN 73	15:22:37.5	157	414	3.0	5.85	RAIN	0.241	-0.030	NO
30 JUN 73	15:29:01.5	158	417	3.0	72.55	RAIN	0.252	0.061	NO
30 JUN 73	17:12:51.0	158	417	3.0	88.30	RAIN	0.250	0.061	YES
30 JUN 73	18:44:22.1	158	417	3.0	117.30	RAIN	0.250	0.061	NO

TABLE III (continued)

DATE	UT START	SFC	MPR	SSP	DUR	WEATHER	RA-OFF	DEC-OFF	ACT
01 JUL 73	11:57:43.0	158	417	3.0	40.50	CLOUDY	0.225	0.061	NO
01 JUL 73	12:52:30.7	158	417	3.0	13.00	CLOUDY	0.225	0.061	NO
01 JUL 73	13:08:26.5	158	417	3.0	51.15	CLOUDY	0.225	0.061	NO
01 JUL 73	14:10:54.4	158	417	3.0	51.82	CLOUDY	0.225	0.061	NO
01 JUL 73	15:15:14.5	158	417	3.0	40.45	CLOUDY	0.225	0.061	NO
01 JUL 73	16:04:47.7	158	417	3.0	53.35	CLOUDY	0.225	0.061	NO
04 JUL 73	13:41:40.4	158	417	3.0	50.20	CLOUDY	0.050	0.042	NO
04 JUL 73	14:41:09.6	158	417	3.0	49.95	CLOUDY	0.050	0.042	NO
04 JUL 73	15:34:23.7	158	417	3.0	58.25	CLOUDY	0.050	0.042	YES
04 JUL 73	16:43:44.6	158	417	3.0	31.45	CLOUDY	0.050	0.042	NO
05 JUL 73	14:17:31.2	158	417	3.0	51.35	RAIN	0.023	0.042	NO
05 JUL 73	15:19:15.3	158	417	3.0	15.60	RAIN	0.023	0.042	YES
07 JUL 73	14:16:20.9	158	417	3.0	11.00	CLEAR	-0.126	0.036	NO
07 JUL 73	14:54:46.7	162	427	3.0	91.05	CLEAR	-0.025	-0.006	YES
07 JUL 73	16:28:30.8	162	427	3.0	87.05	CLEAR	-0.025	-0.006	YES
08 JUL 73	12:48:09.2	162	427	3.0	38.40	CLEAR	-0.091	-0.018	NO
08 JUL 73	13:48:03.5	162	427	3.0	66.75	CLEAR	-0.091	-0.018	NO
08 JUL 73	15:26:28.8	158	417	0.6	4.35	CLEAR	-0.206	0.036	YES
08 JUL 73	15:31:58.8	158	417	0.6	21.24	CLEAR	-0.196	0.036	YES
08 JUL 73	15:53:16.2	158	417	3.0	30.25	CLEAR	-0.196	0.036	YES
11 JUL 73	15:06:30.3	158	417	3.0	82.25	RAIN	-0.271	0.055	YES
11 JUL 73	16:32:18.6	158	417	3.0	18.25	RAIN	-0.271	0.055	NO
11 JUL 73	17:00:00.6	158	417	3.0	25.55	RAIN	-0.271	0.055	NO
11 JUL 73	17:41:15.4	158	417	3.0	21.40	RAIN	-0.272	0.055	NO
11 JUL 73	18:08:37.6	158	417	3.0	46.34	RAIN	-0.271	0.055	NO
12 JUL 73	13:57:44.3	158	417	3.0	49.75	PTLY CLDY	-0.280	0.061	YES
12 JUL 73	15:03:57.6	158	417	3.0	52.65	PTLY CLDY	-0.280	0.061	YES
12 JUL 73	16:09:24.0	158	417	3.0	105.80	PTLY CLDY	-0.280	0.061	YES

TABLE III (continued)

DATE	UT START	SFC	MPR	SSP	DUR	WEATHER	RA-OFF	DEC-OFF	ACT
17 JUL 73	16:18:55.4	171	448	3.0	17.65	CLOUDY	0.017	-0.061	NO
17 JUL 73	16:47:57.0	?	442	3.0	75.90	CLOUDY	0.220	-0.052	NO
17 JUL 73	18:12:58.5	?	442	3.0	23.50	CLOUDY	0.220	-0.052	NO
17 JUL 73	18:40:01.4	?	442	3.0	12.90	CLOUDY	0.220	-0.052	NO
21 JUL 73	13:30:04.3	171	448	3.0	25.45	RAIN	-0.228	-0.028	NO
21 JUL 73	13:58:33.0	171	448	3.0	93.25	RAIN	-0.228	-0.028	NO
21 JUL 73	15:42:28.0	171	448	3.0	86.15	RAIN	-0.029	-0.023	NO
22 JUL 73	13:54:14.3	171	448	3.0	32.60	CLEAR	-0.244	-0.024	NO
22 JUL 73	14:30:24.8	171	448	3.0	56.75	CLEAR	-0.244	-0.024	NO
22 JUL 73	15:52:23.2	171	448	3.0	95.30	CLEAR	-0.241	-0.024	NO
22 JUL 73	17:30:58.7	171	448	3.0	4.10	CLEAR	-0.241	-0.024	NO
26 JUL 73	16:23:53.1	177	460	3.0	49.55	RAIN	0.241	-0.067	NO
26 JUL 73	17:22:54.2	177	460	3.0	31.65	RAIN	0.241	-0.067	NO
06 JUN 74	18:37:22.5	416	972	3.0	51.90	CIRRUS	-0.050	-0.080	NO
06 JUN 74	19:51:13.8	416	972	3.0	62.00	CIRRUS	-0.055	-0.085	NO
07 JUN 74	18:18:20.3	416	972	6.0	26.90	CIRRUS	-0.106	-0.092	NO
07 JUN 74	19:20:21.8	416	972	3.0	21.00	CIRRUS	-0.106	-0.092	NO
07 JUN 74	19:44:15.8	416	972	3.0	58.60	CIRRUS	-0.106	-0.092	YES
08 JUN 74	17:31:01.5	416	972	3.0	28.45	CLEAR	-0.249	-0.104	NO
08 JUN 74	18:02:37.2	416	972	3.0	53.50	CLEAR	-0.249	-0.104	NO
08 JUN 74	19:01:13.2	416	972	3.0	25.90	CLEAR	-0.249	-0.104	NO
08 JUN 74	19:27:52.8	416	972	3.0	31.90	CLEAR	-0.249	-0.104	NO
08 JUN 74	20:06:44.7	416	972	3.0	53.00	CLEAR	-0.249	-0.104	NO
09 JUN 74	13:57:58.6	416	972	3.0	57.70	CLEAR	-0.217	-0.104	YES
09 JUN 74	14:58:34.9	416	972	3.0	62.90	CLEAR	-0.217	-0.104	YES
09 JUN 74	16:06:11.8	416	972	3.0	162.30	CLEAR	-0.217	-0.104	YES

TABLE III (continued)

DATE	UT START	SFC	MPR	SSP	DUR	WEATHER	RA-OFF	DEC-OFF	ACT
12 JUL 74	15:37:30.3	438	057	3.0	111.90	CLEAR	0.126	-0.066	NO
12 JUL 74	17:32:40.8	438	057	3.0	41.45	CLEAR	0.126	-0.066	NO
12 JUL 74	18:26:17.7	438	057	3.0	22.80	CLEAR	0.125	-0.068	NO
12 JUL 74	18:52:41.4	438	057	3.0	50.60	CLEAR	0.125	-0.068	NO
13 JUL 74	14:19:26.1	438	057	3.0	73.75	PTLY CLDY	0.072	-0.067	YES
13 JUL 74	15:39:11.4	438	057	3.0	30.15	PTLY CLDY	0.072	-0.067	NO
13 JUL 74	16:13:31.5	438	057	3.0	149.45	PTLY CLDY	0.072	-0.067	YES
14 JUL 74	14:20:37.9	438	057	3.0	88.15	CLEAR	0.004	-0.061	YES
14 JUL 74	16:08:00.4	438	057	3.0	132.40	CLEAR	-0.005	-0.059	YES
14 JUL 74	19:30:34.0	?	?	0.6	37.76	CLEAR	-0.020	-0.060	NO
15 JUL 74	15:04:30.8	438	057	3.0	51.00	CIRRUS	-0.064	-0.055	YES
15 JUL 74	16:07:16.7	438	057	3.0	210.20	CIRRUS	-0.064	-0.055	YES
17 JUL 74	15:07:04.3	438	057	3.0	16.20	CLEAR	-0.183	-0.042	NO
17 JUL 74	16:11:00.7	442	062	3.0	55.20	CLEAR	-0.033	-0.076	YES
17 JUL 74	17:15:11.5	438	057	3.0	35.55	CLEAR	-0.182	-0.044	NO
17 JUL 74	18:02:54.7	443	067	3.0	31.10	CLEAR	0.185	-0.092	NO
17 JUL 74	18:42:27.7	442	062	3.0	93.60	CLEAR	-0.039	-0.077	YES
18 JUL 74	15:04:40.0	438	057	3.0	6.35	CLOUDY	-0.231	-0.036	NO
18 JUL 74	15:14:46.9	438	057	3.0	51.25	CLOUDY	-0.231	-0.036	YES
18 JUL 74	16:19:09.4	443	067	3.0	89.95	CLOUDY	0.125	-0.096	YES
18 JUL 74	17:58:10.3	442	062	3.0	74.35	CLOUDY	-0.216	-0.059	YES
20 JUL 74	15:08:32.2	438	057	3.0	42.60	PTLY CLDY	-0.238	-0.033	YES
20 JUL 74	16:06:10.9	442	062	3.0	91.35	PTLY CLDY	-0.238	-0.036	YES
20 JUL 74	17:45:42.4	451	?	3.0	34.70	PTLY CLDY	0.251	-0.079	YES
20 JUL 74	18:28:01.3	442	062	3.0	30.55	PTLY CLDY	-0.238	-0.034	NO

TABLE III (continued)

DATE	UT START	SFC	MPR	SSP	DUR	WEATHER	RA-OFF	DEC-OFF	ACT
21 JUL 74	14:55:11.5	451	088?	3.0	64.05	PTLY CLDY	0.260	-0.083	YES
21 JUL 74	16:22:47.2	451	088?	3.0	153.90	PTLY CLDY	0.255	-0.088	YES
18 SEP 74	14:38:29.7	487	225	3.0	246.53	CLEAR	-0.165	0.090	YES
19 SEP 74	13:38:51.2	487	225	3.0	136.85	CLOUDY	-0.187	0.106	NO
19 SEP 74	16:24:01.7	487	225	3.0	136.05	CLOUDY	-0.198	0.107	NO
20 SEP 74	13:47:13.8	487	225	3.0	57.45	CLOUDY	-0.206	0.131	NO
20 SEP 74	14:55:27.0	487	225	3.0	116.30	CLOUDY	-0.206	0.131	NO
20 SEP 74	16:51:54.0	487	225	3.0	7.30	CLOUDY	-0.206	0.131	NO
20 SEP 74	17:13:48.0	487	225	3.0	101.00	CLOUDY	-0.206	0.131	NO
21 SEP 74	14:05:43.7	487	225	3.0	141.10	RAIN	-0.222	0.143	YES
21 SEP 74	16:51:36.8	487	225	3.0	36.75	RAIN	-0.222	0.143	YES
21 SEP 74	17:46:35.9	487	225	3.0	170.95	RAIN	-0.207	0.140	YES
22 SEP 74	13:47:40.7	CAL	---	3.0	27.15	CLEAR	0.000	0.202	NO
22 SEP 74	14:30:26.6	487	225	3.0	42.05	CLEAR	-0.201	0.151	NO
23 SEP 74	14:06:59.1	487	250	3.0	67.60	CLEAR	0.043	0.016	NO
24 SEP 74	14:24:21.3	494	250	3.0	66.30	CLEAR	0.043	0.016	NO
24 SEP 74	15:42:14.1	494	250	3.0	9.90	CLEAR	0.044	0.015	NO
24 SEP 74	16:08:25.2	494	250	3.0	13.00	CLEAR	0.044	0.015	NO
25 SEP 74	14:12:19.6	494	250	3.0	88.50	PTLY CLDY	-0.004	0.050	NO
25 SEP 74	18:23:03.7	494	250	3.3	11.33	PTLY CLDY	-0.013	0.047	NO
25 SEP 74	18:34:26.8	494	250	3.0	15.80	PTLY CLDY	-0.013	0.047	NO

TABLE III (continued)

DATE	UT START	SFC	MPR	SSP	DUR	WEATHER	RA-OFF	DEC-OFF	ACT
26 SEP 74	14:40:10.5	494	250	0.6	6.10	CLOUDY	-0.062	0.075	NO
26 SEP 74	14:46:20.7	494	250	3.0	47.05	CLOUDY	-0.062	0.075	NO
26 SEP 74	17:58:11.1	?	257	3.0	47.40	CLOUDY	0.184	-0.153	NO
27 SEP 74	15:05:21.0	495	262	3.0	26.30	CLEAR	0.202	-0.007	NO
28 SEP 74	13:50:34.5	495	262	3.0	60.20	FOG, CLDY	0.234	-0.078	YES
28 SEP 74	14:50:49.5	495	262	3.0	66.75	FOG, CLDY	0.234	-0.078	YES
28 SEP 74	16:03:27.6	495	262	3.0	38.80	FOG, CLDY	0.234	-0.078	NO
29 SEP 74	14:03:19.0	497	257	3.0	107.30	FOG, CLDY	0.192	-0.140	YES
29 SEP 74	16:06:44.8	497	257	3.0	148.60	FOG, CLDY	0.192	-0.140	YES
24 JUN 75	15:55:45.5	603	736	3.0	77.70	CLEAR	-0.071	-0.055	NO
25 JUN 75	15:49:45.3	603	736	3.0	112.30	CLEAR	-0.136	-0.067	YES
25 JUN 75	17:49:34.9	603	736	3.0	40.55	CLEAR	-0.136	-0.067	NO
04 AUG 75	14:50:14.4	618	786	3.0	55.40	CLOUDY	0.048	-0.012	YES
04 AUG 75	15:46:53.4	618	786	3.0	6.04	CLOUDY	0.048	-0.012	NO
04 AUG 75	16:23:45.0	617	786	3.0	31.50	CLOUDY	0.046	-0.016	YES
04 AUG 75	17:02:38.4	619	790	3.0	38.95	CLOUDY	0.256	-0.030	YES
04 AUG 75	17:45:23.1	617	786	3.0	115.75	CLOUDY	0.046	-0.016	YES
04 AUG 75	19:42:07.5	619	790	3.0	8.20	CLOUDY	0.256	-0.030	NO
05 AUG 75	15:21:45.1	619	790	3.0	3.65	PTLY CLDY	0.219	-0.030	NO
05 AUG 75	15:27:11.8	619	790	3.0	85.65	PTLY CLDY	0.219	-0.030	NO
05 AUG 75	17:01:57.7	618	786	3.0	171.45	PTLY CLDY	-0.020	-0.006	YES

TABLE III (continued)

DATE	UT START	SFC	MPR	SSP	DUR	WEATHER	RA-OFF	DEC-OFF	ACT
06 AUG 75	14:23:48.0	618	786	3.0	177.55	PTLY CLDY	-0.082	0.018	YES
07 AUG 75	14:51:19.5	618	786	3.0	279.00	RAIN	-0.132	0.024	YES
08 AUG 75	17:03:51.4	618	786	3.0	30.95	RAIN	-0.182	0.046	NO
08 AUG 75	17:35:40.0	619	790	3.0	24.95	RAIN	0.070	-0.006	NO
08 AUG 75	18:02:05.5	618	786	3.0	40.30	RAIN	-0.182	0.046	NO
08 AUG 75	18:48:47.5	618	786	3.0	64.30	RAIN	-0.182	0.046	NO
10 AUG 75	15:04:56.2	618	786	3.0	42.70	CLEAR	-0.238	0.074	NO
10 AUG 75	15:48:19.6	619	790	3.0	91.49	CLEAR	-0.045	0.023	YES
10 AUG 75	17:20:39.7	618	786	3.0	108.06	CLEAR	-0.238	0.074	YES
21 AUG 75	14:31:24.9	?	808	3.0	45.41	CLEAR	-0.172	0.165	YES
21 AUG 75	15:16:49.8	?	808	0.6	4.88	CLEAR	-0.172	0.165	YES
21 AUG 75	15:49:14.4	?	808	0.6	5.96	CLEAR	-0.172	0.165	YES
21 AUG 75	15:55:16.2	?	808	3.0	105.90	CLEAR	-0.172	0.165	YES
21 AUG 75	19:33:39.0	?	808	3.0	3.29	CLEAR	-0.177	0.165	YES
21 AUG 75	19:36:56.7	?	808	0.6	16.90	CLEAR	-0.177	0.165	YES
21 AUG 75	20:03:21.3	?	808	0.6	5.24	CLEAR	-0.177	0.165	YES
23 AUG 75	17:01:37.9	?	808	3.0	66.00	CLEAR	-0.031	0.031	NO
23 AUG 75	18:18:22.6	?	808	3.0	61.15	CLEAR	-0.031	0.031	NO
31 AUG 75	15:17:47.1	?	826	3.0	3.05	?	0.240	-0.067	NO
31 AUG 75	15:42:00.6	?	826	3.0	138.45	?	0.240	-0.067	YES
01 SEP 75	13:32:01.5	?	826	3.0	94.80	CLEAR	0.209	-0.060	NO
01 SEP 75	17:17:32.4	?	826	3.0	131.85	CLEAR	0.209	-0.060	NO

TABLE III (continued)

DATE	UT START	SFC	MPR	SSP	DUR	WEATHER	RA-OFF	DEC-OFF	ACT
08 NOV 75	14:44:02.9	664	926	3.0	158.90	RAIN	0.149	-0.052	NO
08 NOV 75	17:52:44.9	664	926	3.0	11.65	RAIN	0.137	-0.055	NO
08 NOV 75	18:36:20.3	664	926	3.0	17.80	RAIN	0.137	-0.055	YES
08 NOV 75	19:13:39.8	664	926	3.0	4.60	RAIN	0.137	-0.055	NO
08 NOV 75	19:25:16.7	664	926	3.0	28.60	RAIN	0.137	-0.055	NO
08 NOV 75	19:59:11.0	664	926	3.0	45.55	RAIN	0.137	-0.055	NO
09 NOV 75	14:09:37.6	664	926	3.0	42.20	CLEAR	0.091	-0.026	NO
09 NOV 75	14:52:49.6	664	926	3.0	87.90	CLEAR	0.091	-0.026	NO
09 NOV 75	16:27:04.0	664	926	3.0	129.55	CLEAR	0.091	-0.026	NO
09 NOV 75	18:40:07.0	664	926	3.0	5.85	CLEAR	0.091	-0.026	NO
10 NOV 75	13:52:57.2	664	926	3.0	12.11	FOG, CLDY	0.023	0.001	YES
10 NOV 75	14:09:53.6	664	926	0.6	8.94	FOG, CLDY	0.023	0.001	NO
10 NOV 75	14:18:54.2	664	926	3.0	90.60	FOG, CLDY	0.023	0.001	YES
10 NOV 75	15:52:28.4	664	926	3.0	67.65	FOG, CLDY	0.023	0.001	NO
10 NOV 75	17:25:23.0	664	926	0.6	4.29	FOG, CLDY	0.023	0.001	NO
10 NOV 75	17:29:46.1	664	926	3.0	40.05	FOG, CLDY	0.023	0.001	NO
10 NOV 75	18:13:02.0	664	926	3.0	23.32	FOG, CLDY	0.023	0.001	NO
10 NOV 75	18:39:23.0	664	926	3.0	22.30	FOG, CLDY	0.023	0.001	NO

Finally from these long plots, some of them several feet long, we chose 30 minute segments which included the most important events observed and which could be demonstrated in the space of a normal 8.5" × 11.0" page. These are shown in the figures that follow.

3.3 Selected Flare Events

A total of 22 flare events were selected for the special and diverse features which they display in the behavior of T_a and %P. A brief description of these 22 events is given below:

FIGURE 3.1. 25 May 1973. Starting time 18:56:00 UT, McMath 357. Weather: cloudy. A small event where an increase of approximately 10% in T_a was not accompanied by any detectable change in %P.

FIGURE 3.2. 28 June 1973. Starting time 17:32:00 UT, McMath 397. Weather: high overcast. A small event with a very sharp commencement where the %P shows also some small changes during the initial spikes of the flare event.

FIGURE 3.3. 28 June 1973. Starting time 18:44:00 UT, McMath 397. Weather: high overcast. A small event with a relatively gradual rise and no detectable change in %P.

FIGURE 3.4. 29 June 1973. Starting time 16:31:00 UT, McMath 417. Weather: cloudy and light rain. A small event in a relatively strongly polarized active region. The sharp drop in T_a after the event might be the result of weather conditions. The oscillations in both T_a and %P are due to antenna tracking

difficulties which occur when the antenna is pointing in a specific direction. This usually occurred near solar transit.

FIGURE 3.5. 7 July 1973. Starting time 15:49:00 UT, McMath 427. Weather: clear. A strong and most interesting event with three distinct spikes in T_a and corresponding spikes in %P. The interesting observation in this event is that while the first two spikes of T_a produced a decrease in %P, the third and largest of the three spikes in T_a produced a reversal in %P which changed towards larger values. It is also to be noticed that no characteristic variations in either T_a or %P occurred before this event which could be interpreted as a forecaster of the flare event.

FIGURE 3.6. 12 July 1973. Starting time 15:03:00 UT, McMath 417. Weather: partly cloudy. A rather small event with an almost one to one correspondence between the changes recorded in T_a and %P. Some activity more noticeable in %P 10-15 minutes before the event could be taken as a precursor. It is interesting that T_a showed little change during what could have been a precursor in %P.

FIGURE 3.7. 7 June 1974. Starting time 19:54:00 UT, McMath 972. Weather: sunny with cirrus clouds. A small event with a slow rise in T_a and an even slower change in %P.

FIGURE 3.8. 13 July 1974. Starting time 14:29:00 UT, McMath 057. Weather: partly cloudy. A small event with a parallel behavior in T_a and %P which demonstrate the same features. Before the event T_a was quiet while the %P showed some significant fluctuations.

FIGURE 3.9. 21 July 1974. Starting time 15:16:00 UT, McMath 088(?). Weather: partly cloudy. A small event with very similar behavior in T_a and in %P. It is interesting that in this case T_a showed first a slight increase followed by a substantial decrease before the event, while %P showed no corresponding change.

FIGURE 3.10. 21 July 1974. Starting time 17:13:00 UT. McMath 088(?). Weather: partly cloudy. A substantial event with a large spike of short duration (less than one minute) in both T_a and %P. A smaller event followed approximately 12 minutes after the large spike, which occurred 105 minutes after the event of Figure 3.9.

FIGURE 3.11. 18 September 1974. Starting time 15:33:00 UT. McMath 225. Weather: clear. A small event with corresponding features in T_a and %P. It is interesting that while the %P shows substantial fluctuations before the event, T_a shows no significant changes before the event.

FIGURE 3.12. 18 September 1974. Starting time 16:48:00 UT. McMath 225. Weather: clear. A much larger event which occurred in the same active region approximately 72 minutes after the smaller event shown in Figure 3.11. While the earlier smaller event produced a substantial enhancement of the negative polarization of the active region, the much larger increase in T_a seen in this figure produced essentially no change in %P.

FIGURE 3.13. 21 September 1974. Starting time 16:51:00 UT. McMath 225. Weather: cloudy with some rain. An interesting event with a close correlation between the features seen in T_a and %P.

FIGURE 3.14. 21 September 1974. Starting time 18:01:00 UT. McMath 225. Weather: cloudy with some rain. A large event in which T_a increased by nearly 2.5 times. The peak value of the brightness temperature was close to 9 times higher than the background temperature of the solar disk. The %P showed a similar major decrease changing from about -9% to -33%. This change in %P was so large that in order to maintain the same scale in %P, we had to plot at the top of the diagram the segment of the %P which would have gone beyond the lower boundary of the figure. This major event occurred approximately 75 minutes after the smaller event shown in Figure 3.13.

FIGURE 3.15. 21 September 1974. Starting time 19:27:00 UT. McMath 225. Weather: cloudy with some rain. A relatively small event with a significant change in %P. This event followed the large one plotted in Figure 3.14 by approximately 97 minutes. It should be noted that this active region remained in a state of high activity during the entire day showing continous fluctuations both in T_a and in %P with several flares.

FIGURE 3.16. 6 August 1975. Starting time 16:03:00 UT. McMath 786. Weather: partly cloudy. A rather large event of short duration consisting of a sudden spike, both in T_a and %P, which lasted for less than one minute. During the two hours preceeding this event (not shown in this figure) both T_a and %P showed substantial fluctuations.

FIGURE 3.17. 7 August 1975. Starting time 14:51:00 UT. McMath 786. Weather: rainy. A large event consisting of a sudden spike both in T_a and %P lasting for only about one minute. Approximately 10 minutes after the spike-like flare, a second event occurred which was less pronounced but of substantially longer duration. It is interesting that though the large increase in T_a in the first event produced an increase in %P to higher positive values, in the smaller but longer lasting event that followed, the increase in T_a produced a decrease in the polarization.

FIGURE 3.18. 7 August 1975. Starting time 16:06:00 UT. McMath 786. Weather: rainy. A large event again of a spike-like nature both in T_a and %P. This event consists of two distinct spikes each less than one minute in duration and separated by about three minutes. The first spike is much smaller than the second one in the case of T_a but both are of approximately equal magnitude in the case of %P. This event followed the ones plotted in Figure 3.17 by about 75 minutes.

FIGURE 3.19. 7 August 1975. Starting time 17:16:00 UT. McMath 786. Weather: rainy. A small event showing a single prominent peak in T_a and three peaks in %P. It is interesting that the peak in T_a coincides with a valley in %P, i.e., it occured at a time when the %P was returning to normal values between two peaks to higher values. This event occurred approximately 65 minutes after the one plotted in Figure 3.18.

FIGURE 3.20. 7 August 1975. Starting time 18:31:00 UT. McMath 786. Weather: rainy. A moderately large event showing clearly three peaks in %P while T_a shows the corresponding peaks in a less pronounced way as it increases continously towards its maximum value at the third peak. This event occurred approximately 75 minutes after the one plotted in Figure 3.19. This active region remained in a highly active state during the entire monitoring period which lasted for almost five hours. Both T_a and %P showed continuous fluctuations perhaps indicating that the active region was bound to produce several flare events, as it actually did.

FIGURE 3.21. 10 August 1975. Starting time 18:02:00 UT. McMath 786. Weather: clear. A moderately large event in T_a, again in the form of a spike approximately one minute in duration, which surprisingly produced almost no change in %P. T_a and %P had been quiet for more than one hour before this sudden event, and returned to a quiet state after this brief flaring event.

FIGURE 3.22. 21 August 1975. Starting time 14:47:00 UT. McMath 808. Weather: clear. A large event which saturated our receivers which on this day were set at a high sensitivity and, therefore, could not accommodate large excursions in T_a and %P. The interesting observation in this event is that there was a substantial drop in T_a prior to the flare event, though no corresponding change in %P was observed.

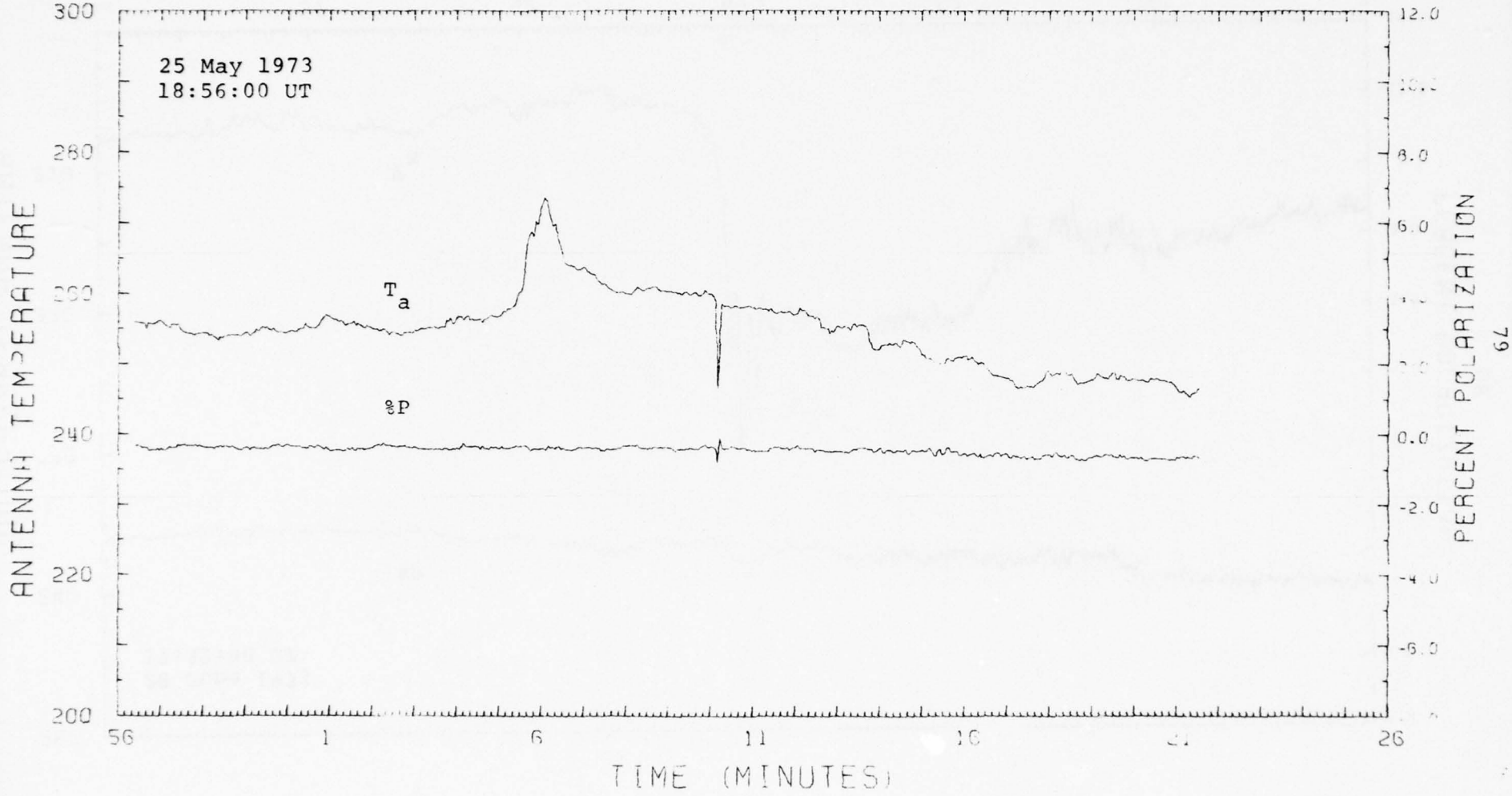
25 May 1973
18:56:00 UT
T_a
%P
ANTENNA TEMPERATURE
PERCENT POLARIZATION
TIME (MINUTES)
300
280
240
220
200
12.0
8.0
6.0
0.0
-2.0
-6.0
56
1
6
11
26

FIGURE 3.1

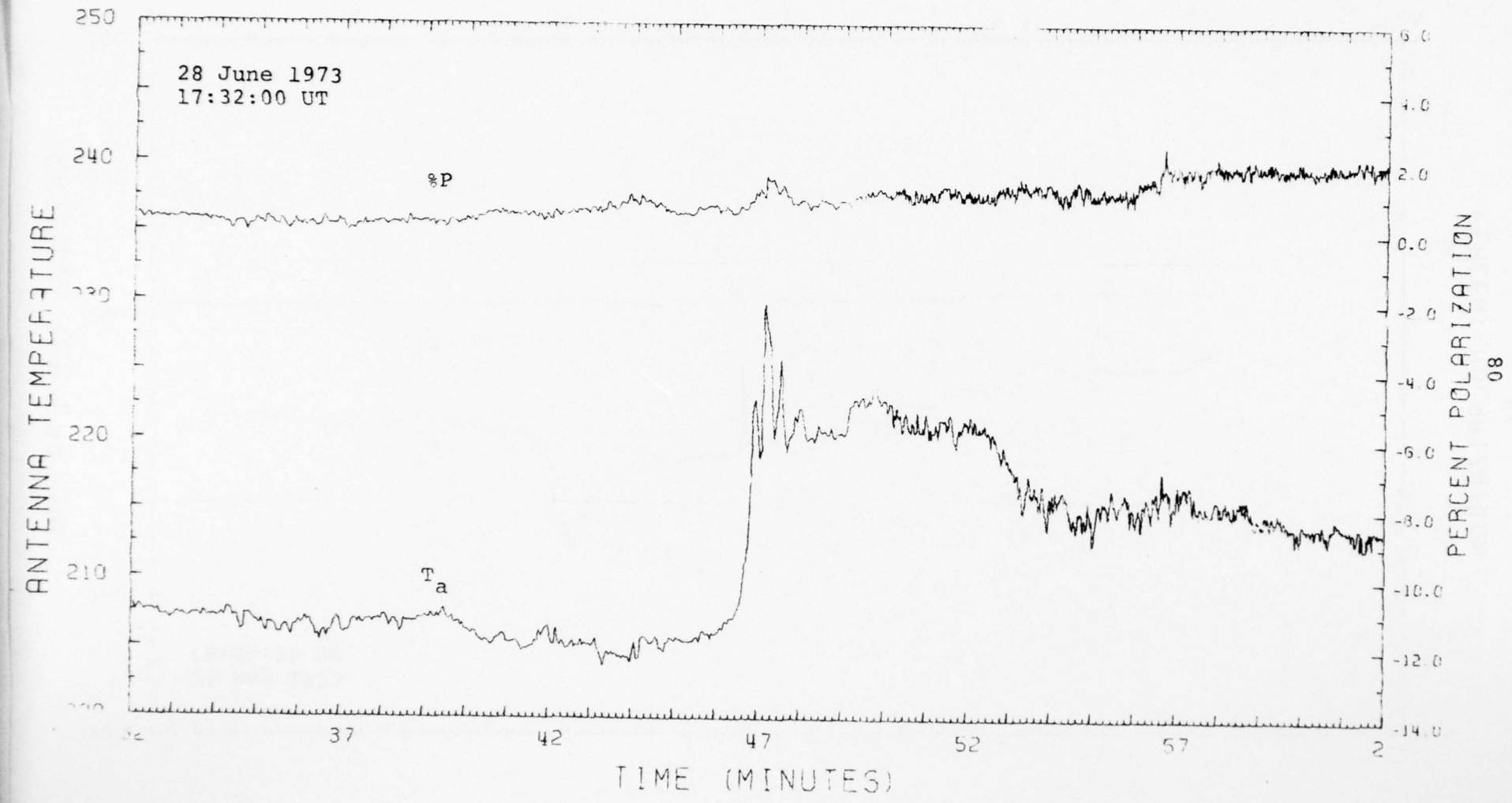
28 June 1973
17:32:00 UT
%P
T_a
250
240
230
220
210
ANTENNA TEMPERATURE
6.0
4.0
2.0
0.0
-2.0
-4.0
-6.0
-8.0
-10.0
-12.0
-14.0
PERCENT POLARIZATION
37
42
47
52
57
2
TIME (MINUTES)

FIGURE 3.2

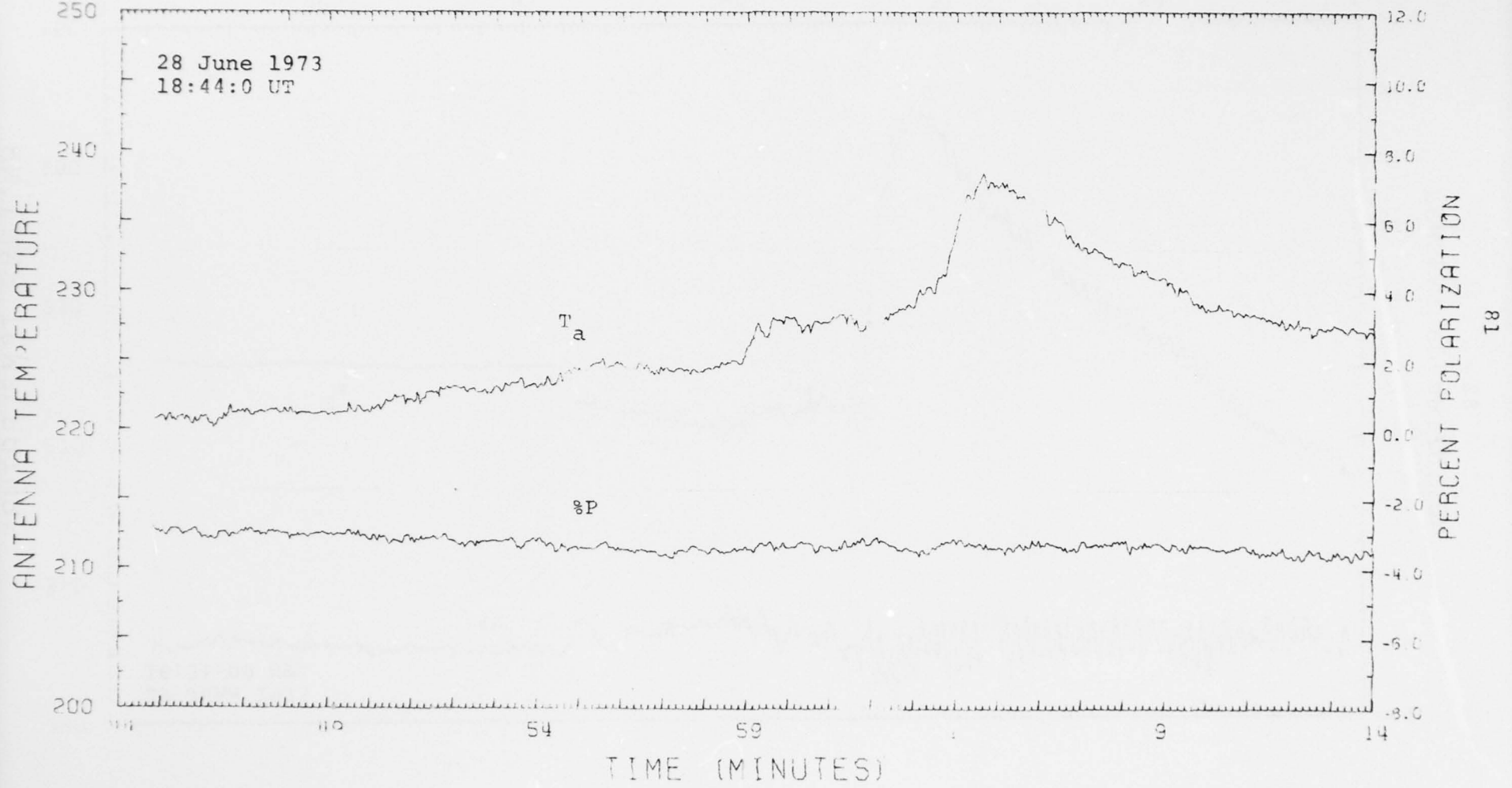
28 June 1973
18:44:0 UT
T_a
%P
ANTENNA TEMPERATURE
PERCENT POLARIZATION
TIME (MINUTES)
250
240
230
220
210
200
12.0
10.0
8.0
6.0
4.0
2.0
0.0
-2.0
-4.0
-6.0
-8.0
54
59
9
14

FIGURE 3.3

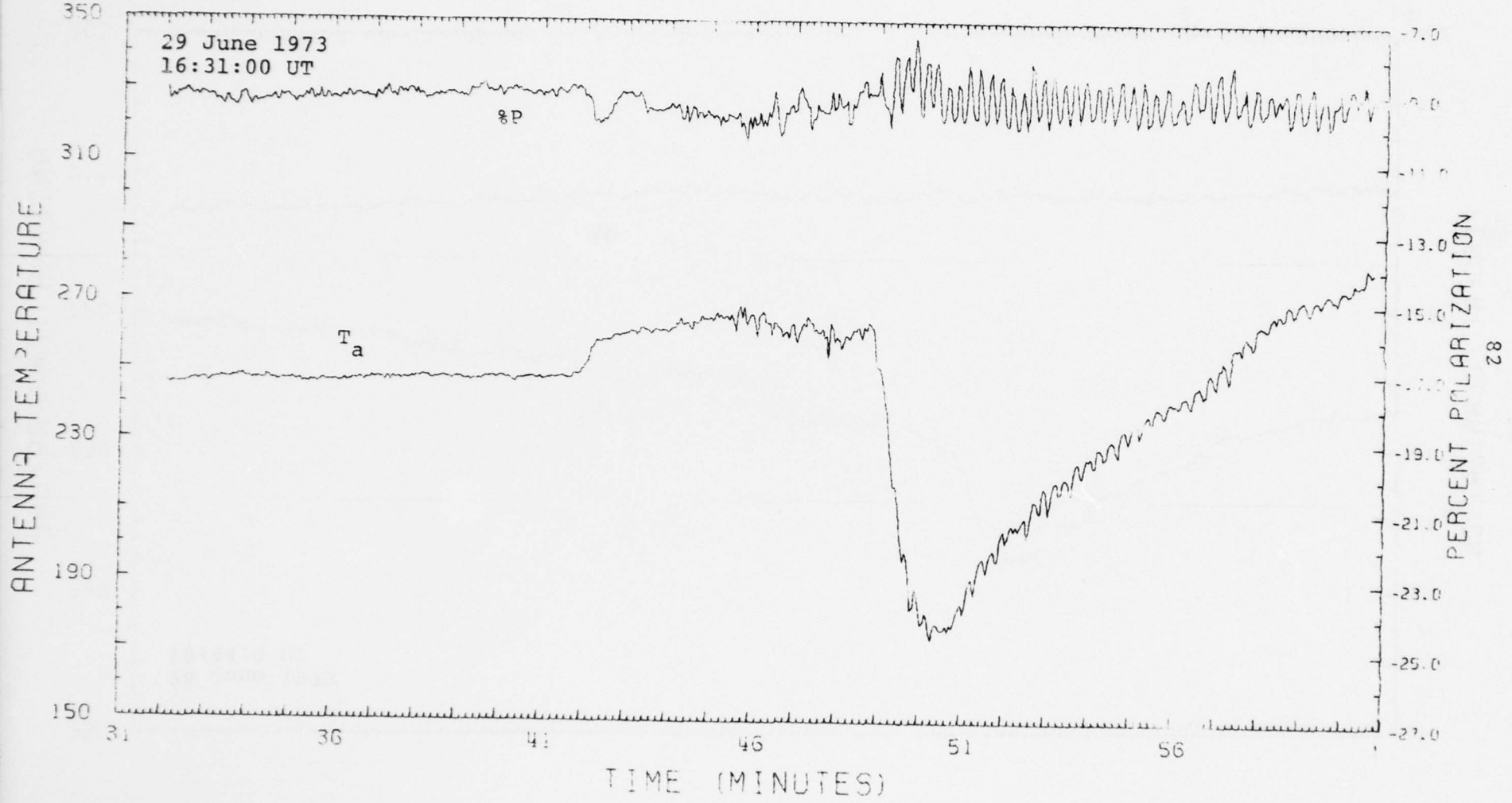
29 June 1973
16:31:00 UT
%P
T_a
ANTENNA TEMPERATURE
350
310
270
230
190
150
PERCENT POLARIZATION
-7.0
-13.0
-15.0
-19.0
-21.0
-23.0
-25.0
-27.0
31
36
41
46
51
56
TIME (MINUTES)

FIGURE 2.4

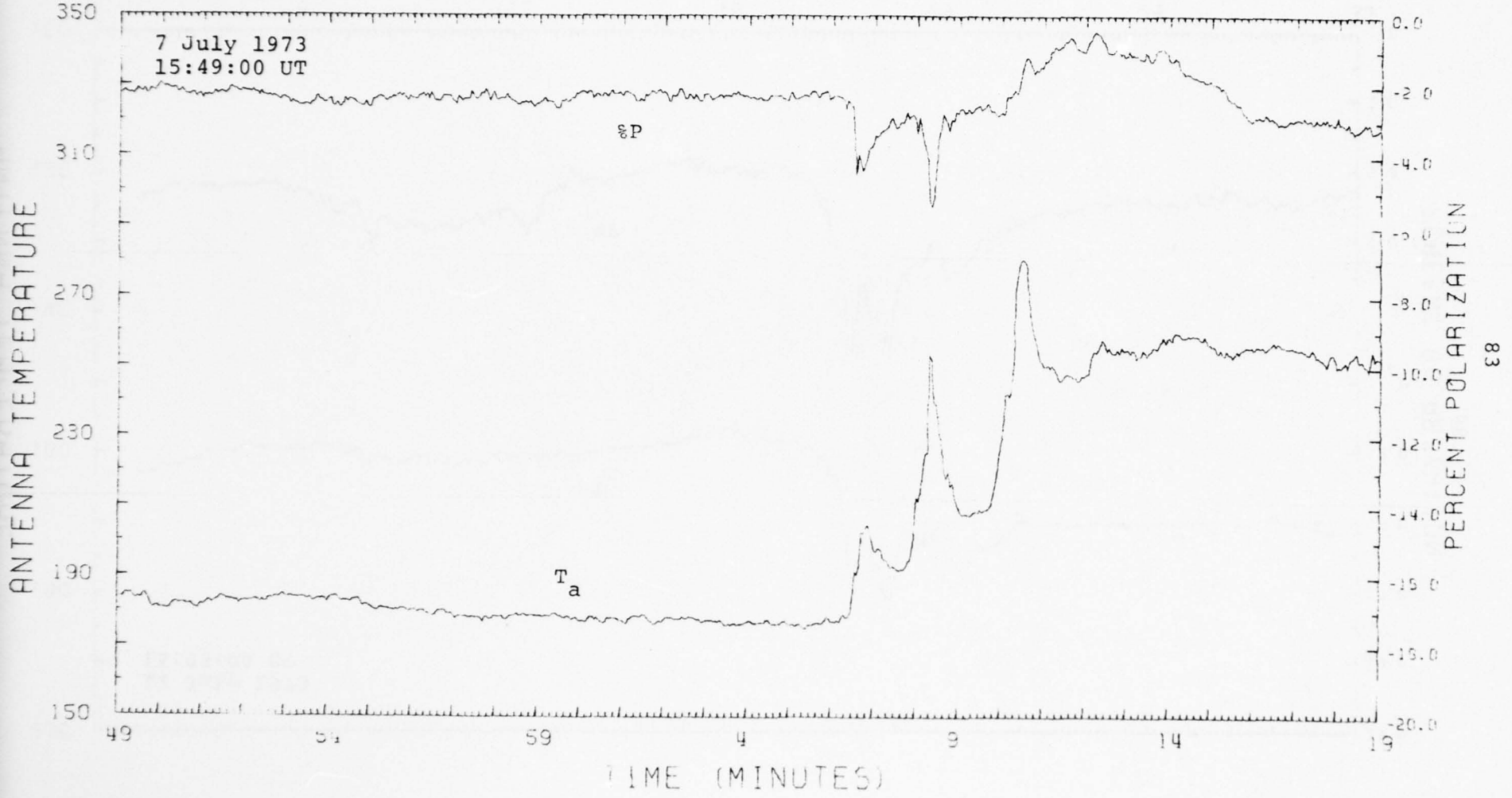
7 July 1973
15:49:00 UT
%P
T_a
ANTENNA TEMPERATURE
PERCENT POLARIZATION
TIME (MINUTES)
350
310
270
230
190
150
0.0
-2.0
-4.0
-6.0
-8.0
-10.0
-12.0
-14.0
-16.0
-18.0
-20.0
49
54
59
4
9
14
19

FIGURE 3.5

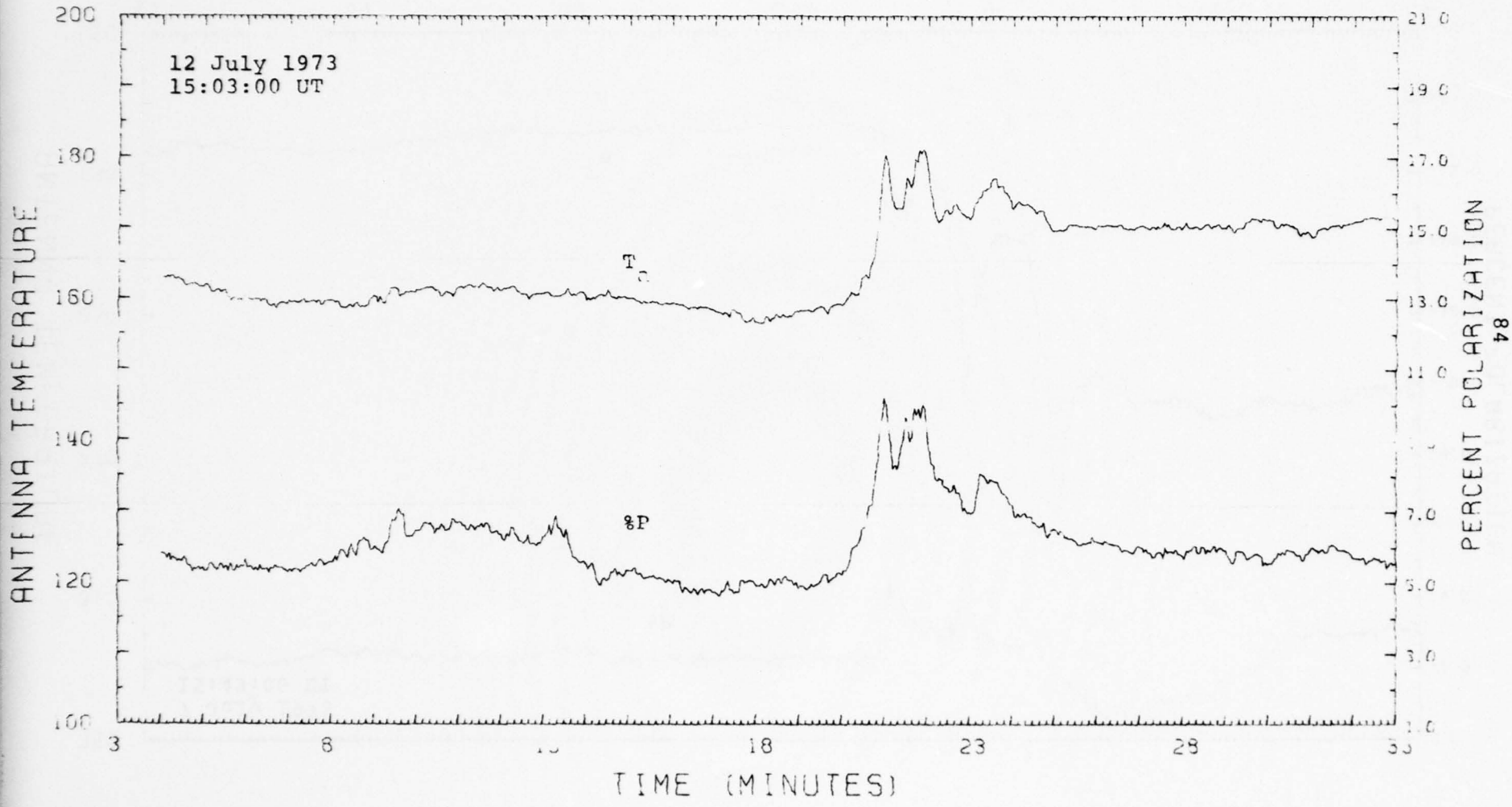
12 July 1973
15:03:00 UT
T_a
%P
ANTENNA TEMPERATURE
PERCENT POLARIZATION
TIME (MINUTES)
200
180
160
140
120
100
21.0
19.0
17.0
15.0
13.0
11.0
7.0
5.0
3.0
1.0
3
8
18
23
28

FIGURE 3.6

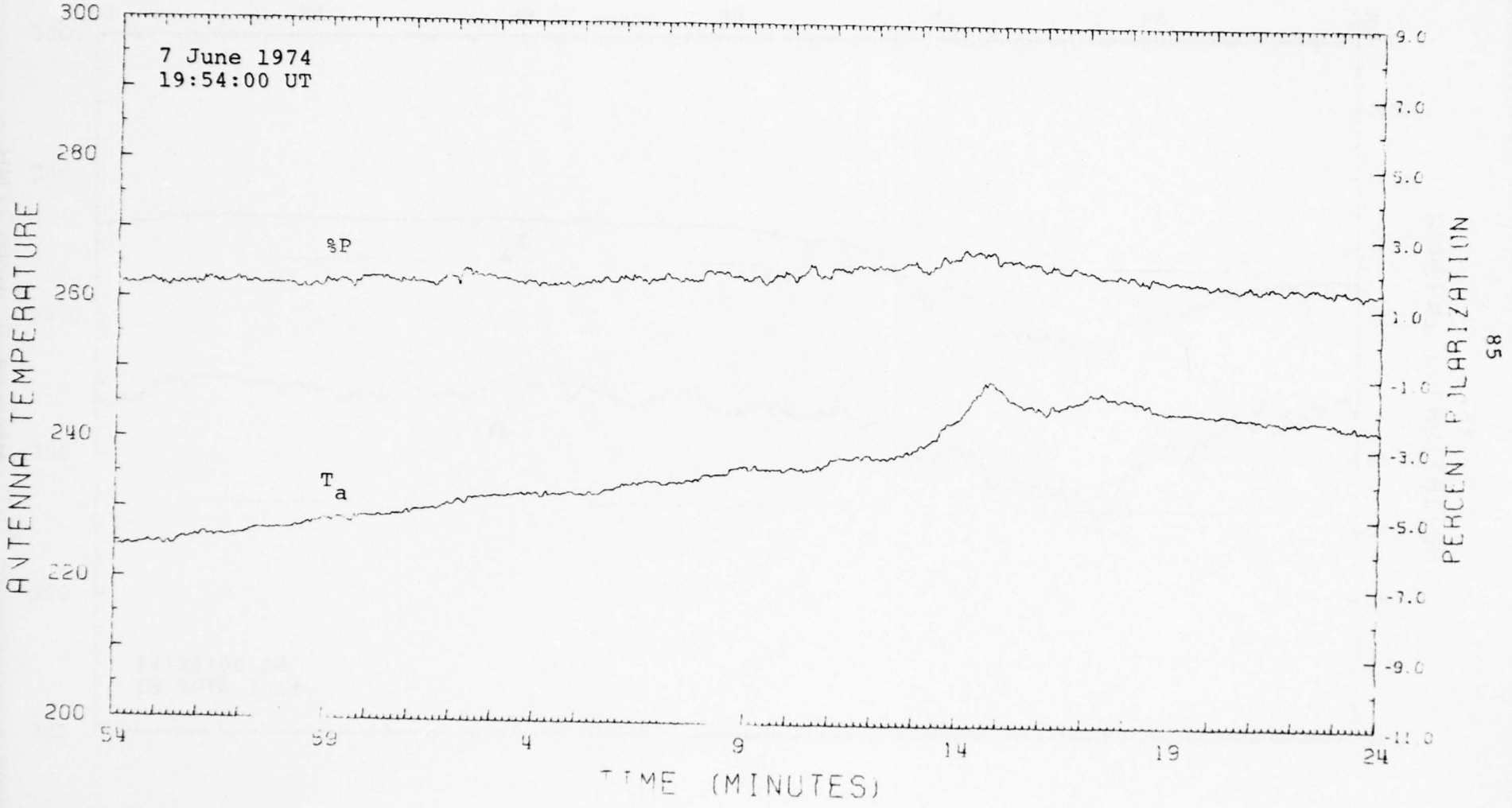
7 June 1974
19:54:00 UT
300
280
260
240
220
200
%P
T_a
ANTENNA TEMPERATURE
9.0
7.0
5.0
3.0
1.0
-1.0
-3.0
-5.0
-7.0
-9.0
-11.0
PERCENT POLARIZATION
54
59
4
9
14
19
24
TIME (MINUTES)

FIGURE 3.7

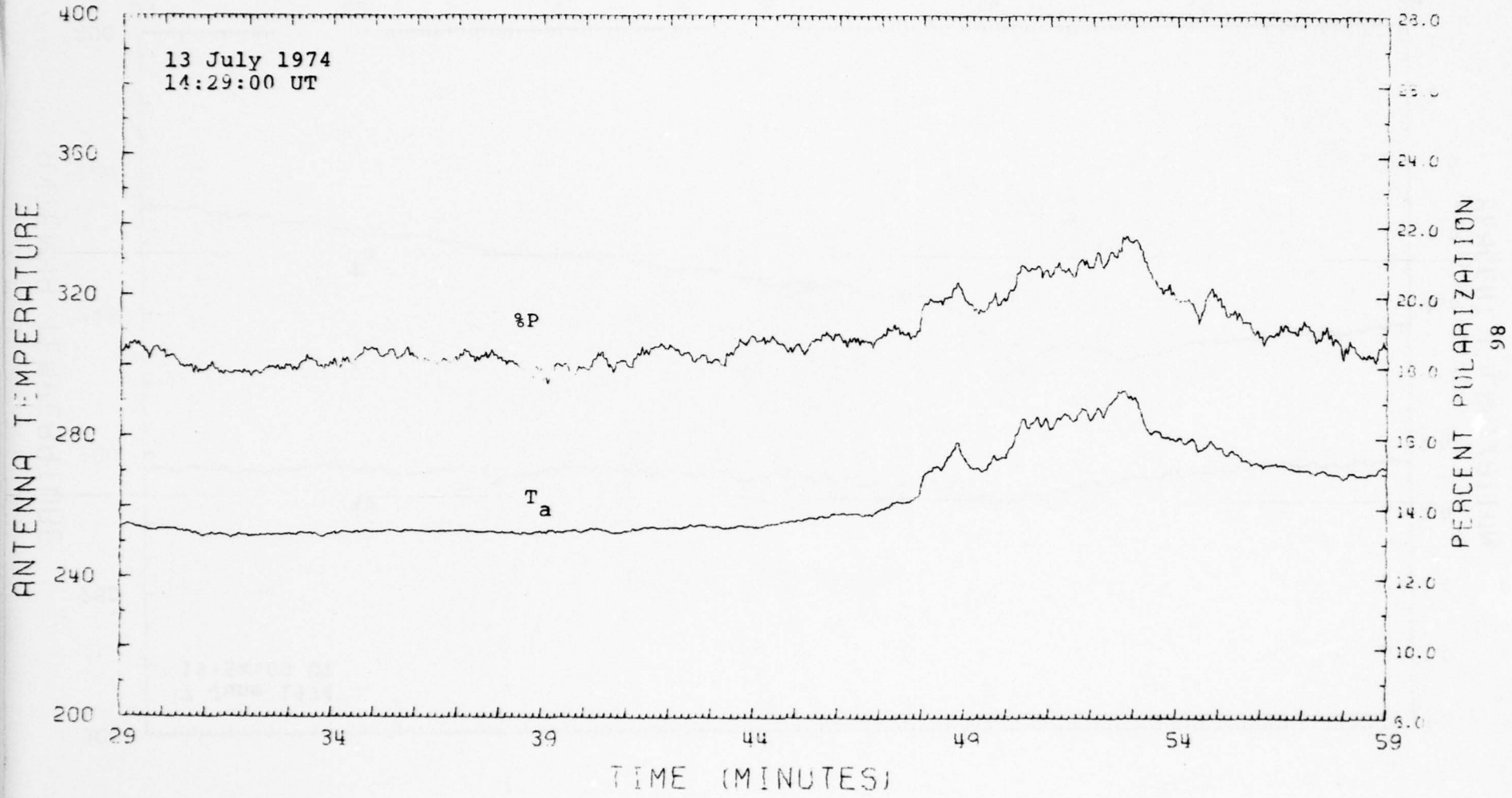
13 July 1974
14:29:00 UT
%P
T_a
ANTENNA TEMPERATURE
PERCENT POLARIZATION
TIME (MINUTES)
400
360
320
280
240
200
28.0
24.0
22.0
20.0
18.0
16.0
14.0
12.0
10.0
8.0
29
34
39
44
49
54
59

FIGURE 3.8

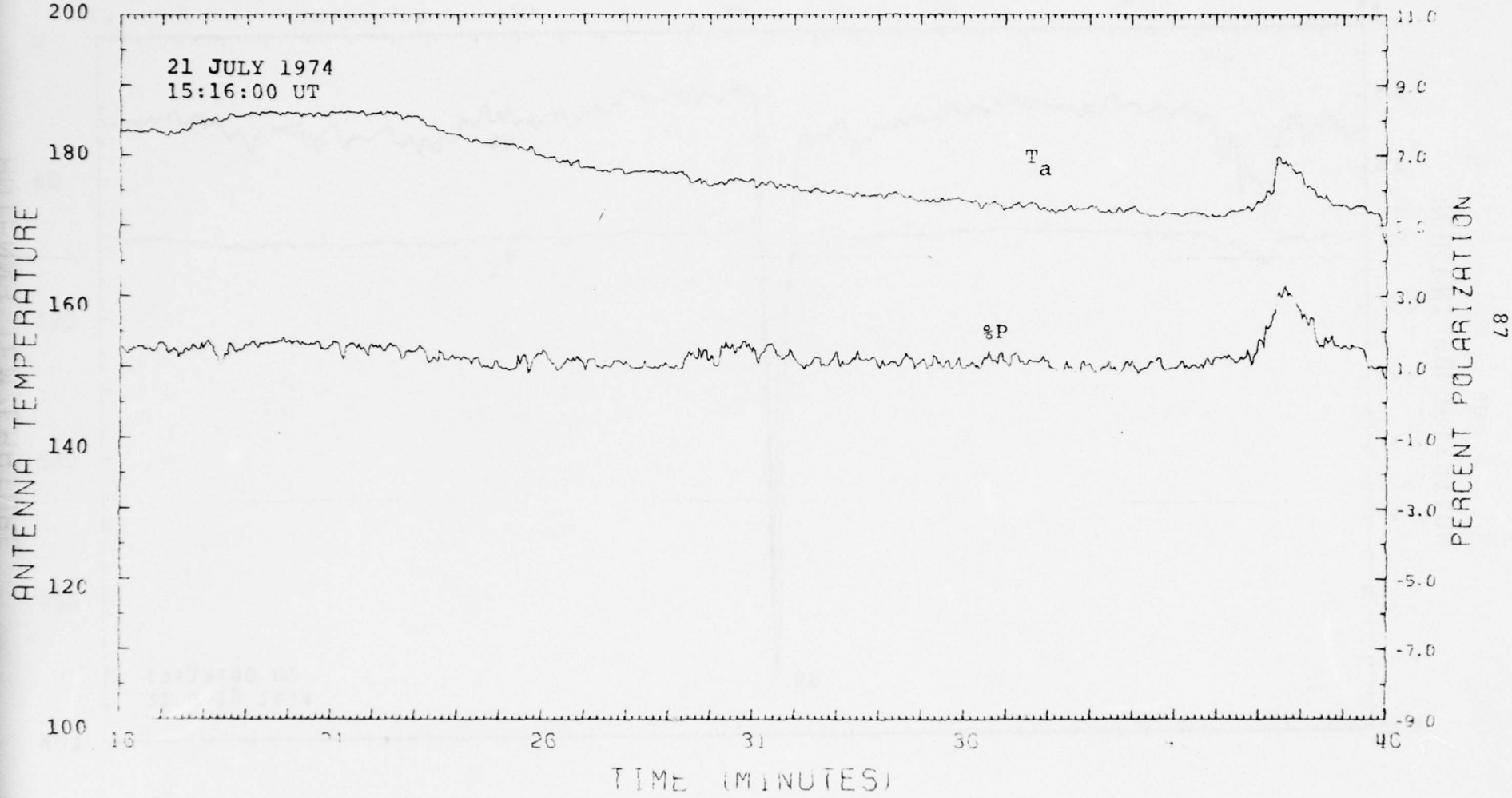
21 JULY 1974
15:16:00 UT
T_a
%P
ANTENNA TEMPERATURE
PERCENT POLARIZATION
TIME (MINUTES)
200
180
160
140
120
100
11.0
9.0
7.0
3.0
1.0
-1.0
-3.0
-5.0
-7.0
-9.0
16
21
26
31
36
40

FIGURE 3.9

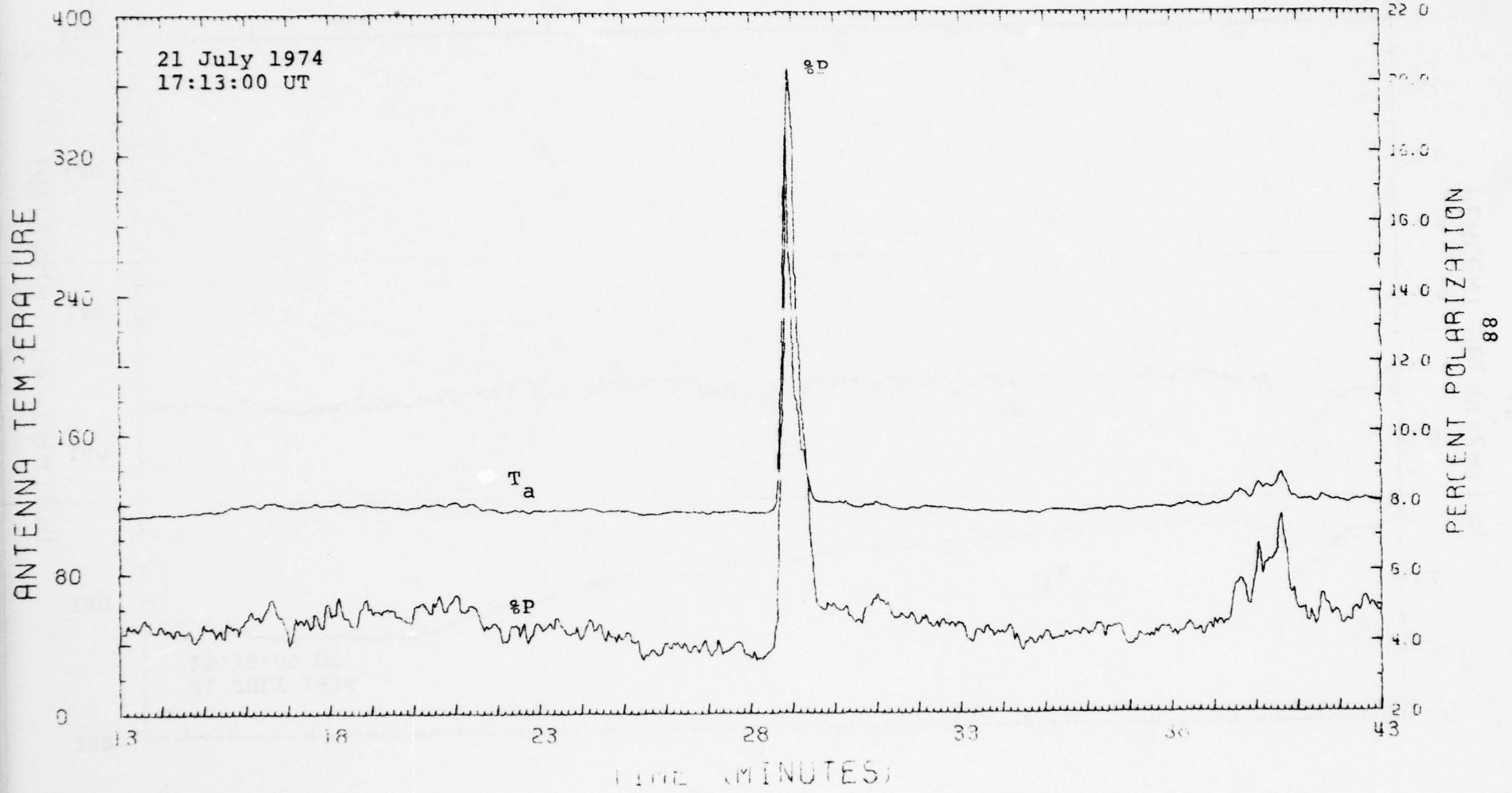
21 July 1974
17:13:00 UT
%D
T_a
%P
ANTENNA TEMPERATURE
PERCENT POLARIZATION
400
320
240
160
80
0
22.0
18.0
16.0
14.0
12.0
10.0
8.0
6.0
4.0
2.0
13
18
23
28
33
43
TIME (MINUTES)

FIGURE 3.10

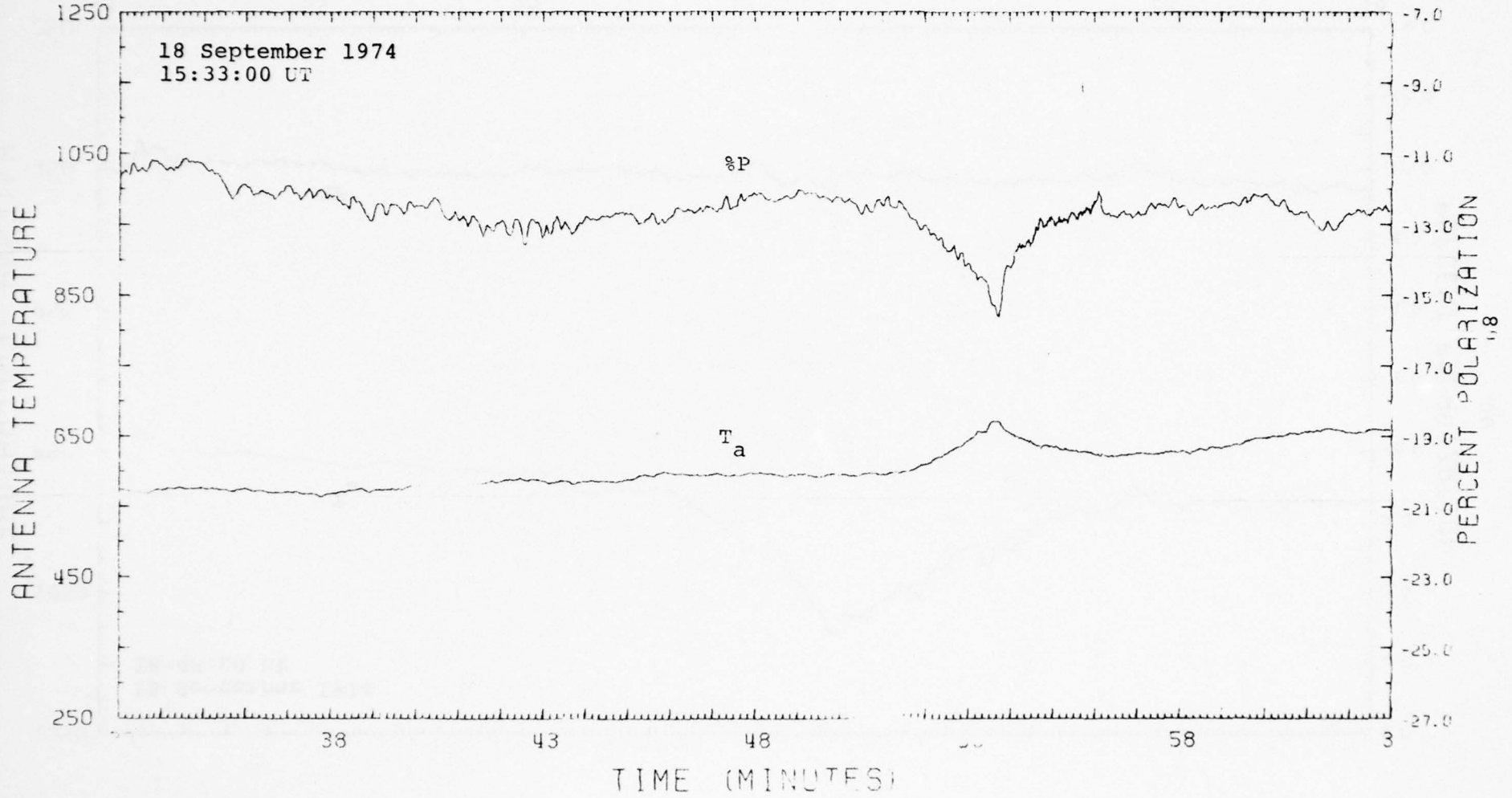
18 September 1974
15:33:00 UT
%P
T_a
ANTENNA TEMPERATURE
PERCENT POLARIZATION
1250
1050
850
650
450
250
-7.0
-9.0
-11.0
-13.0
-15.0
-17.0
-19.0
-21.0
-23.0
-25.0
-27.0
38
43
48
58
3
TIME (MINUTES)

FIGURE 3.11

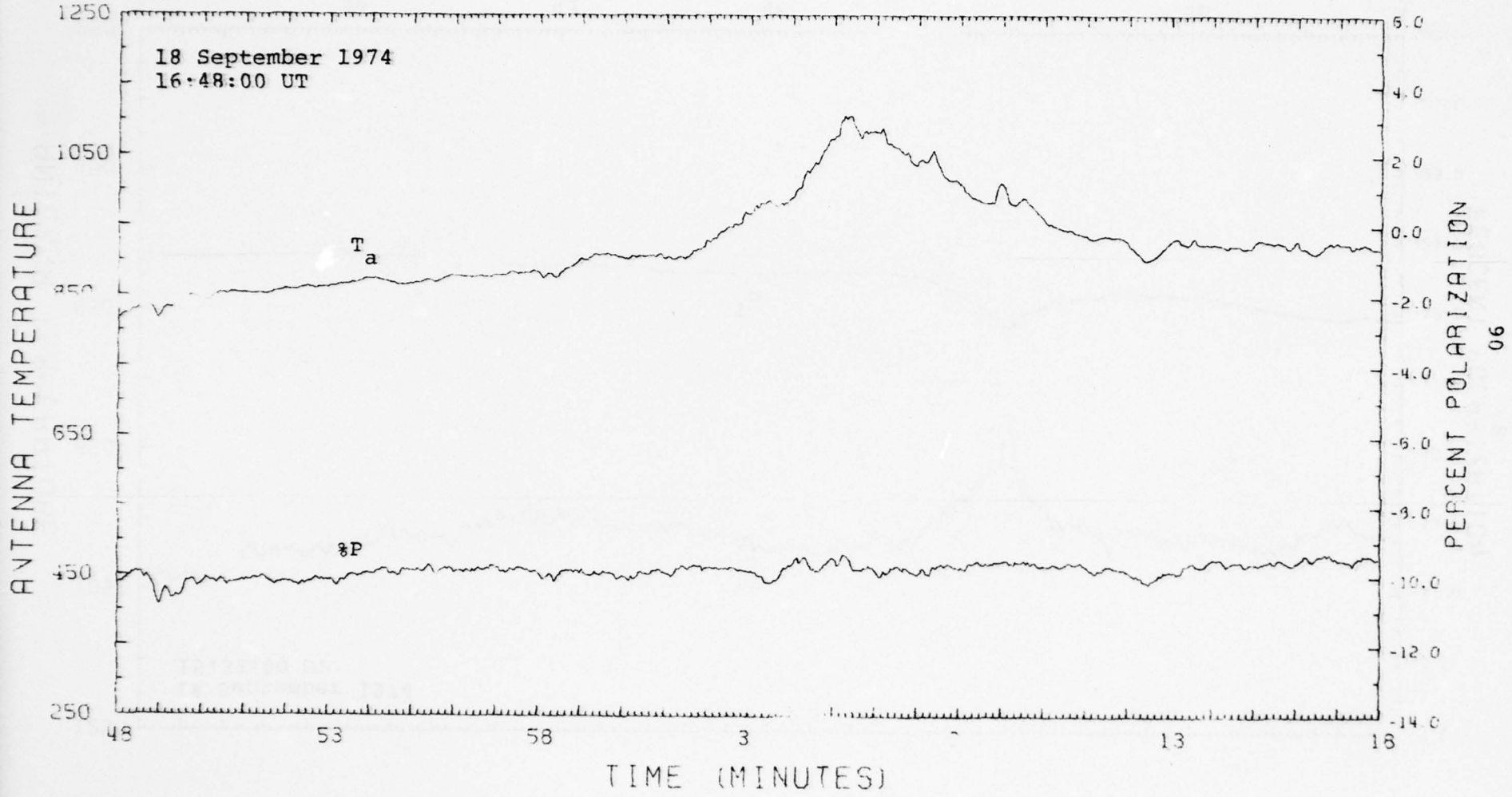
18 September 1974
16:48:00 UT
T_a
%P
ANTENNA TEMPERATURE
PERCENT POLARIZATION
TIME (MINUTES)
1250
1050
650
250
6.0
4.0
2.0
0.0
-2.0
-4.0
-6.0
-8.0
-10.0
-12.0
-14.0
48
53
58
3
13
18

FIGURE 3.12

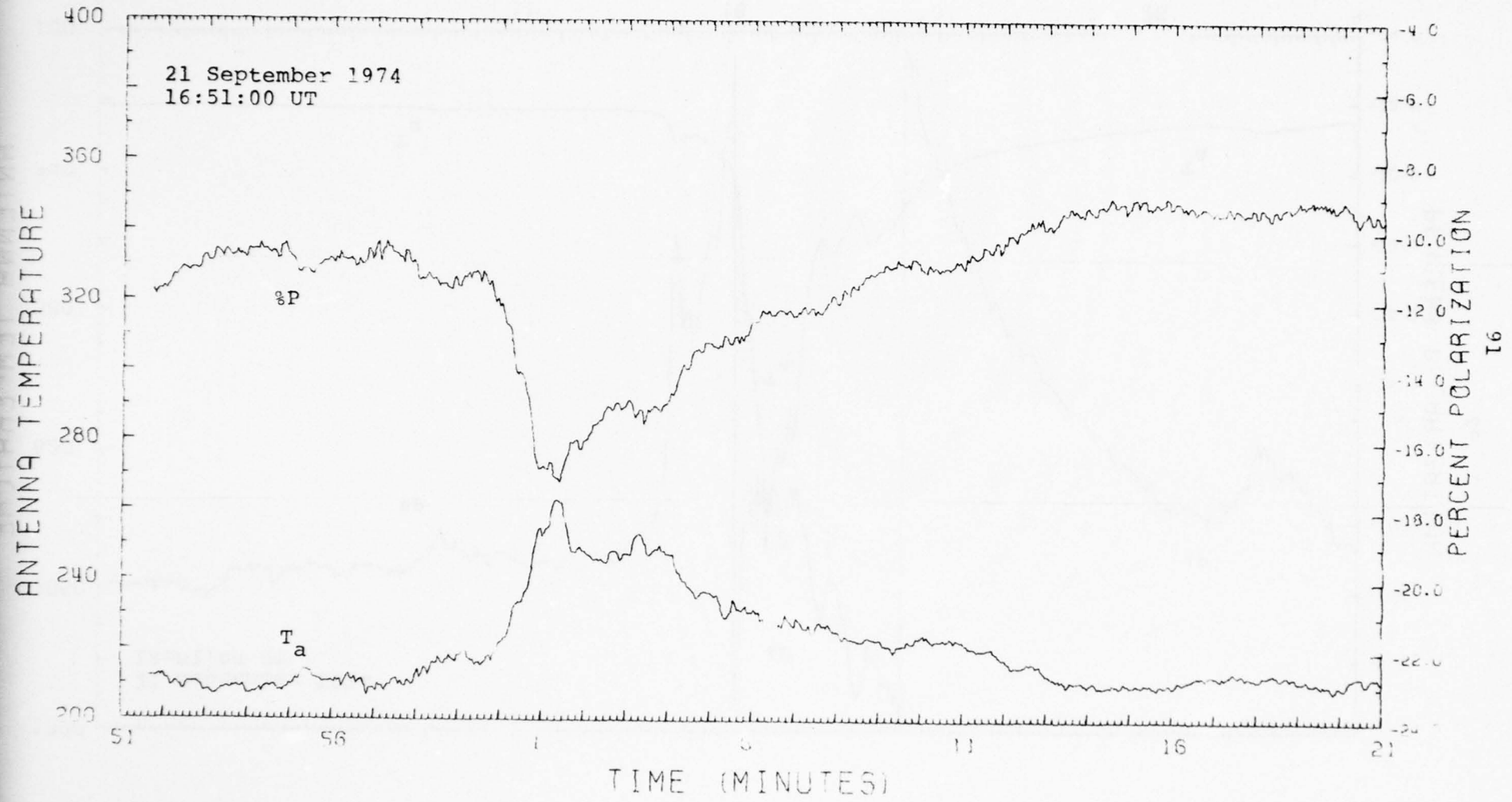
21 September 1974
16:51:00 UT
400
360
320
280
240
200
ANTENNA TEMPERATURE
%P
T_a
-4.0
-6.0
-8.0
-10.0
-12.0
-14.0
-16.0
-18.0
-20.0
PERCENT POLARIZATION
51
56
1
6
11
16
21
TIME (MINUTES)

FIGURE 3.13

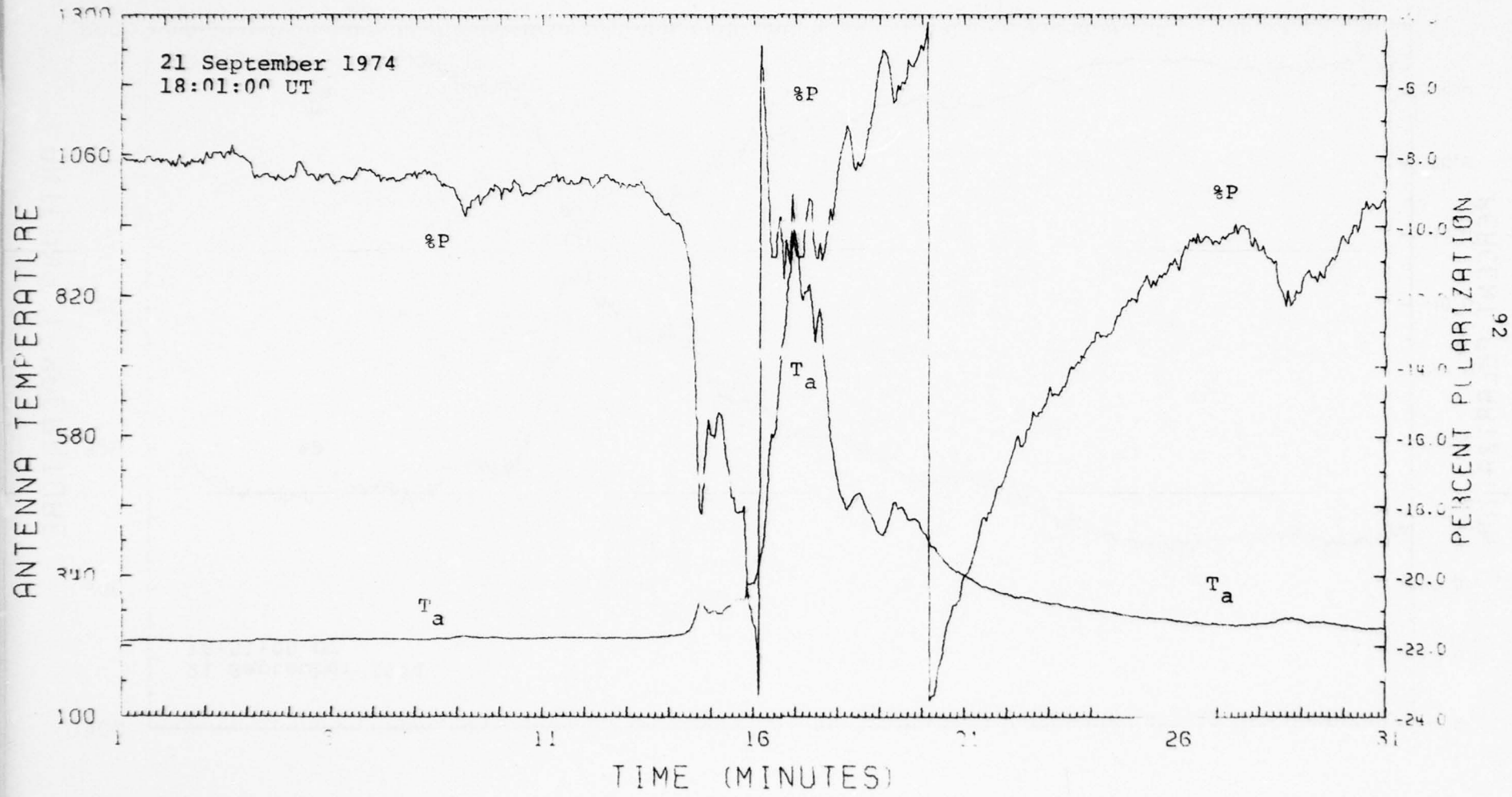
21 September 1974
18:01:00 UT
%P
%P
%P
T_a
T_a
T_a
1060
820
580
100
1
11
16
26
ANTENNA TEMPERATURE
PERCENT POLARIZATION
-8.0
-10.0
-16.0
-20.0
-22.0
TIME (MINUTES)

FIGURE 3.14

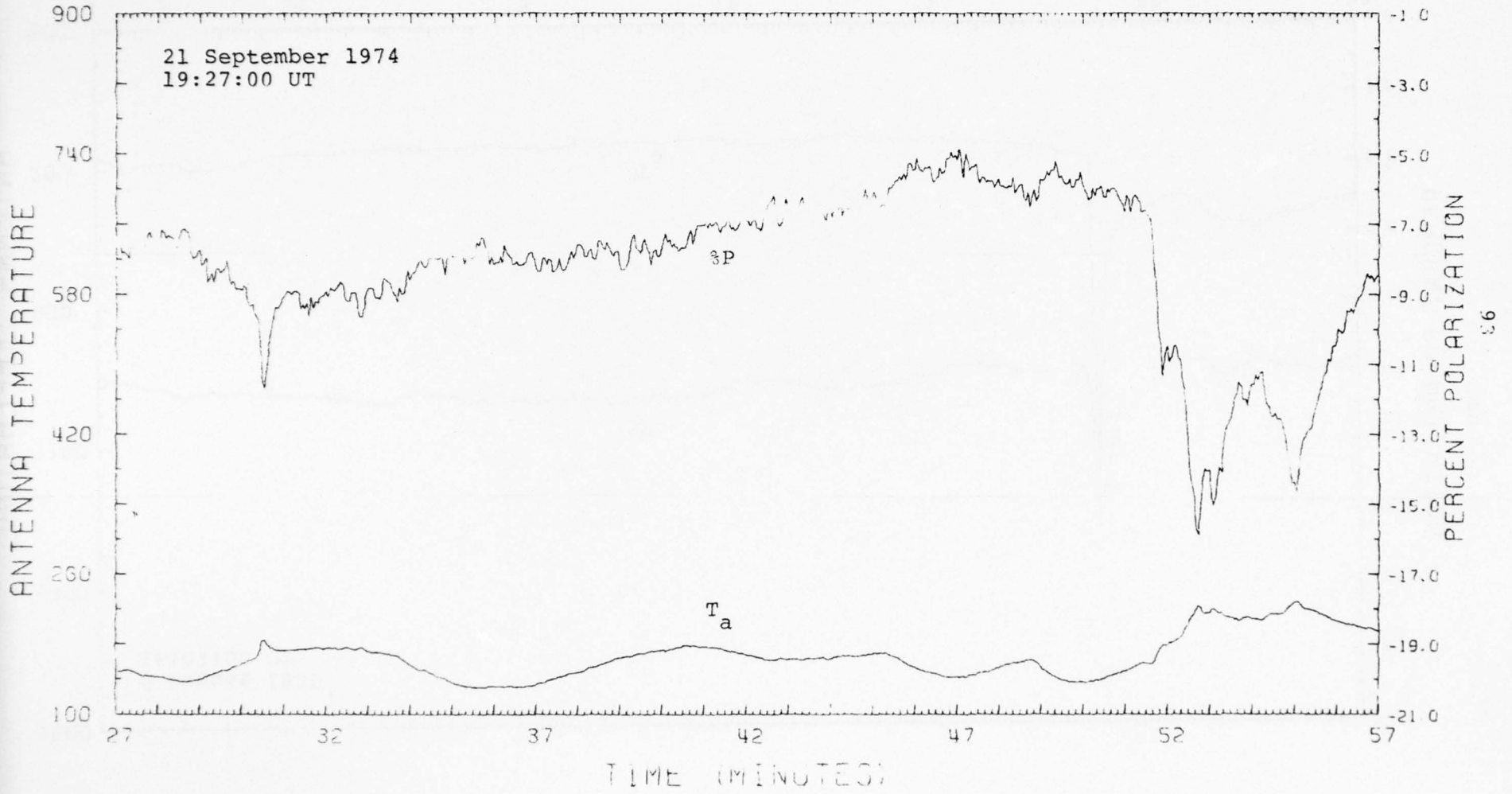
21 September 1974
19:27:00 UT
900
740
580
420
260
100
ANTENNA TEMPERATURE
3P
T_a
-1.0
-3.0
-5.0
-7.0
-9.0
-11.0
-13.0
-15.0
-17.0
-19.0
-21.0
PERCENT POLARIZATION
27
32
37
42
47
52
57
TIME (MINUTES)

FIGURE 3.15

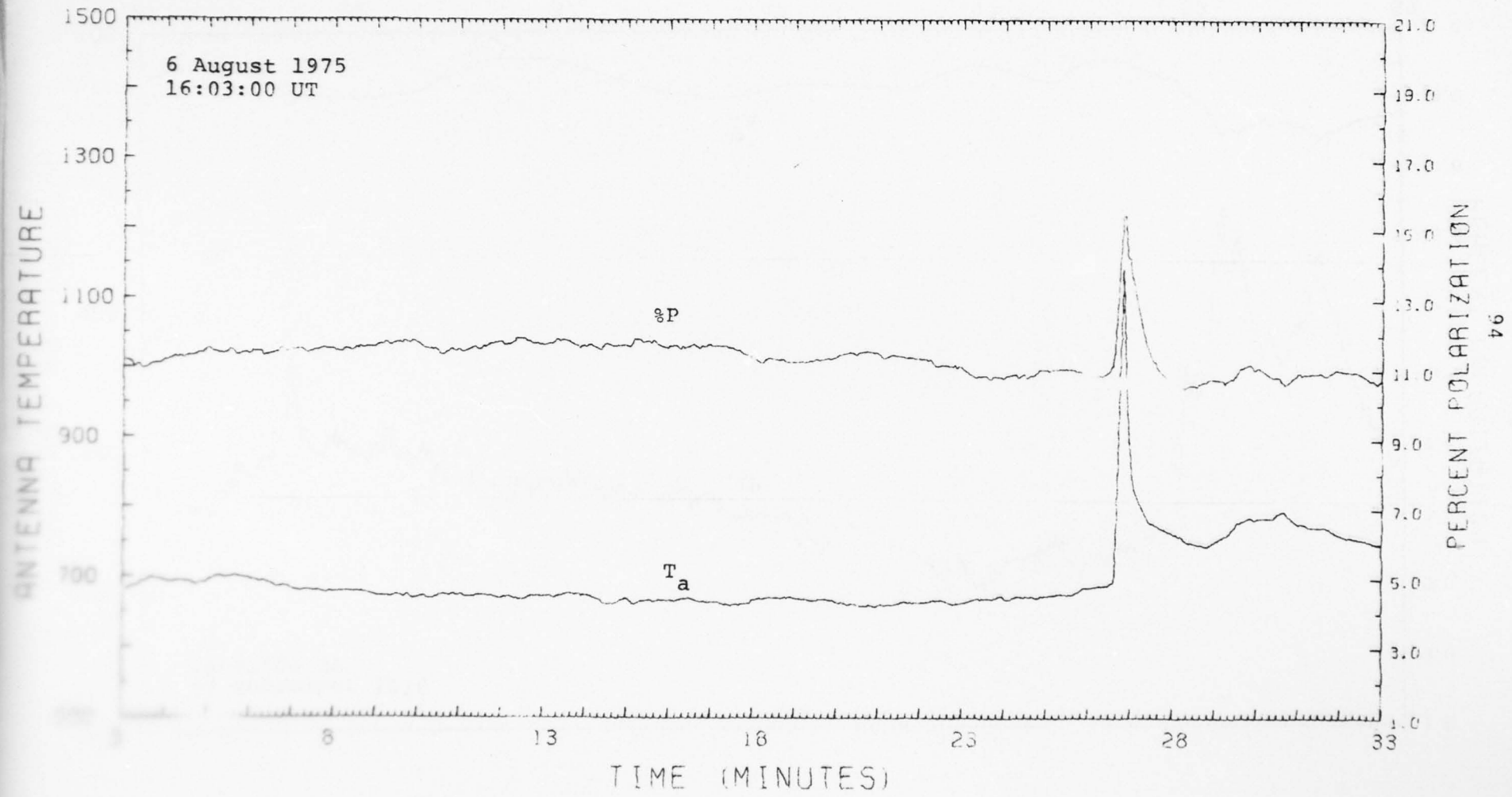
6 August 1975
16:03:00 UT
%P
T_a
ANTENNA TEMPERATURE
PERCENT POLARIZATION
TIME (MINUTES)
1500
1300
1100
900
700
21.0
19.0
17.0
13.0
11.0
9.0
7.0
5.0
3.0
1.0
8
13
18
23
28
33

FIGURE 3.16

AD-A052 360 BOSTON UNIV MASS DEPT OF ASTRONOMY F/G 3/2
RADIO FLARE STUDIES AT 4 CM.(U)
JAN 78 M D PAPAGIANNIS, F L WEFER F19628-76-C-0027
UNCLASSIFIED SER-II-NO-66 AFGL-TR-78-0014 NL

2 OF 2
ADA
052360

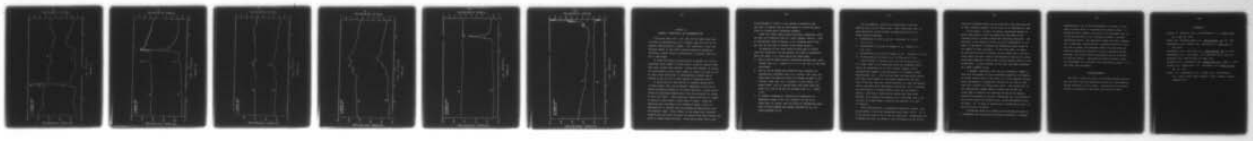

END
DATE
FILMED
5-78
DDC

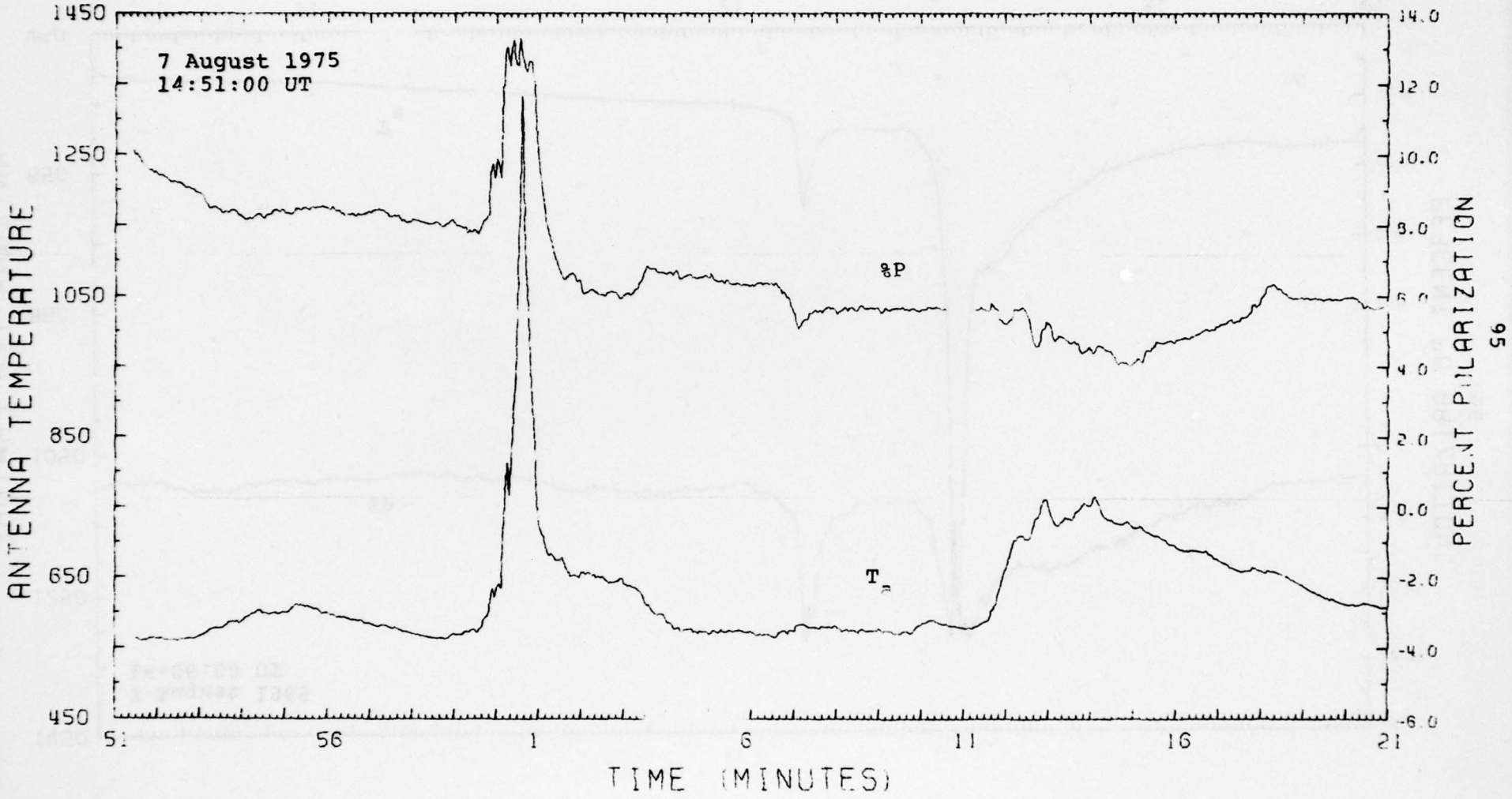
7 August 1975
14:51:00 UT
%P
T_a
ANTENNA TEMPERATURE
PERCENT POLARIZATION
TIME (MINUTES)
1450
1250
1050
850
650
450
14.0
12.0
10.0
8.0
4.0
2.0
0.0
-2.0
-4.0
-6.0
51
56
1
6
11
16
21

FIGURE 3.17

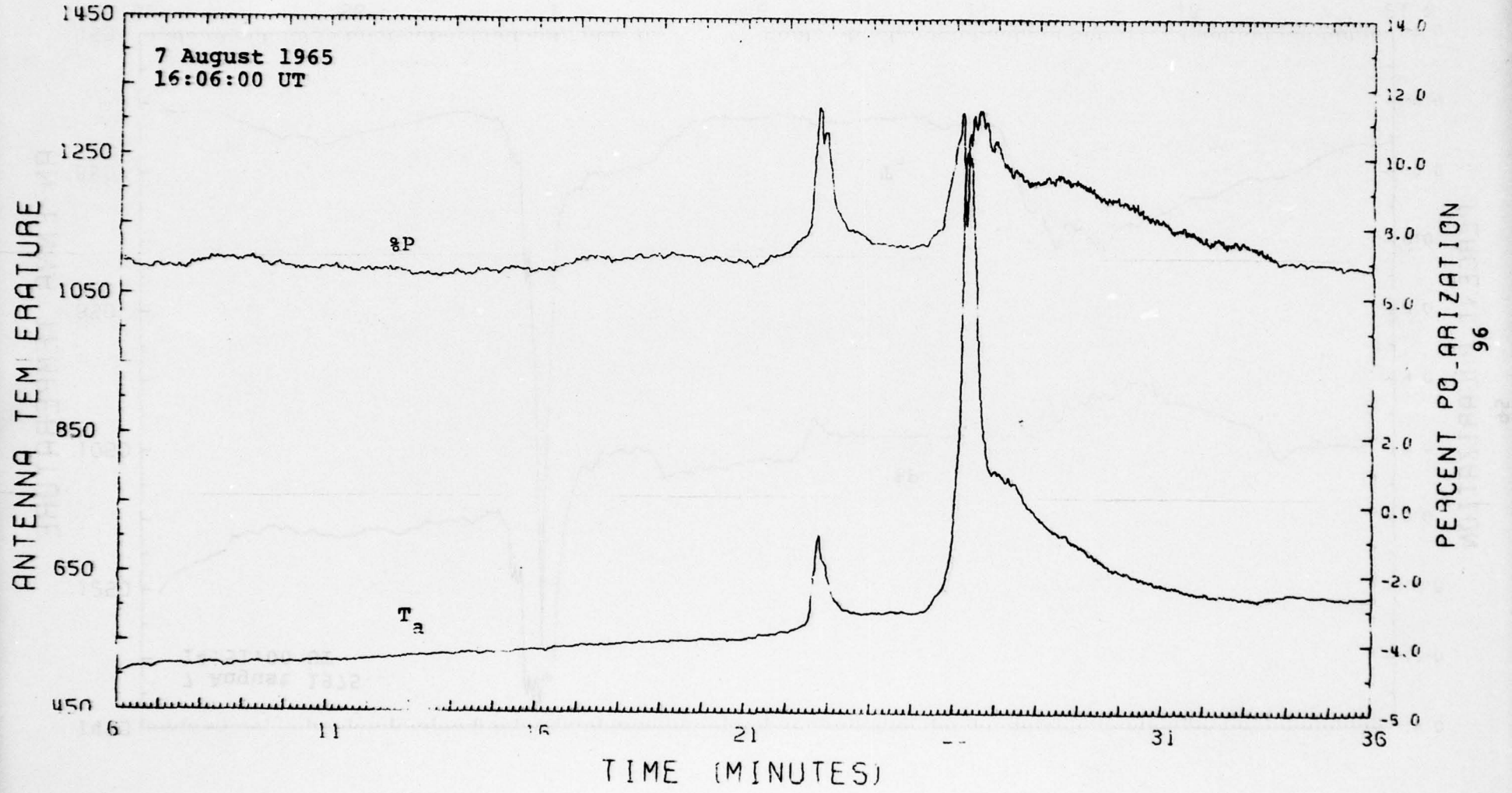
7 August 1965
16:06:00 UT
1450
1250
1050
850
650
450
ANTENNA TEMPERATURE
%P
T_a
14.0
12.0
10.0
8.0
6.0
2.0
0.0
-2.0
-4.0
-5.0
PERCENT POLARIZATION
96
6
11
16
21
31
36
TIME (MINUTES)

FIGURE 3.18

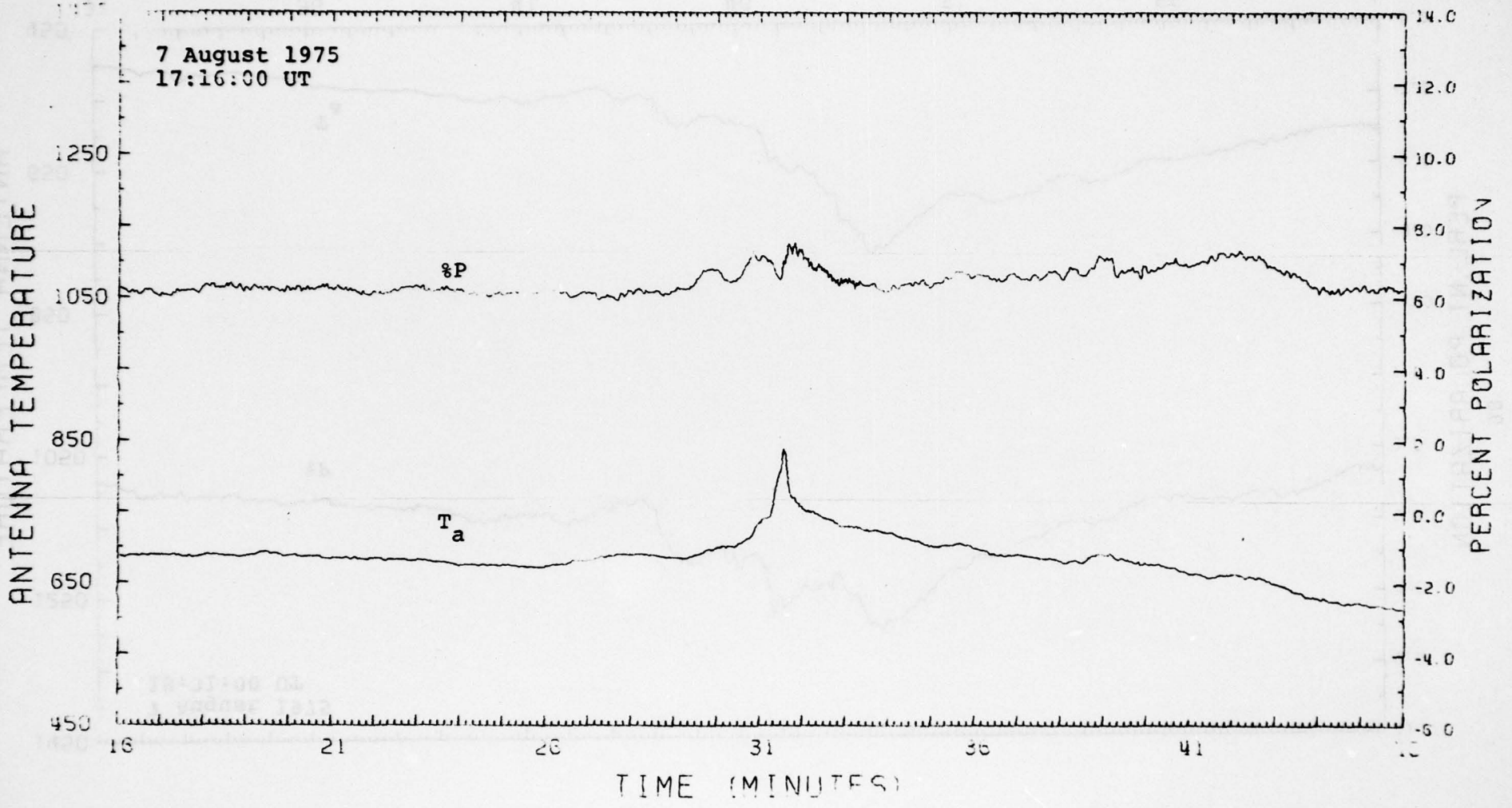
7 August 1975
17:16:00 UT
%P
T_a
ANTENNA TEMPERATURE
PERCENT POLARIZATION
TIME (MINUTES)
1250
1050
850
650
450
14.0
12.0
10.0
8.0
6.0
4.0
2.0
0.0
-2.0
-4.0
-6.0
16
21
26
31
36
41

FIGURE 3.19

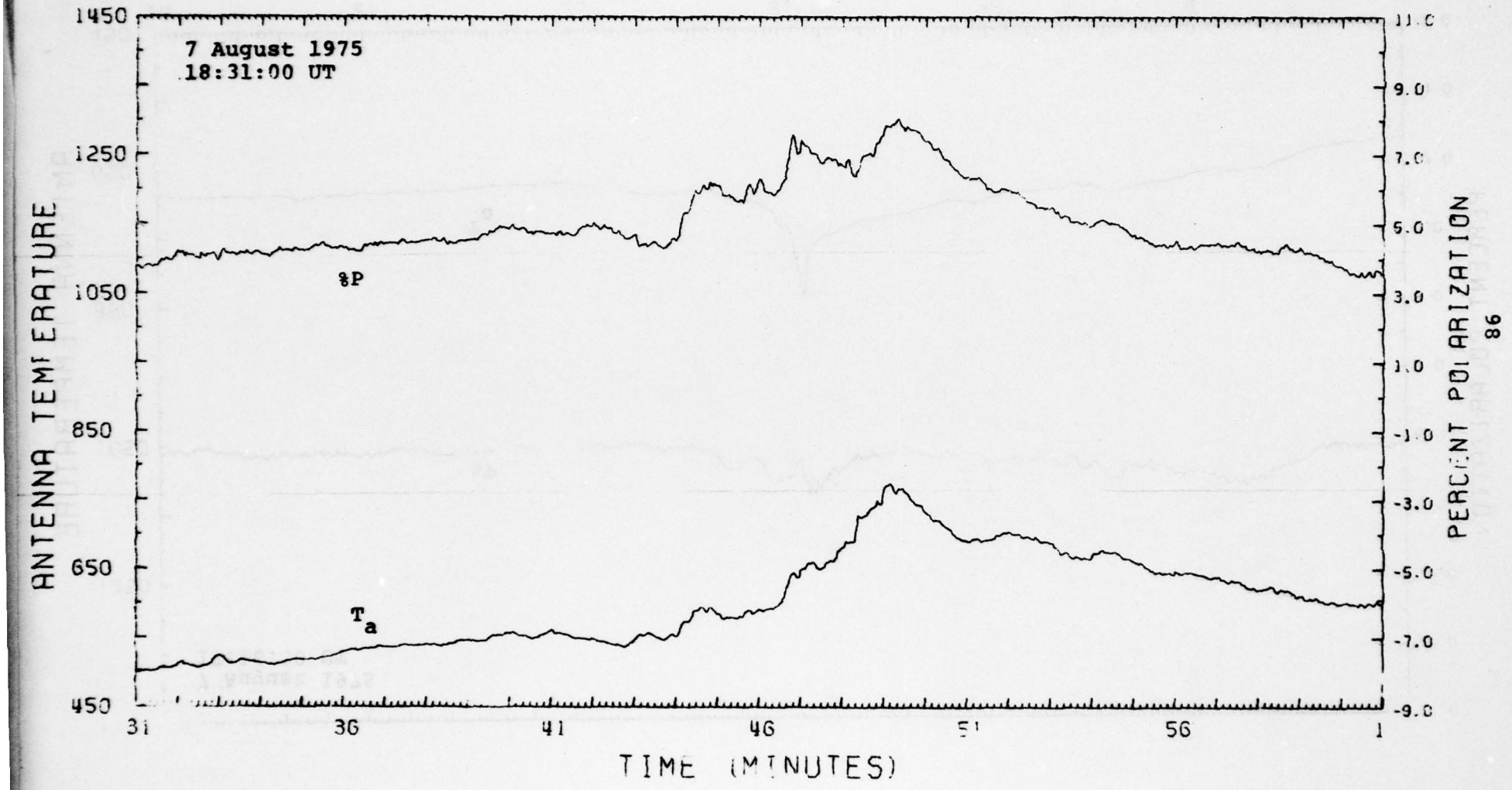
7 August 1975
18:31:00 UT
%P
T_a
ANTENNA TEMPERATURE
PERCENT POLARIZATION
TIME (MINUTES)
1450
1250
1050
850
650
450
11.0
9.0
7.0
5.0
3.0
1.0
-1.0
-3.0
-5.0
-7.0
-9.0
31
36
41
46
51
56
1
86

FIGURE 3.20

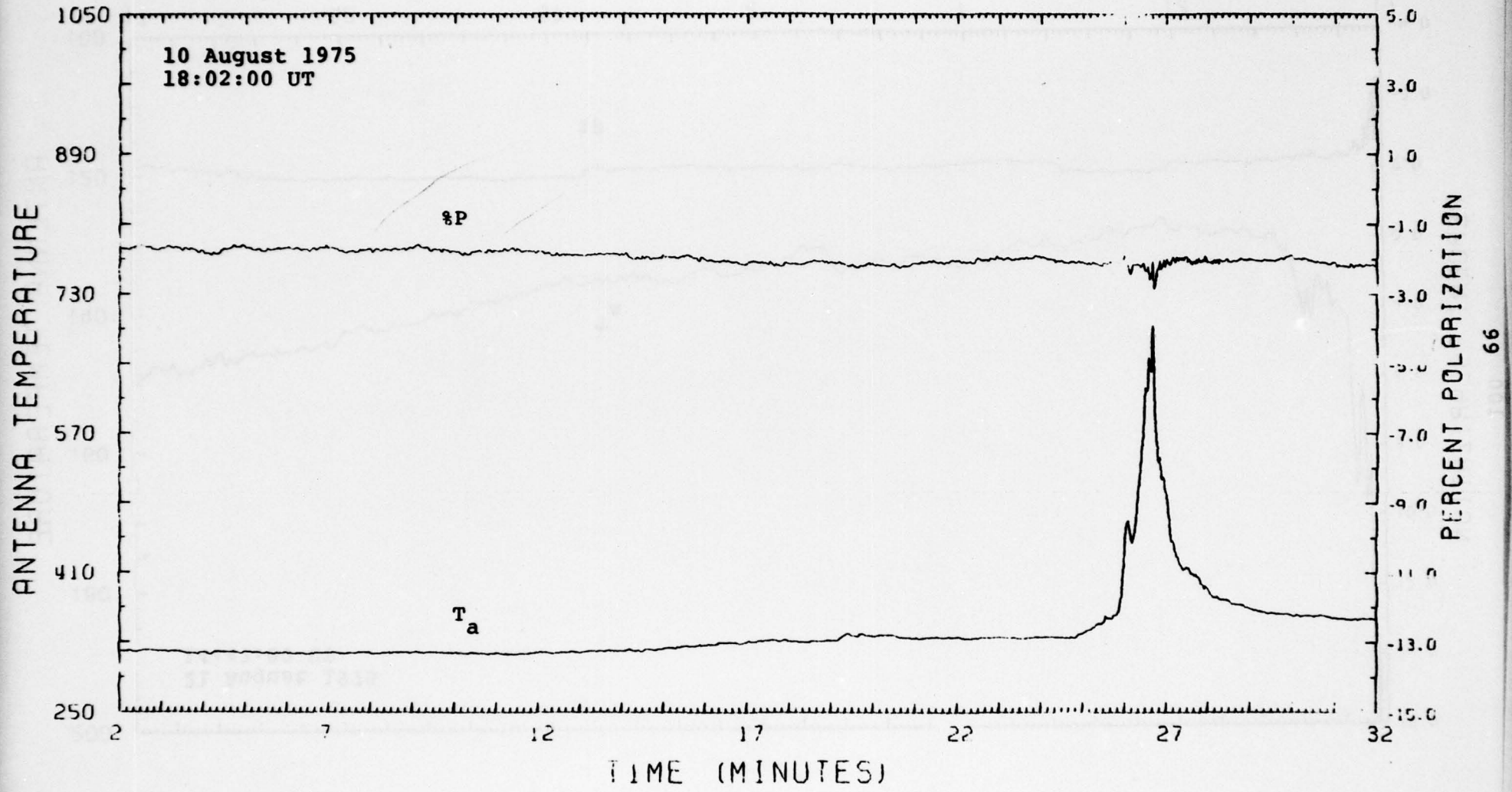
10 August 1975
18:02:00 UT
%P
T_a
1050
890
730
570
410
250
ANTENNA TEMPERATURE
5.0
3.0
1.0
-1.0
-3.0
-7.0
-13.0
PERCENT POLARIZATION
2
7
12
17
22
27
32
TIME (MINUTES)

FIGURE 3.21

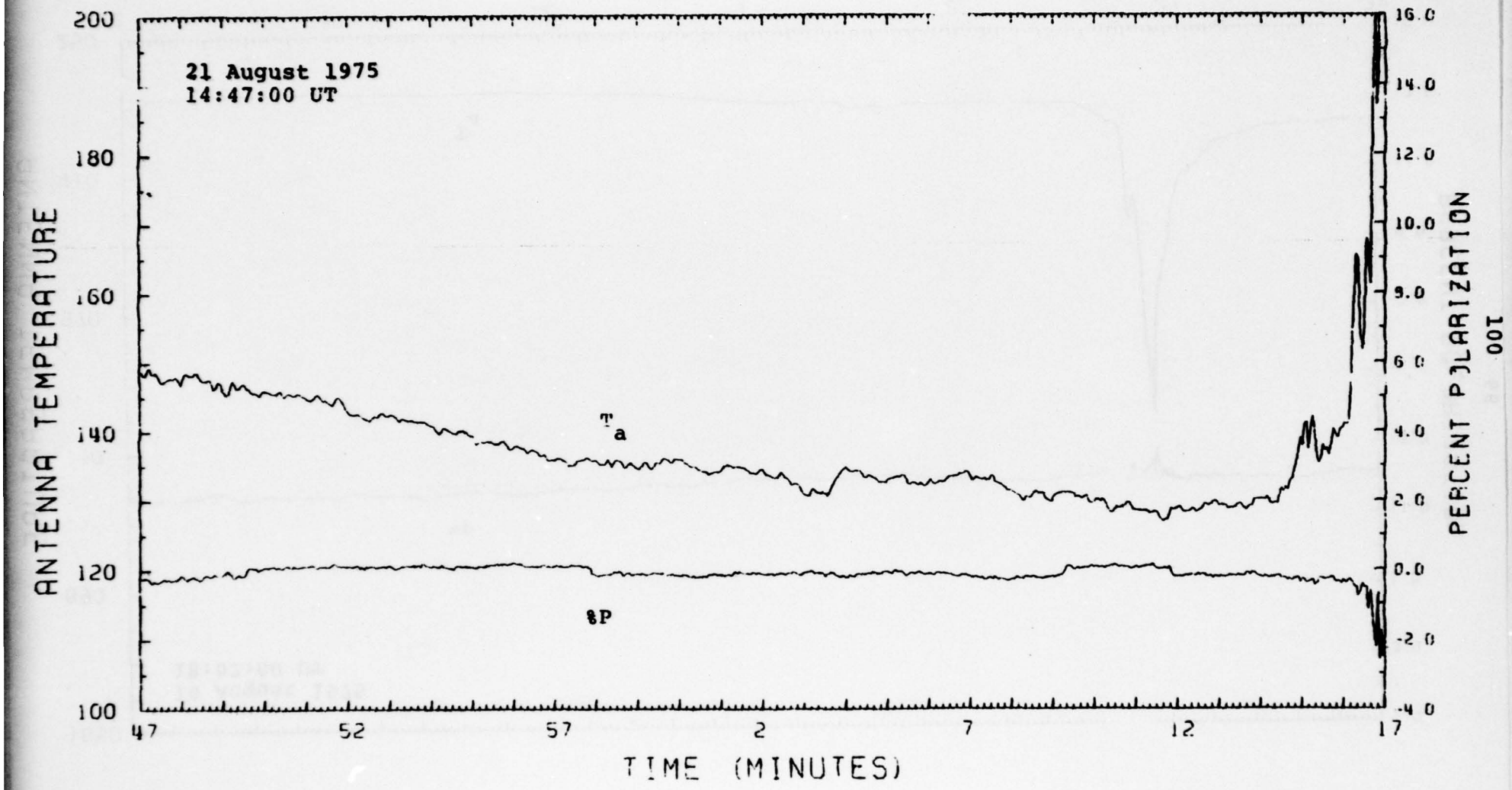
21 August 1975
14:47:00 UT
ANTENNA TEMPERATURE
200
180
160
140
120
100
T_a
$P
PERCENT POLARIZATION
16.0
14.0
12.0
10.0
9.0
6.0
4.0
2.0
0.0
-2.0
-4.0
100
47
52
57
2
7
12
17
TIME (MINUTES)

FIGURE 3.22

Chapter IV

SUMMARY, CONCLUSIONS, AND RECOMMENDATIONS

During the years 1973, 1974, and 1975 we logged more than 330 hours of observations on 63 different days with the 120 ft. Haystack radiotelescope of NEROC. This represents a very substantial amount of data which required extensive processing, including a rather painful transcription of computer tapes from CDC to IBM format.

In these long hours of observations we managed to record a relatively small number of flare events, primarily because these were years around solar minimum. During solar maxima, of course, one would expect a much larger number of events, but they are not as clean since there might be simultaneously several active regions on the sun all of them capable of producing flares.

In three years of observations we recorded approximately 30 minor events (with the brightness temperature of the active region increasing between 10% and 100%) and about 3 major events (with the brightness temperature of the active region increasing by more than 250%). This essentially implies that one can expect to observe a small event roughly every 10 hours. Since our observing days consisted on the average of about 5 hours of observations, it implies that we recorded one small event every two observing days. Major events, on the other hand, occurred roughly only once every 100 hours of observations which implies one event in twenty observing days. Since during these three years

we had managed to obtain on the average 21 observing days per year, it implies that we could expect to record one major event in a whole year's observing schedule.

These are rather discouraging statistics, especially given the fact that observing time on a major research facility, such as the Haystack radio telescope, is at a premium and 21 days per year are not easy to obtain by any single project.

An analysis of the flare events we were able to record show that essentially one can observe all kinds of situations. There are cases, e.g., where during the flare event:

a. Both T_a and %P showed similar excursions matching each other closely (see, e.g., Figures 3.9, 3.13, 3.14, and 3.5 the first two spikes).

b. Both T_a and %P showed excursions but their behavior was substantially different (see, e.g., Figure 3.20) including cases where the absolute value of %P decreased when T_a was hitting a peak (see, e.g., Figures 3.5 third spike, 3.21 second event, and 3.17 second event) and cases where the peaks of T_a and of %P did not coincide (see, e.g., Figure 3.19).

c. T_a showed a substantial increase with essentially no observable change in %P (see, Figures 3.12 and 3.21).

There were, of course, also all kinds of intermediate cases when we would compare the changes recorded for T_a with those recorded for %P.

We also observed events with substantially different behavior prior to the flare event. Thus, there were cases in which during the 50-100 minutes of monitoring prior to the flare event we recorded:

a. Fluctuations in both T_a and %P. (Figures 3.9, 313-15, 3.16, 3.20)

b. Fluctuations in %P with no changes in T_a. (Figures 3.6, 3.8, 3.11)

c. Fluctuations in T_a with no changes in %P. (Figures 3.9, 3.22)

d. No fluctuations in either T_a or %P (Figures 3.5, 3.21)

The diversity in behavior of T_a and %P during and prior to a flare event is not surprising given the parameters which affect the morphology of an active region (magnetic field configuration; number, sizes and extent of sunspots; plasma temperatures; etc.). Also the fact that the same active region will most likely behave in a different manner near the east limb of the sun, near the central meridian, and near the western limb of the solar disk (Papagiannis and Straka, 1977), increases the multiplicity of diverse behavior that one can expect to observe. Each one of these active regions and flare event deserves to be studied and analyzed as an individual case so as to build the proper model to explain the behavior of T_a and %P observed.

This undertaking has a substantial scientific interest and was attempted in one case (Papagiannis and Straka, 1977), but it is not an easy task to try it out for each case. In addition, for a complete analysis one needs to have information on the active

region at different points on the solar disk, plus data obtained at other spectral regions such as X-ray and UV spectrohelio rams.

On the whole, in order to devise a prediction scheme for major flare events, which was essentially the hope of this research project, we have reached the following conclusion: The diversity in the behavior of both T_a and %P observed at $\lambda \simeq 4$ cm makes it impossible to develop any forecasting scheme based on the number of cases available. On the other hand, the number of days and the hours of observations we logged over a period of three years, was very close to the maximum of what any one group could have expected to obtain from a major national facility such as Haystack. It also streched to the limit the human resources of a small academic group.

It appears, therefore, that the only reasonable scheme to deal with the problem of flare forecasting based on the behavior of active regions prior to an event, is to use a smaller facility which can dedicate a substantial fraction of its time to this task over a period of a whole solar cycle. The routine part of the observations, namely making a raster scan of the sun (solar map) to identify the locations of the active regions, pointing the antenna to the most interesting one, and monitoring this active region for several hours, can be pattended to such an extent as to make it possible for a technician to carry it out on a day to day basis.

A scientist could be in charge of the project analyzing in a systematic way the data and collecting statistics. Parallel

observations at two or more wavelengths, if possible, might prove of great value in a potential forecasting scheme. It should be noted, however, that there is no guarantee that such a long lasting project will ultimately produce a reliable forecasting scheme. Our experience, never the less, suggests that a long term operation with a dedicated facility is the only way to obtain the necessary number of events that can assure a statistical reliability to any forecasting scheme proposed. The price would be substantial and the task would be long and tedious. The potential reward, however, namely, the development of a reliable flare forecasting scheme, may be well worth the investment.

ACKNOWLEDGEMENTS

We want to thank the staff of the NEROC Haystack Observatory for their valuable assistantce during the long observing periods described in this report. Research with the Haystack antenna is supported by NSF under Grant MPS71-02 09A07.

REFERENCES

Edelson, S., Mayfield, E.B., and Shimabukuro, F.I., Nature Phys. Sc ., 232, 82, 1971.

Kundu, M.R., and McCullough, T.P., Solar Physics, 24, 133, 1972.

Papagiannis, M.D., Straka, R.M., and Kogut J.A., Bull. AAS, 7, 523, 1975.

Papagiannis, M.D., and Kogut, J.A., Solar Physics, 48, 49, 1976.

Papagiannis, M.D., and Straka, R.M., AFGL-TR-77-0115, May 1977.

Richards, D.W., AFGL-72-0090, February 1972.

Richards, D.W., and Straka, R.M. Nature Phys. Sci., 233, 9 , 1971.

Straka, R.M., Papagiannis, M.D., and Kogut, J.A., Solar Physics, 45, 131, 1975.

Wefer, F.L., Papagiannis, M.D., Straka, R.M., and Bleiweiss, M.P., Topic. Conf. Solar Interplan. Phys., Tuscon, Arizona, January, 1977.